

105p.

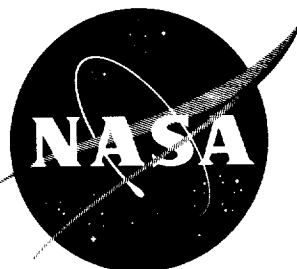
162-15429

N

15421

NASA TN D-1333

NASA TN D-1333



11

# TECHNICAL NOTE

## D-1333

CHARTS FOR EQUILIBRIUM FLOW PROPERTIES OF AIR  
IN HYPERVELOCITY NOZZLES

By Leland H. Jorgensen and Gayle M. Baum

Ames Research Center  
Moffett Field, Calif.

NATIONAL AERONAUTICS AND SPACE ADMINISTRATION  
WASHINGTON

September 1962



## NATIONAL AERONAUTICS AND SPACE ADMINISTRATION

## TECHNICAL NOTE D-1333

CHARTS FOR EQUILIBRIUM FLOW PROPERTIES OF AIR  
IN HYPERVELOCITY NOZZLES

By Leland H. Jorgensen and Gayle M. Baum

## SUMMARY

For initial stagnation pressures up to 1,000 atmospheres and stagnation enthalpies up to 10,000 Btu per pound, nozzle-flow properties for equilibrium air have been computed and plotted on charts. The work of NASA TN D-693 has been extended to include flow properties for closer intervals of specified stagnation enthalpies. Properties which have been charted as a function of Mach number are as follows: temperature, pressure, density, velocity, area ratio, dynamic pressure, Reynolds number, isentropic exponent, and molecular weight ratio. Ratios of temperature, pressure, and density across normal shock waves are also charted, and weight-flow rate is plotted as a function of stagnation enthalpy.

## INTRODUCTION

In order to design hypervelocity nozzles and to define the test conditions, various air-flow properties must be determined. Several theoretical investigations of air in equilibrium, frozen, and nonequilibrium flows have been reported (e.g., refs. 1 to 4). In a recent study (ref. 5) charts for equilibrium and frozen air flows were computed for specified stagnation pressures of 6.8, 68, and 680 atmospheres and stagnation enthalpies of 125, 2,000, 4,500, 8,000, 12,000 and 24,500 Btu per pound. In the present study the work of reference 5 has been extended to include equilibrium air-flow properties for stagnation pressures up to 1,000 atmospheres and for many additional stagnation enthalpies below 10,000 Btu per pound. Also, in contrast to reference 5, the flow properties have been plotted as a function of Mach number instead of area ratio for convenience of use in wind-tunnel operation.

The purpose of this report is to present for specified stagnation pressures and enthalpies the following properties as a function of Mach number: temperature, pressure, density, velocity, area ratio, dynamic pressure, Reynolds number, isentropic exponent, and molecular weight ratio. Also included are temperature, pressure, and density ratios across normal shock waves. Weight-flow rate is plotted as a function of stagnation enthalpy. Because in an actual nozzle the flow may not be in complete equilibrium, care should be exercised in the application of these charts.

## NOTATIONS AND CONSTANTS

A	nozzle cross-section area, ft <sup>2</sup>	
a	isentropic speed of sound, ft/sec	
h	enthalpy (with datum of h = 0 for molecular gas at 0° K), Btu/lb	
$\frac{h}{RT_0}$	enthalpy, dimensionless	
L	characteristic length, ft	A 6
M	Mach number	1 5
m	molecular weight of mixture, lb/mole	
$m_0$	molecular weight of undissociated air, 28.966 lb/mole	
p	pressure, atmospheres unless specified	
q	dynamic pressure ( $1/2 \rho u^2$ ), lb/ft <sup>2</sup>	
Re	Reynolds number, $u\rho L/\mu$	
R	gas constant, 1.987 Btu/mole-°R or 0.7302 ft <sup>3</sup> -atm/mole-°R	
RT <sub>0</sub>	33.73 Btu/lb for air	
S	entropy, Btu/(initial mole) (°R)	
S/R	entropy, dimensionless	
T	temperature, °R or °K as specified	
T <sub>0</sub>	reference temperature, 492° R = 273° K	
u	velocity, ft/sec	
W	weight-flow rate, lb/sec	
Z	molecular weight ratio, $m_0/m$	
$\gamma$	isentropic exponent, $\left(\frac{\partial \ln p}{\partial \ln \rho}\right)_s$	
$\rho$	density, slug/ft <sup>3</sup>	
$\rho_0$	reference density, 0.00251 slug/ft <sup>3</sup> for air	

$\mu$  coefficient of viscosity, lb-sec/ft<sup>2</sup>

( )\* sonic point

#### Subscripts

- o reference condition
- t reservoir condition
- 1 condition in front of normal shock wave
- 2 condition behind normal shock wave

#### THERMODYNAMIC PROPERTIES

For ready reference and convenience, thermodynamic properties of air for temperatures to 10,000° K and pressures to 10<sup>3</sup> atmospheres are plotted in figure 1. These plots give the variation of molecular weight ratio Z (fig. 1(a)), enthalpy  $h/RT_0$  (fig. 1(b)), and entropy S/R (fig. 1(c)) with temperature for specified pressures. The reader is referred to the previous section of the report for values of the constants  $RT_0$  and R. For temperatures to 3,000° K and pressures from 10<sup>-2</sup> to 10<sup>2</sup> atmospheres, the properties were obtained from reference 6. For temperatures from 2,000° K to 10,000° K and pressures from 10<sup>-5</sup> to 10<sup>3</sup> atmospheres, the properties were obtained from reference 7. The properties from references 6 and 7 were in excellent agreement in the overlapping range of temperatures and pressures (2,000° K to 3,000° K and 10<sup>-2</sup> to 10<sup>2</sup> atmospheres). In addition to information from these sources, some of the curves at low pressures and temperatures (p as low as 10<sup>-6</sup> atmosphere and T as low as 50° K) were determined based on the perfect gas law and are identified by dashed lines. For more extensive air charts for temperatures to 15,000° K, the reader is referred to references 8 and 9; and for air properties at temperatures to 100,000° K, the reader is referred to reference 10.

Vapor pressures as a function of temperature for air, oxygen, and nitrogen are presented in figure 2. To estimate the vapor pressures for air a perfect liquid or solid solution of oxygen and nitrogen was assumed in equilibrium with a 20-percent oxygen, 80-percent nitrogen vapor. The vapor-pressure data for oxygen and nitrogen were obtained from references 6, 11, and 12. The approximate saturated vapor line for air is also indicated on the entropy graph in figure 1(c).

## CALCULATION OF NOZZLE FLOW PROPERTIES

The nozzle-flow properties as a function of Mach number were desired for use in wind-tunnel testing. For convenience in the computational procedure, however, the flow properties were computed as a function of the ratio of static to stagnation pressure, with the corresponding Mach number being computed. Stagnation conditions  $p_t$  and  $h_t$  at the reservoir were specified for each case considered. In order to compute the area ratio, Mach number, and Reynolds number, the density was determined from the thermal equation of state

$$\rho = p m_o / ZRT \quad (1)$$

For  $\rho$  in slugs per cubic foot,  $p$  in atmospheres, and  $T$  in  $^{\circ}$ R,

$$\rho = 1.234 p/ZT \quad (2)$$

where

$$p = p_t(p/p_t)$$

An isentropic expansion of the gas from the reservoir to downstream stations in the nozzle was assumed, and the molecular weight ratio  $Z$ , the temperature  $T$ , and the enthalpy  $h = (h/RT_o)RT_o$  were determined from the thermal plots (fig. 1). The velocity was then computed from the energy relation

$$u = 223.6 \sqrt{h_t - h} \quad (3)$$

The area ratio was calculated from the continuity equation

$$A/A^* = \rho^* u^* / \rho u \quad (4)$$

where the mass-flow rate at the throat ( $W/A^* = \rho^* u^*$ ) was determined as the maximum  $\rho u$  for given stagnation conditions  $p_t$  and  $h_t$ . The Mach number was computed from

$$M = \frac{u}{a} = \frac{u}{\sqrt{\gamma ZRT}} \quad (5)$$

For  $T$  in  $^{\circ}$ R the speed of sound  $a$  in feet per second was given by

$$a = 41.43 \sqrt{\gamma Z T} \quad (6)$$

where the isentropic exponent  $\gamma$  was determined from

$$\gamma = \left( \frac{\partial \ln p}{\partial \ln \rho} \right)_s \quad (7)$$

The Reynolds number was calculated from

$$\frac{Re}{L_{Pt}} = \frac{u \rho}{\mu L_{Pt}} \quad (8)$$

with the coefficient of viscosity  $\mu$  computed by the method of reference 13. In reference 13 the effects of molecular dissociation and ionization on  $\mu$  were considered.

An iterative procedure was used to obtain equilibrium temperature ratios, pressure ratios, and density ratios across a normal shock wave. This procedure is outlined in references 3 and 5, but it is repeated here for clarity and convenience. Since the Mach number  $M_1$  in front of the shock was known, the density ratio,  $\rho_2/\rho_1$ , was assumed, and the pressure behind the shock was calculated from the expression

$$p_2 = p_1 + (\rho_1 u_1)(u_1) \left( 1 - \frac{\rho_1}{\rho_2} \right) \quad (9)$$

which resulted from combining the momentum and continuity equations. For the pressure in atmospheres

$$p_2 = p_1 + \frac{1}{2117} (\rho_1 u_1)(u_1) \left( 1 - \frac{\rho_1}{\rho_2} \right) \quad (10)$$

The local enthalpy behind the shock,  $h_2$ , was determined by the energy equation

$$h_2 = h_1 + (1/2)u_1^2 - (1/2)u_2^2 \quad (11)$$

For  $h_2$  in Btu per pound

$$h_2 = h_1 + \frac{1}{50,060} u_1^2 \left[ 1 - \left( \frac{\rho_1}{\rho_2} \right)^2 \right] \quad (12)$$

With  $p_2$  and  $h_2$  known,  $T_2$  and  $Z_2$  were obtained from the thermal plots

(fig. 1). The density behind the normal shock,  $\rho_2$ , was then computed from equation (1), and  $\rho_2/\rho_1$  was compared with the assumed value. This process was repeated until the assumed and computed values of  $\rho_2/\rho_1$  were in agreement. The stagnation pressure behind the normal shock was then determined from the thermal plots with an isentropic compression assumed from  $h_2$  and  $p_2$  to  $h_{t_2} = h_t$ .

## RESULTS

The procedure outlined in the previous section was used to compute nozzle properties for equilibrium flow for various initial stagnation pressures and enthalpies. All calculations were made on an IBM 7090 system, the thermodynamic properties of air (from the references previously cited) having been put on magnetic tape. The nozzle-flow properties determined were temperature, pressure, density, velocity, area ratio, Mach number, dynamic pressure, Reynolds number, isentropic exponent, molecular weight ratio, and weight flow. Ratios of temperature, pressure, and density across normal shock waves were also determined. The initial stagnation pressures for the calculations were 1, 10, 100, and 1,000 atmospheres, and the initial stagnation enthalpies included values from 400 to 10,000 Btu per pound.

Except for weight-flow rate which was plotted as a function of stagnation enthalpy, all properties were plotted as a function of Mach number and are presented on charts which are indexed on page 17. The reader should note that, except on the weight-flow chart (chart 14), symbols are used on the charts only to identify curves, not to indicate the many points computed for each curve. Perfect-air properties (from ref. 14) are presented on most of the charts for comparison with the real-air properties.

Ames Research Center  
National Aeronautics and Space Administration  
Moffett Field, Calif., June 27, 1962

## REFERENCES

1. Bray, K. N. C.: Departure from Dissociation Equilibrium in a Hypersonic Nozzle. British A. R. C. 19,983, March 1958.
2. Li, Ting Yi: Nonequilibrium Flow in Gas Dynamics. Rep. 852-59, American Rocket Soc., June 1959.
3. Erickson, Wayne D., and Creekmore, Helen S.: A Study of Equilibrium Real-Gas Effects in Hypersonic Air Nozzles, Including Charts of Thermodynamic Properties for Equilibrium Air. NASA TN D-231, 1960.
4. Boyer, D. W., Eschenroeder, A. Q., and Russo, A. L.: Approximate Solutions for Nonequilibrium Airflow in Hypersonic Nozzles. AEDC-TN-60-181, Cornell Aero Lab., Inc., Report No. AD-1345-W-3, Aug. 1960.
5. Yoshikawa, Kenneth K., and Katzen, Elliott D.: Charts for Air-Flow Properties in Equilibrium and Frozen Flows in Hypervelocity Nozzles. NASA TN D-693, 1961.
6. Hilsenrath, Joseph, Beckett, Charles W., et al.: Tables of Thermal Properties of Gases. NBS Cir. 564, U. S. Dept. of Commerce, 1955.
7. Hilsenrath, Joseph, and Beckett, Charles W.: Tables of Thermodynamic Properties of Argon-Free Air to 15,000°K. AEDC TN 56-12, Arnold Eng. Dev. Center, Sept. 1956.
8. Feldman, Saul: Hypersonic Gas Dynamic Charts for Equilibrium Air. Avco Res. Lab., Jan. 1957.
9. Moeckel, W. E., and Weston, Kenneth C.: Composition and Thermodynamic Properties of Air in Chemical Equilibrium. NACA TN 4265, 1958.
10. Staff of the Chance Vought Research Center: Thermodynamic Properties of High Temperature Air. Chance Vought Research Center Report No. RE-1R-14, 28 June 1961.
11. Aoyama, S., and Kanda, E.: Vapor Tensions of Solid Oxygen and Nitrogen. Tohoku Univ. Sci. and Tech. Reps., vol. 24, May 1935, pp. 107-115.
12. Hodgman, Charles D. (Editor in Chief): Handbook of Chemistry and Physics, 43rd Ed., Chemical Rubber Pub. Co., Cleveland, Ohio, 1961.
13. Hansen, C. Frederick: Approximations for the Thermodynamic and Transport Properties of High-Temperature Air. NASA TR R-50, 1959.
14. Ames Research Staff: Equations, Tables, and Charts for Compressible Flow. NACA Rep. 1135, 1953.



10

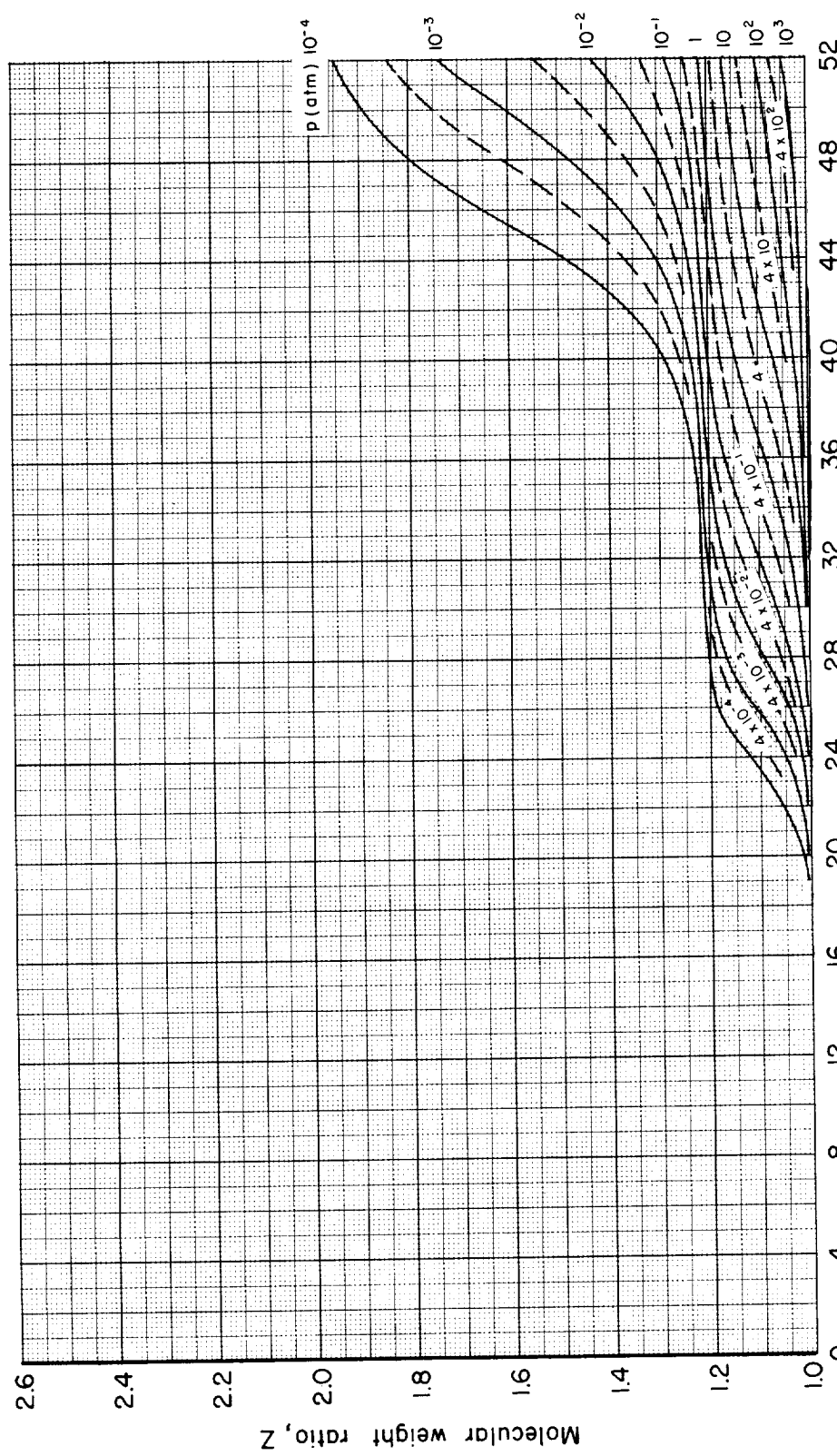
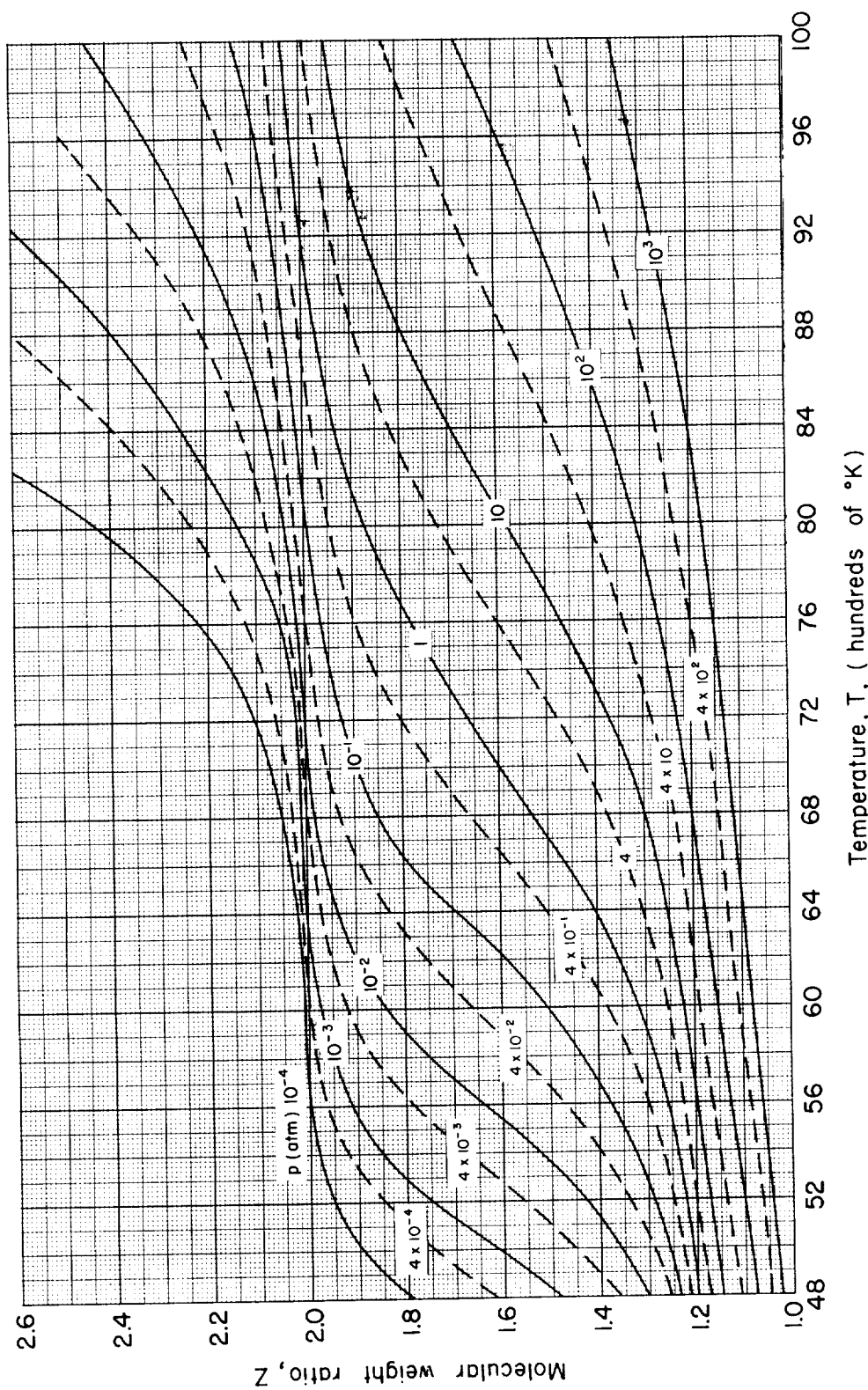


Figure 1.- Thermodynamic properties of air.  
 (a) Molecular weight ratio

1  
5  
L  
5



(a) Molecular weight ratio - Concluded.

Figure 1.- Continued.

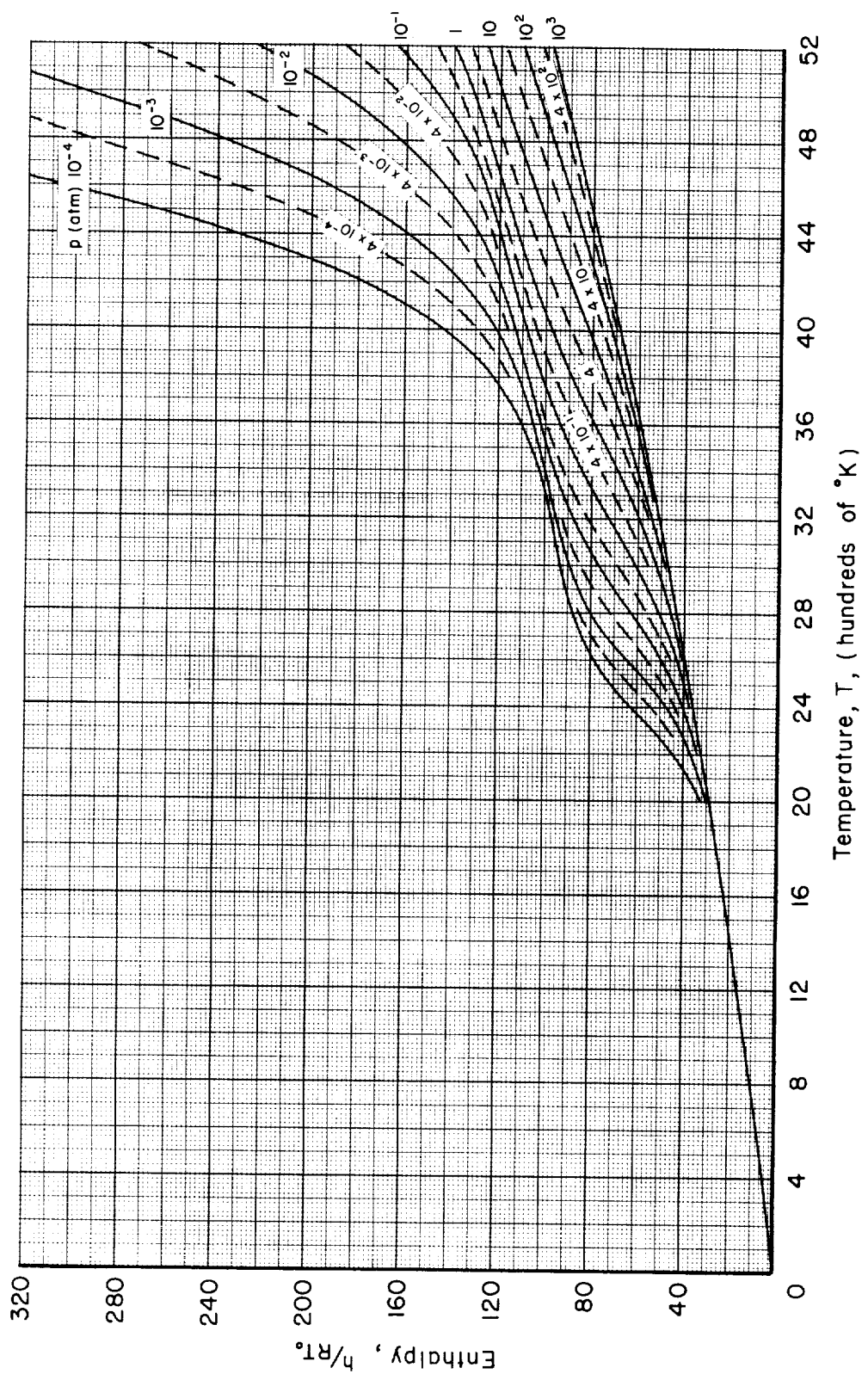
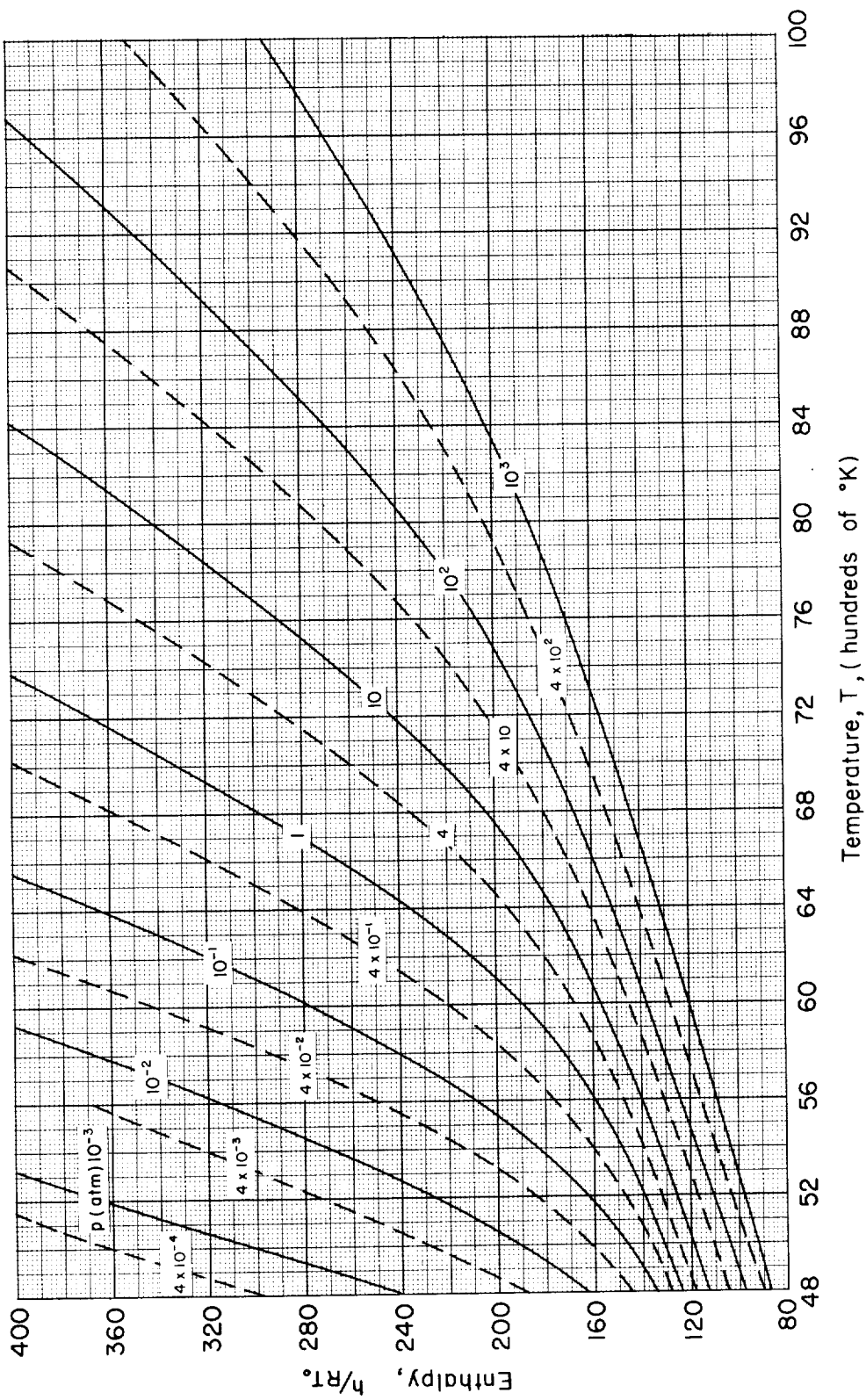


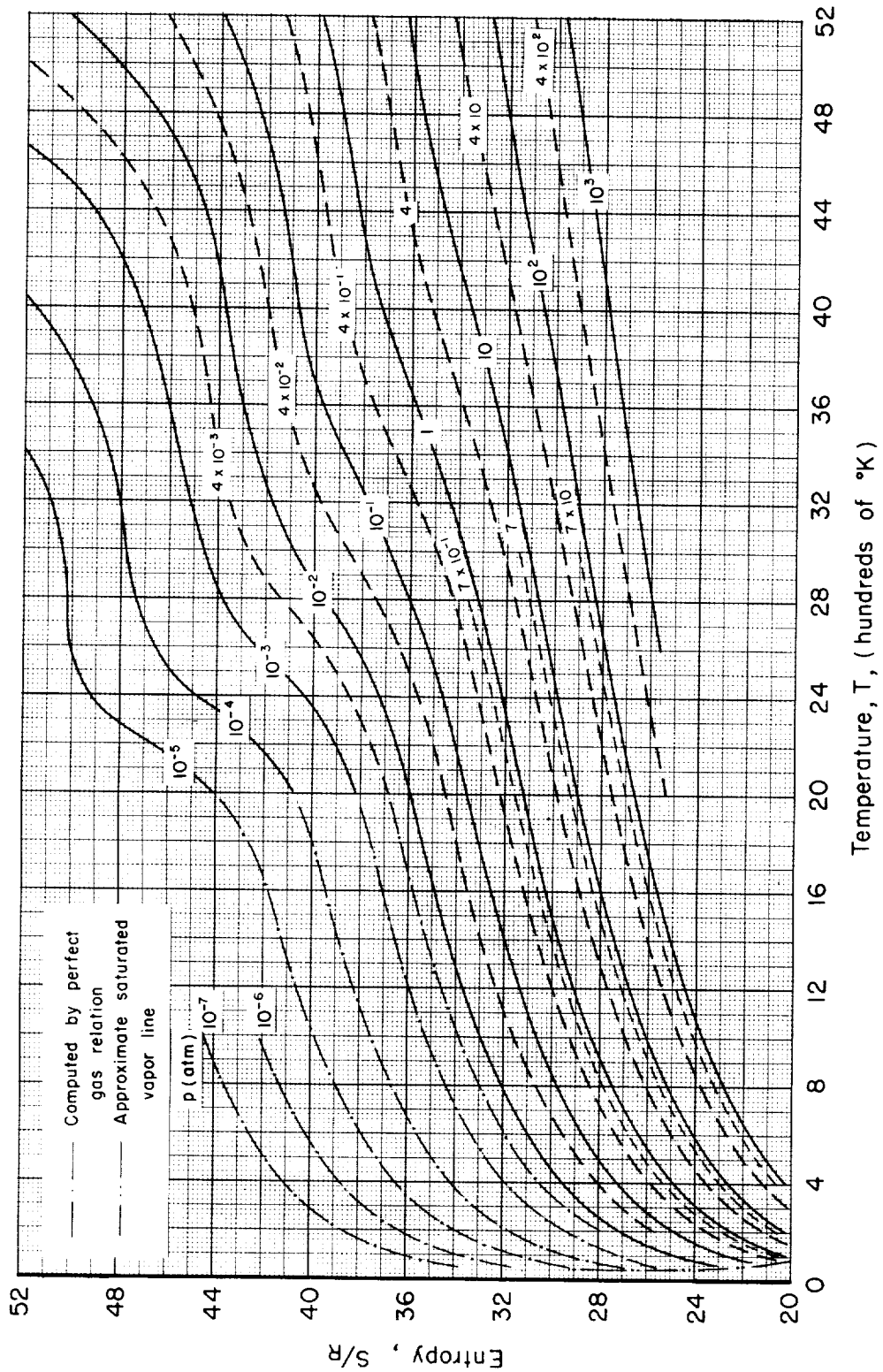
Figure 1.- Continued.  
(b) Enthalpy



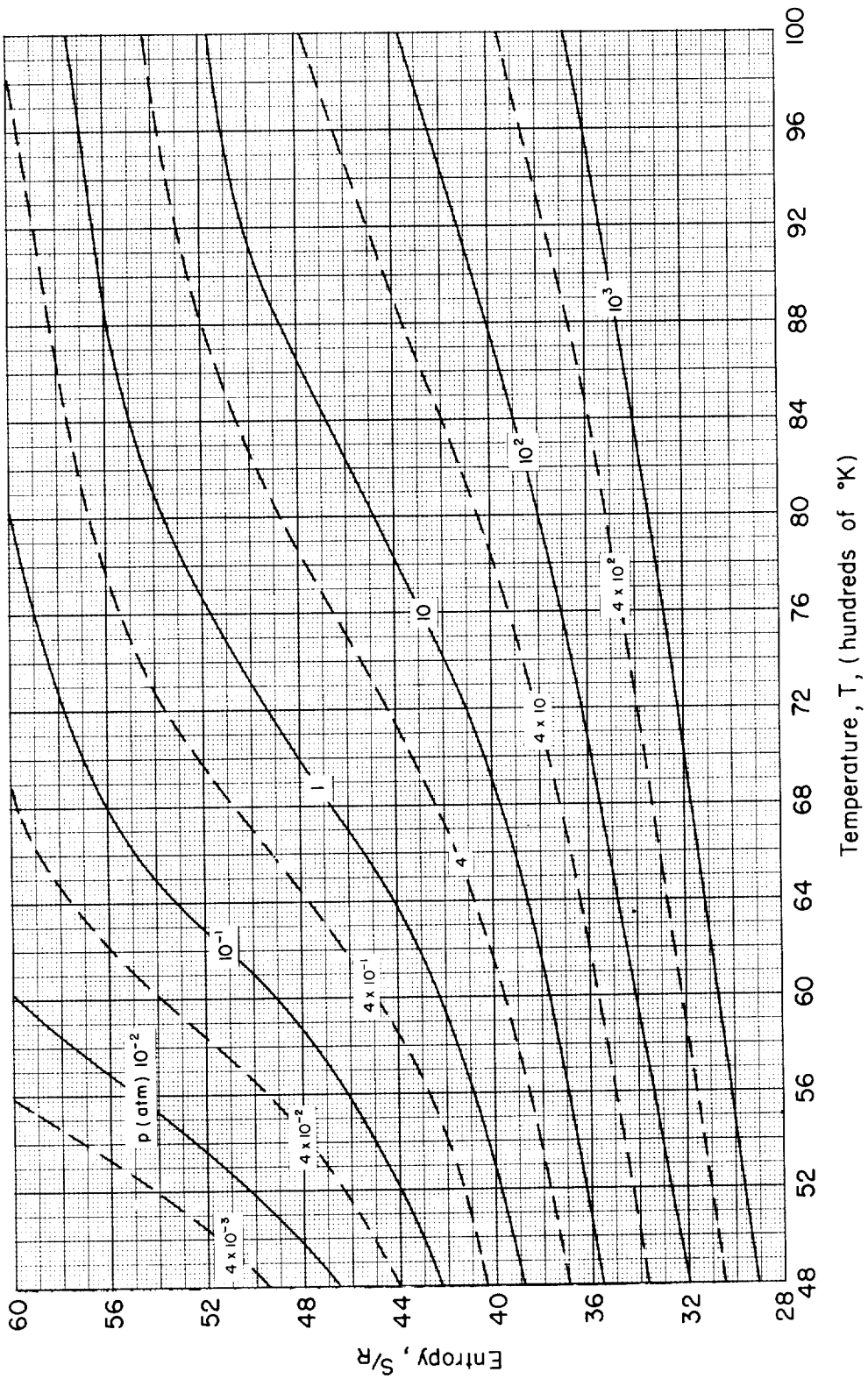
Temperature,  $T$ , (hundreds of  $^{\circ}\text{K}$ )

(b) Enthalpy – Concluded.

Figure 1.— Continued.



(c) Entropy  
Figure 1.- Continued.



(c) Entropy — Concluded.

Figure 1.— Concluded.

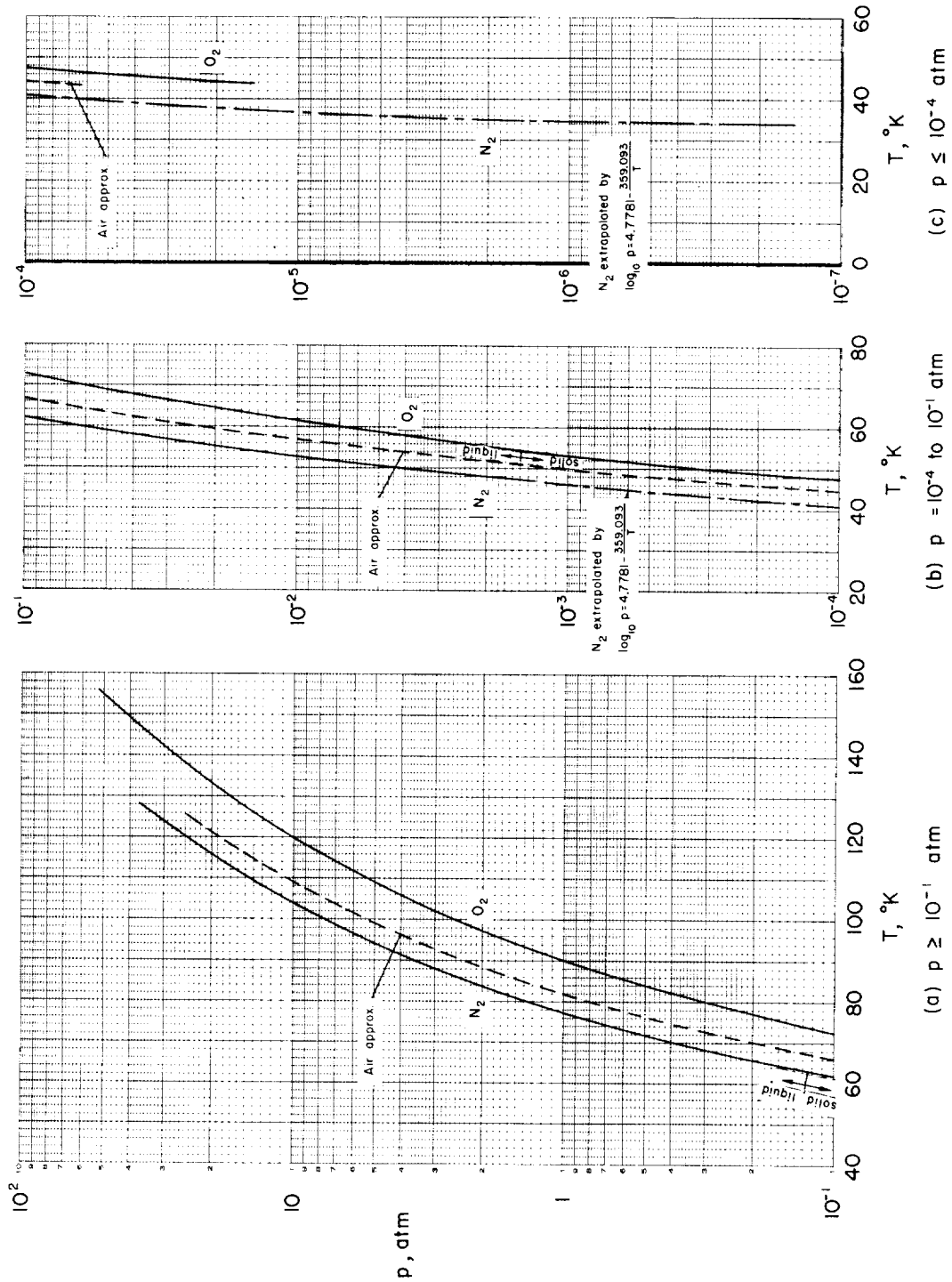


Figure 2.—Vapor pressures of air, oxygen, and nitrogen.

## INDEX TO CHARTS FOR AIR-FLOW PROPERTIES

A  
6  
1  
5

Ordinate		Abscissa	Chart	Page
Temperature	T	M	1	19
	$T_2/T_1$	M	2	23
Pressure	$p/p_t$	M	3	27
	$p_2/p_1$	M	4	34
	$p_{t_2}/p_{t_1}$	M	5	38
Density	$\rho/\rho_0 p_t$	M	6	40
	$\rho_2/\rho_1$	M	7	47
Velocity	u	M	8	51
Area ratio	$A/A^*$	M	9	55
Dynamic pressure	$q/p_t$	M	10	62
Reynolds no.	$Re/p_t L$	M	11	66
Isentropic exponent	$\gamma$	M	12	72
Molecular weight ratio	Z	M	13	73
Weight flow	$w/A^* p_t$	$h_t$	14	74



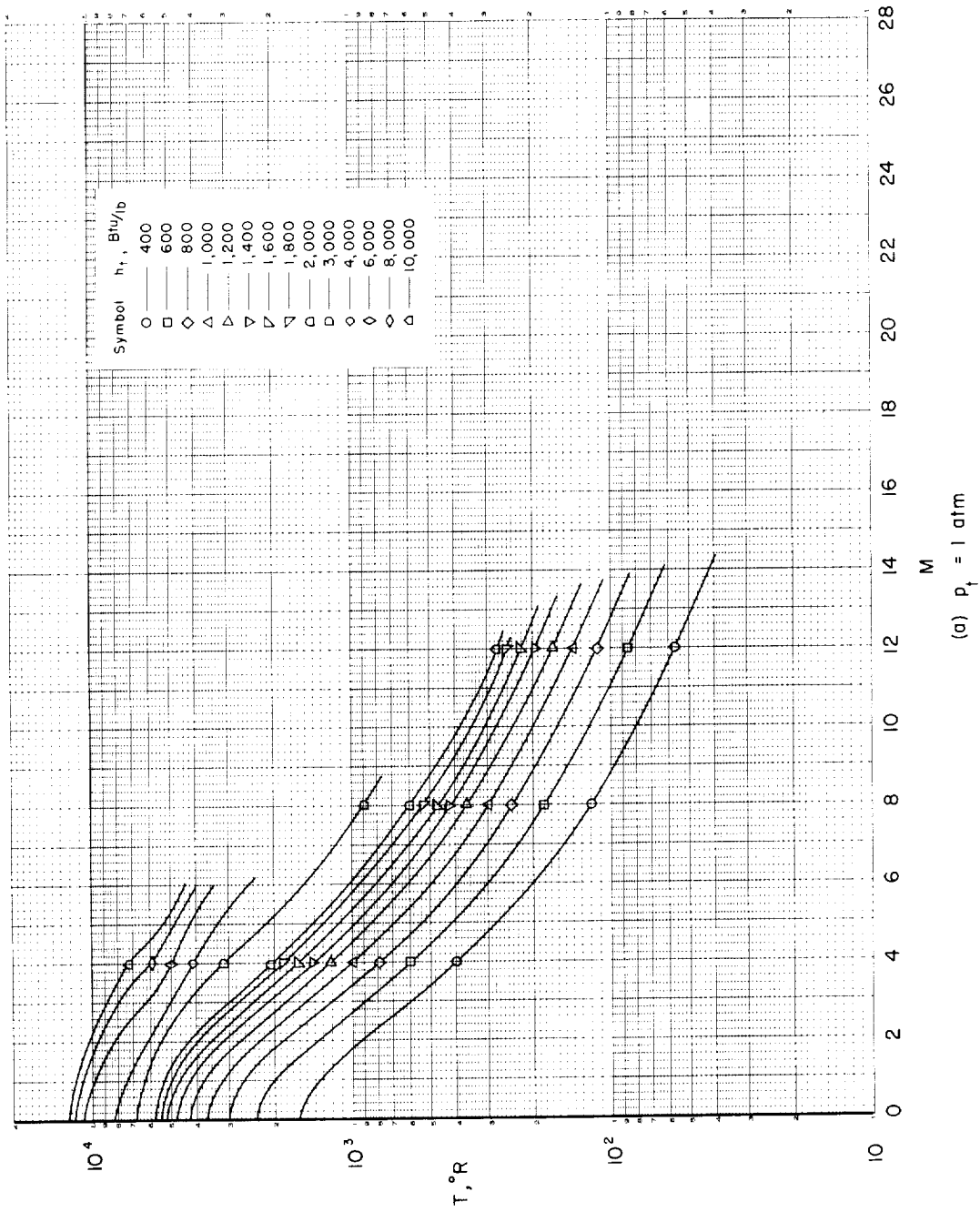
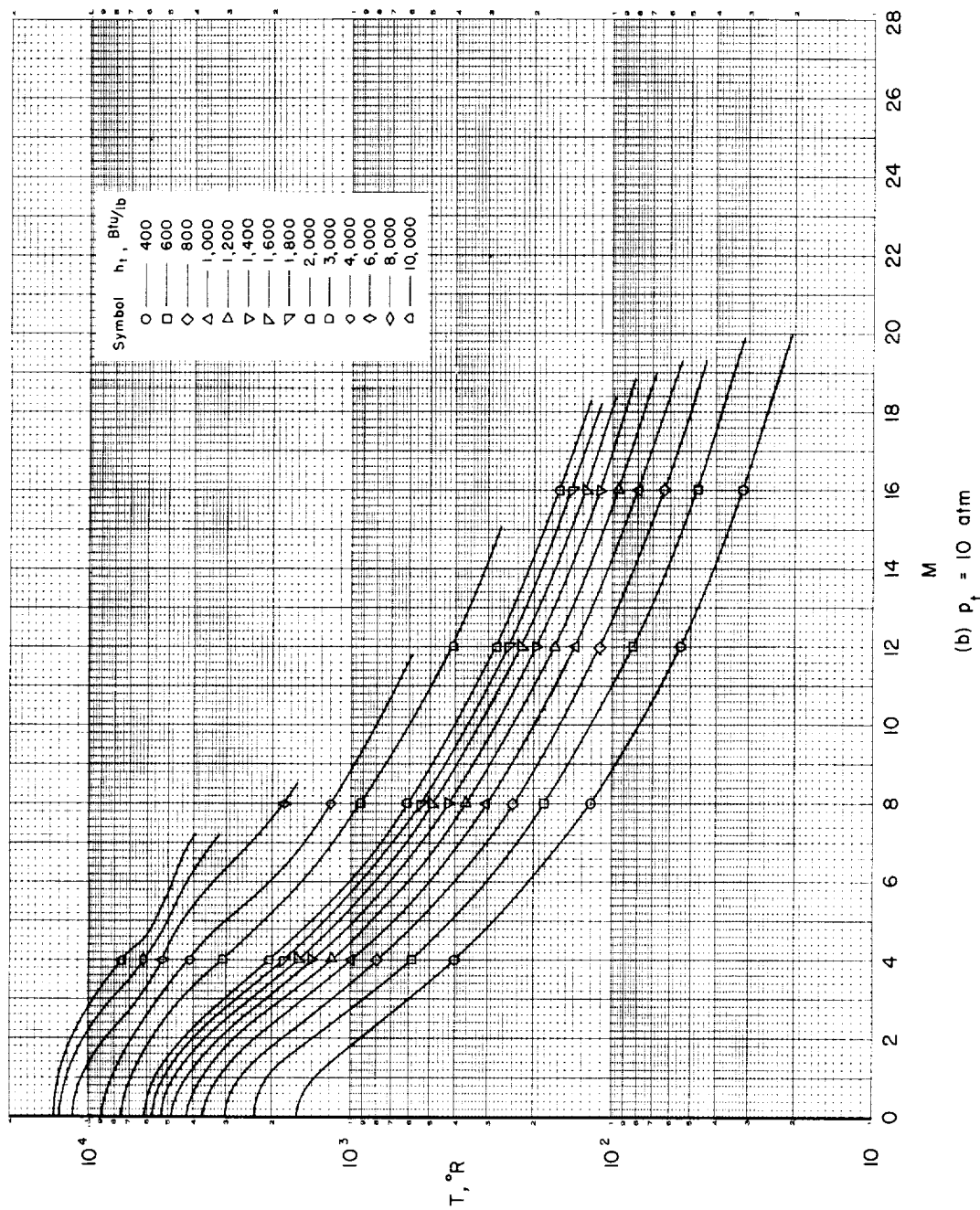


Chart 1.- Variation of temperature with Mach number.



(b)  $p_t = 10 \text{ atm}$

Chart 1.- Continued.

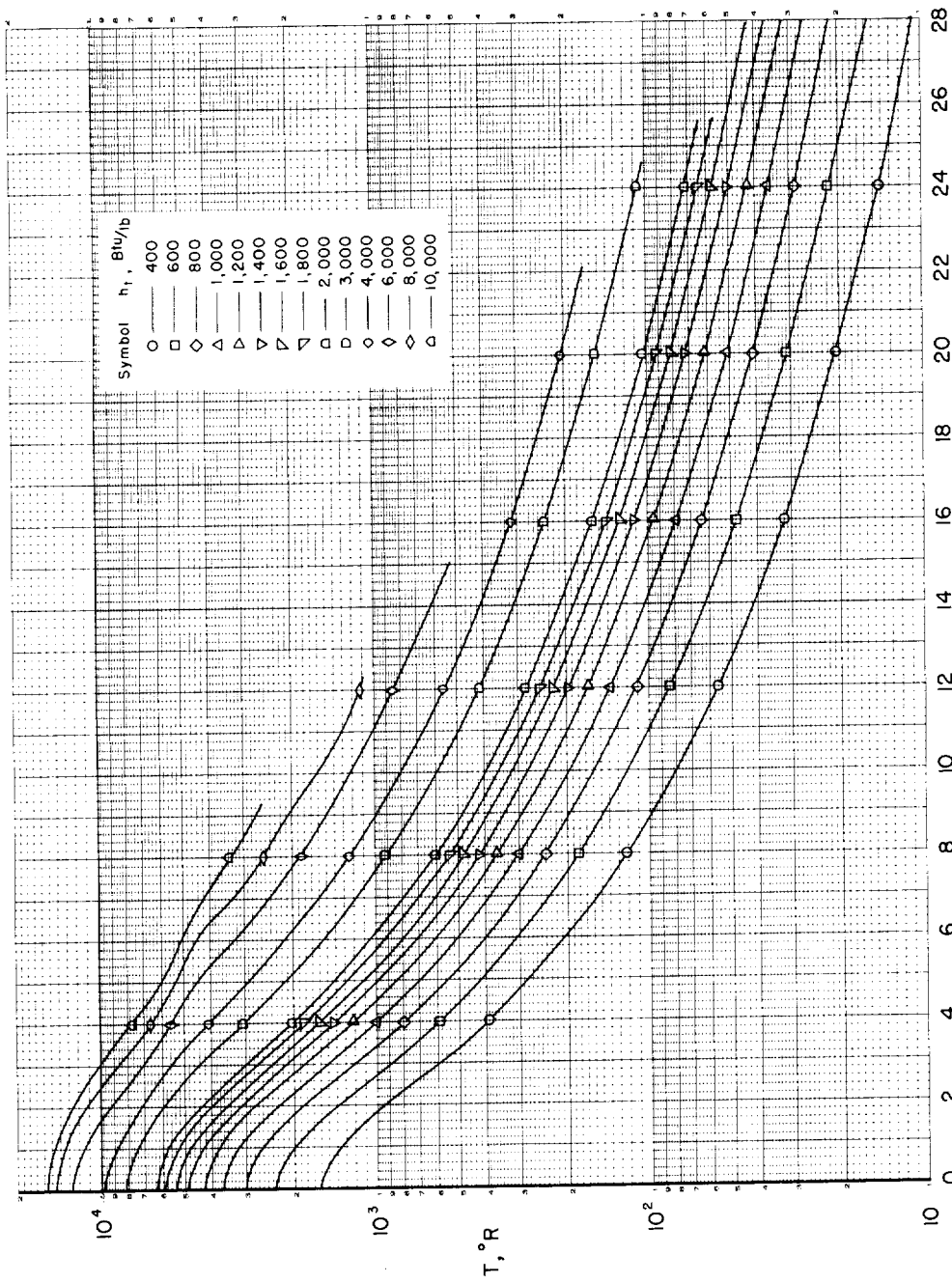
(c)  $P_t = 100$  atm

Chart 1.- Continued.

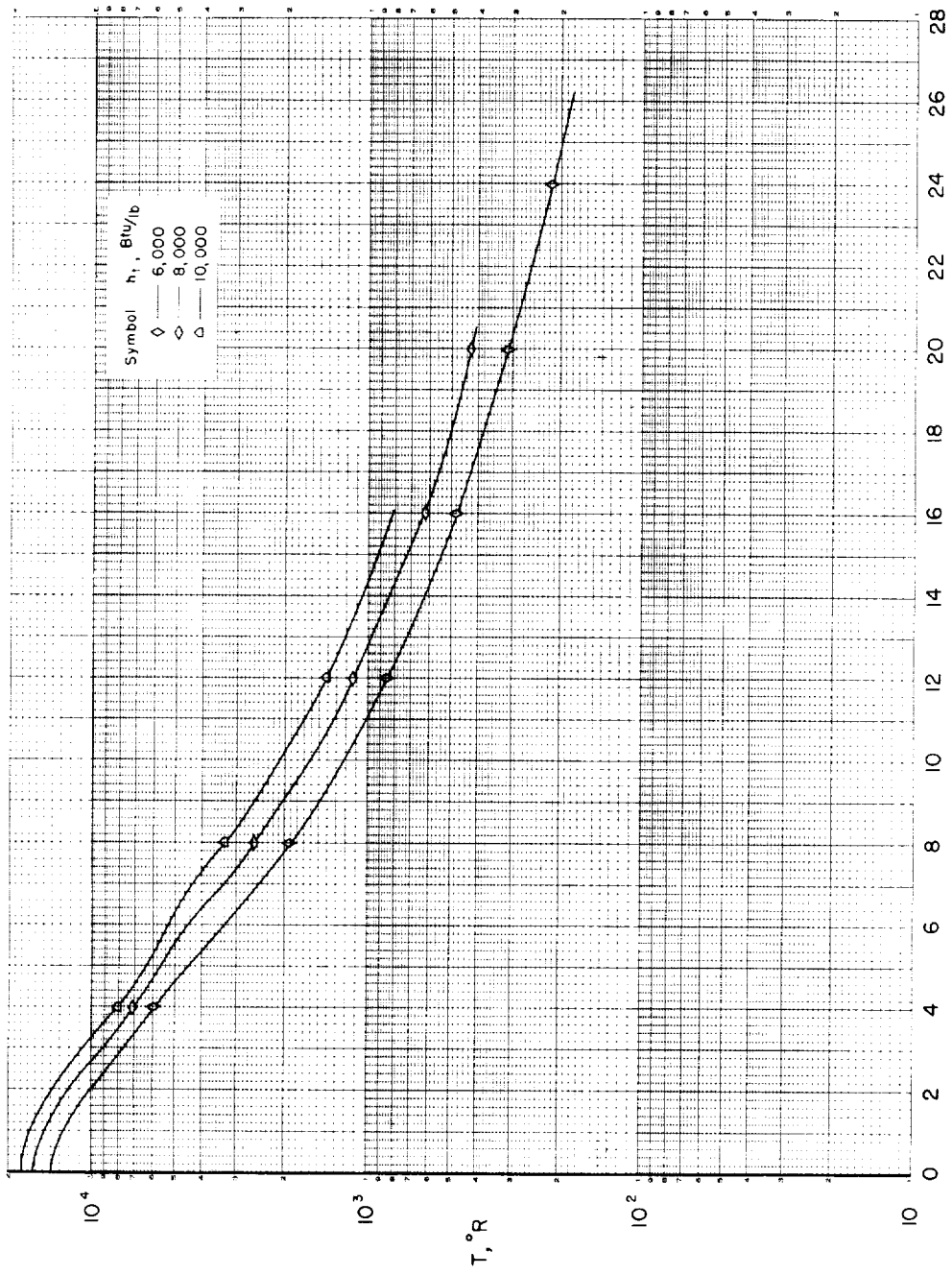


Chart 1.- Concluded.

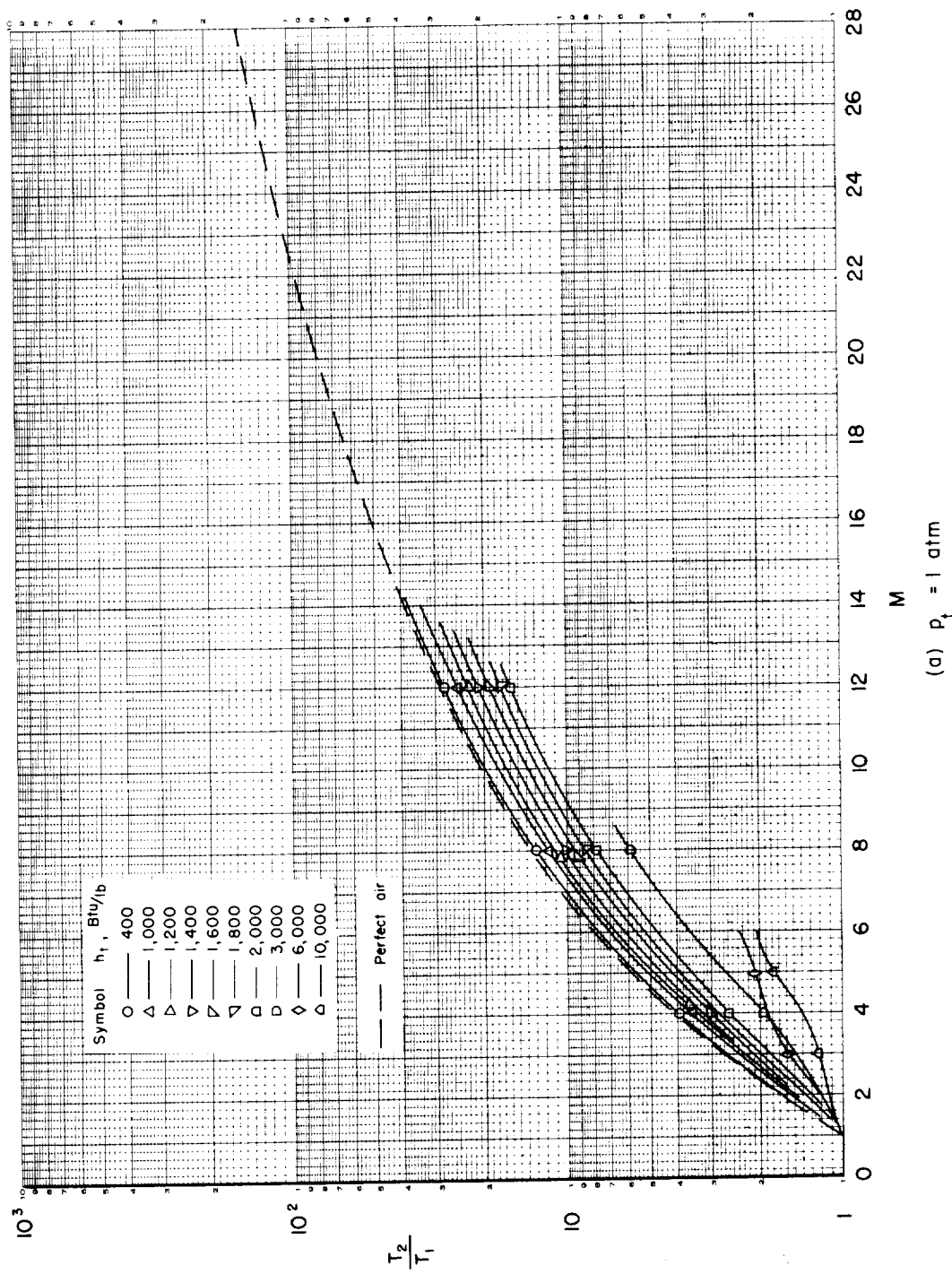


Chart 2.- Variation of temperature ratio across a normal shock wave with Mach number.

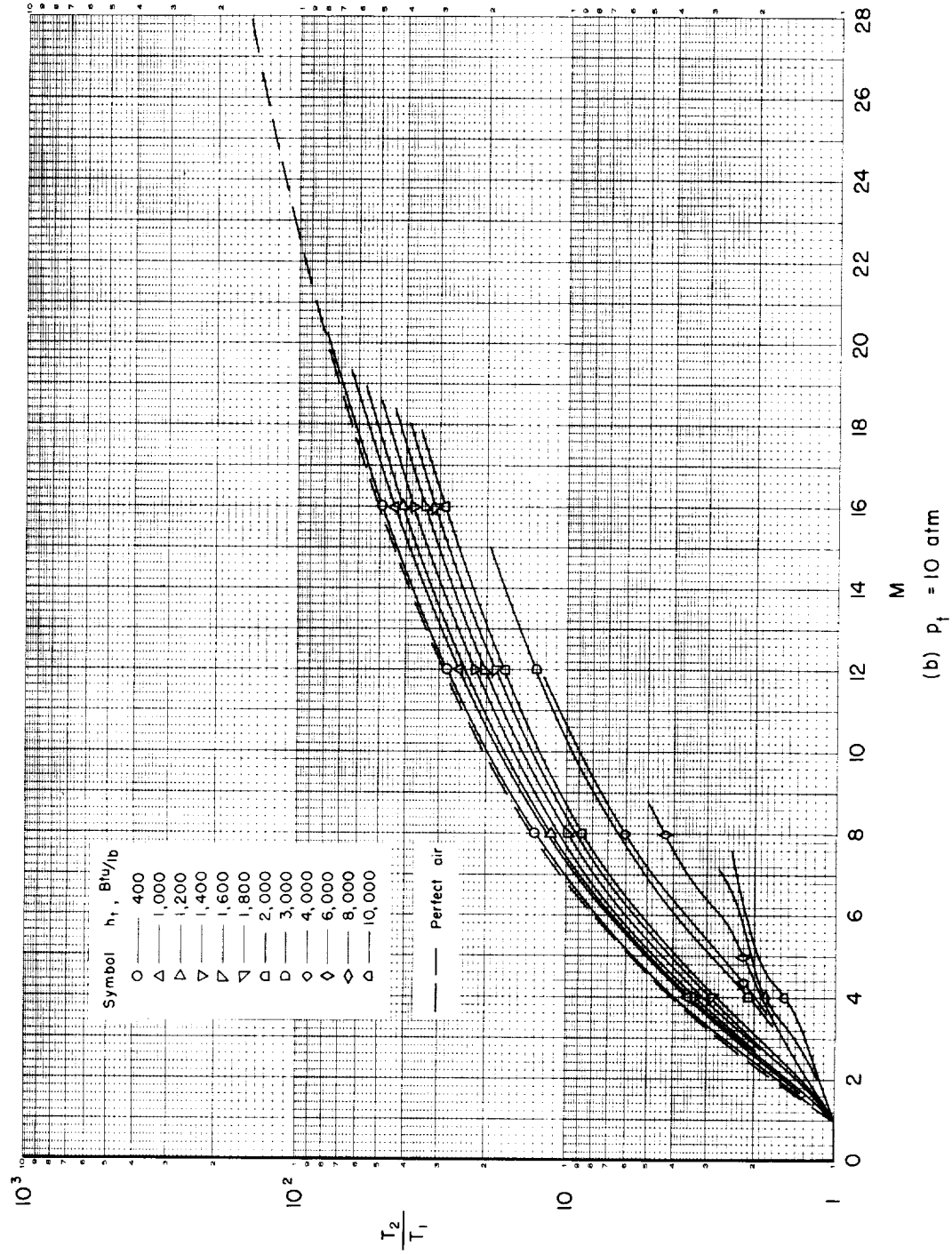
(b)  $P_f = 10$  atm

Chart 2.- Continued.

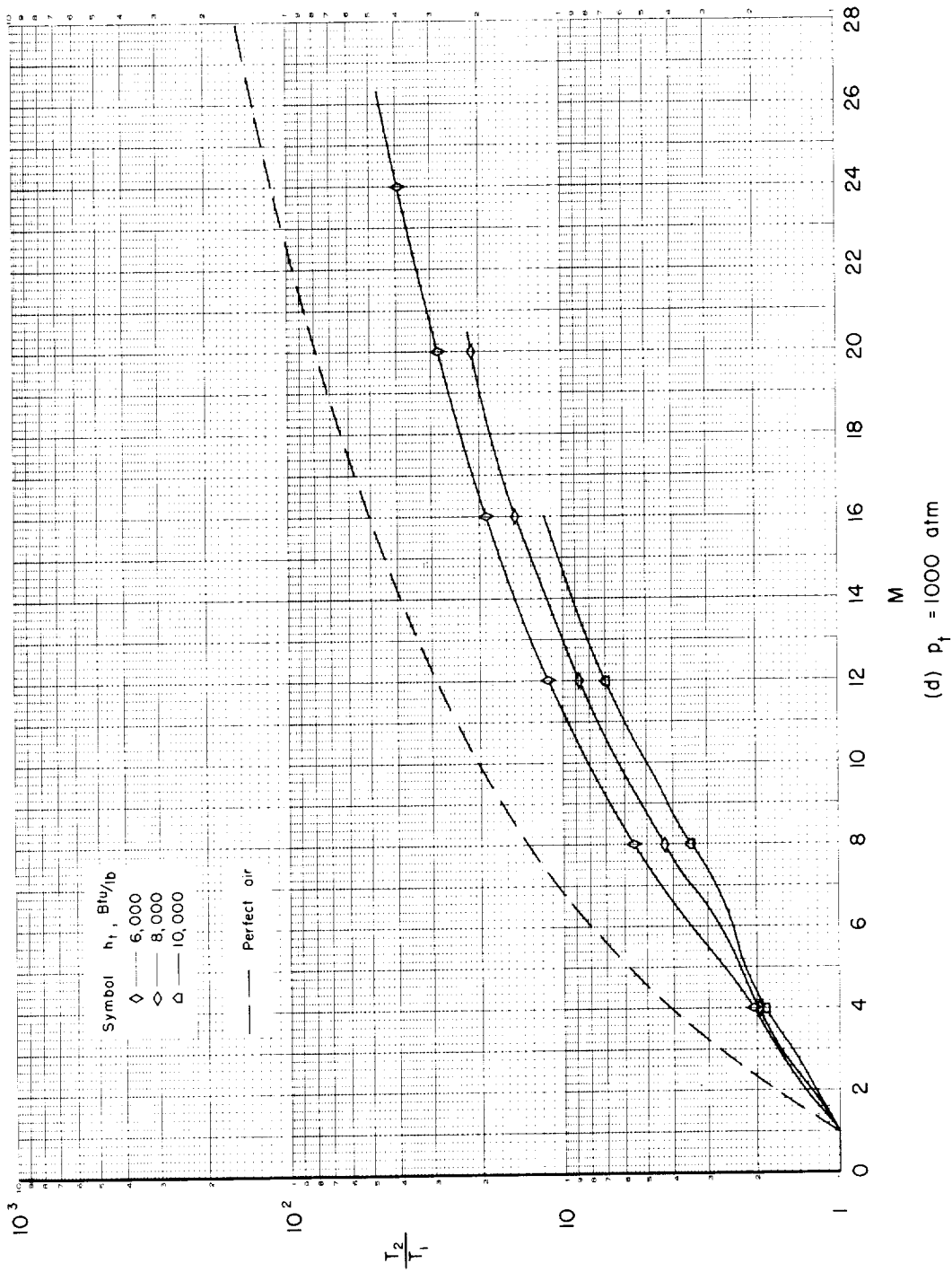
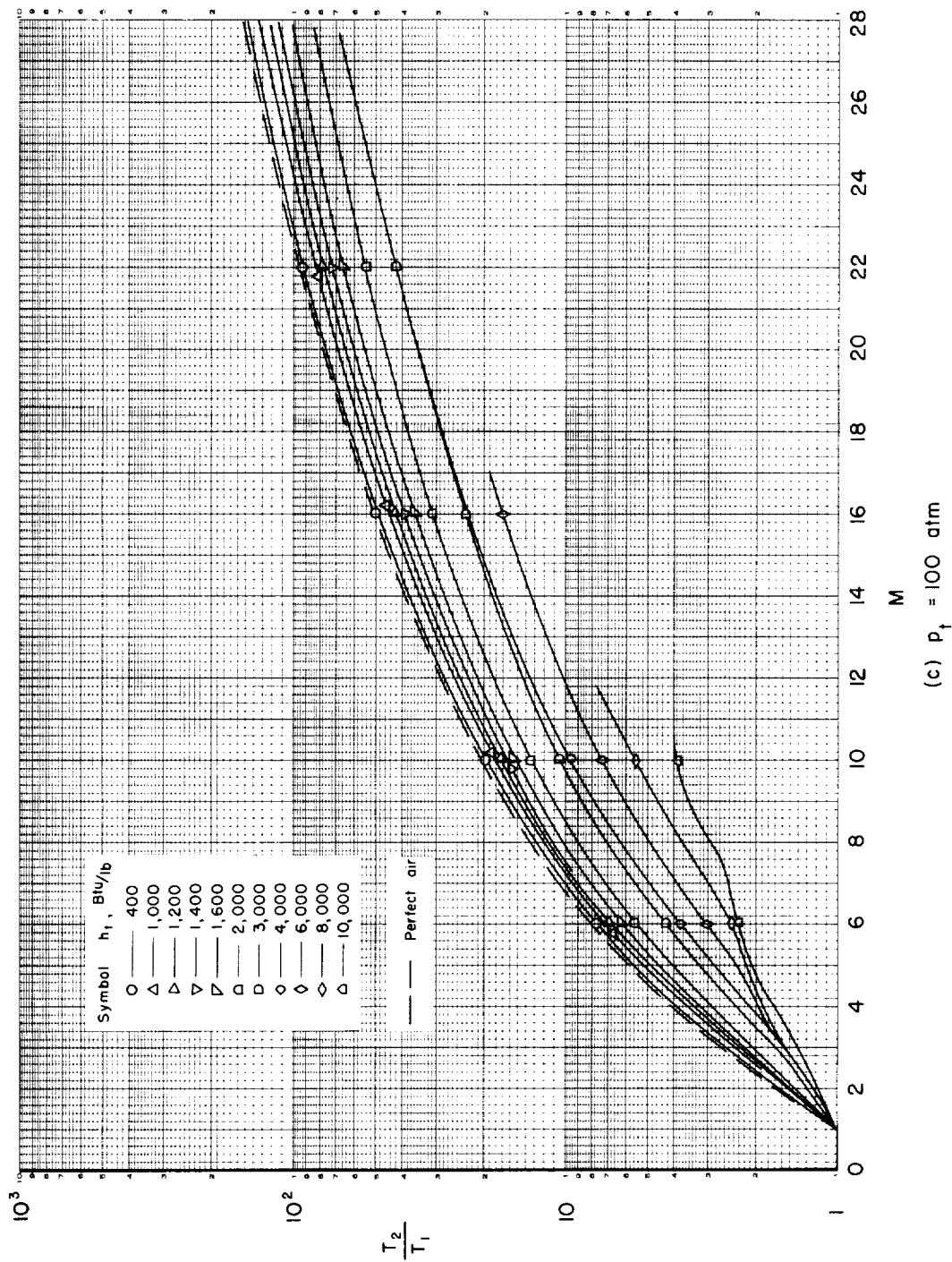
(d)  $p_t = 1000$  atm

Chart 2.— Concluded.



(c)  $P_1 = 100 \text{ atm}$

Chart 2.- Continued.

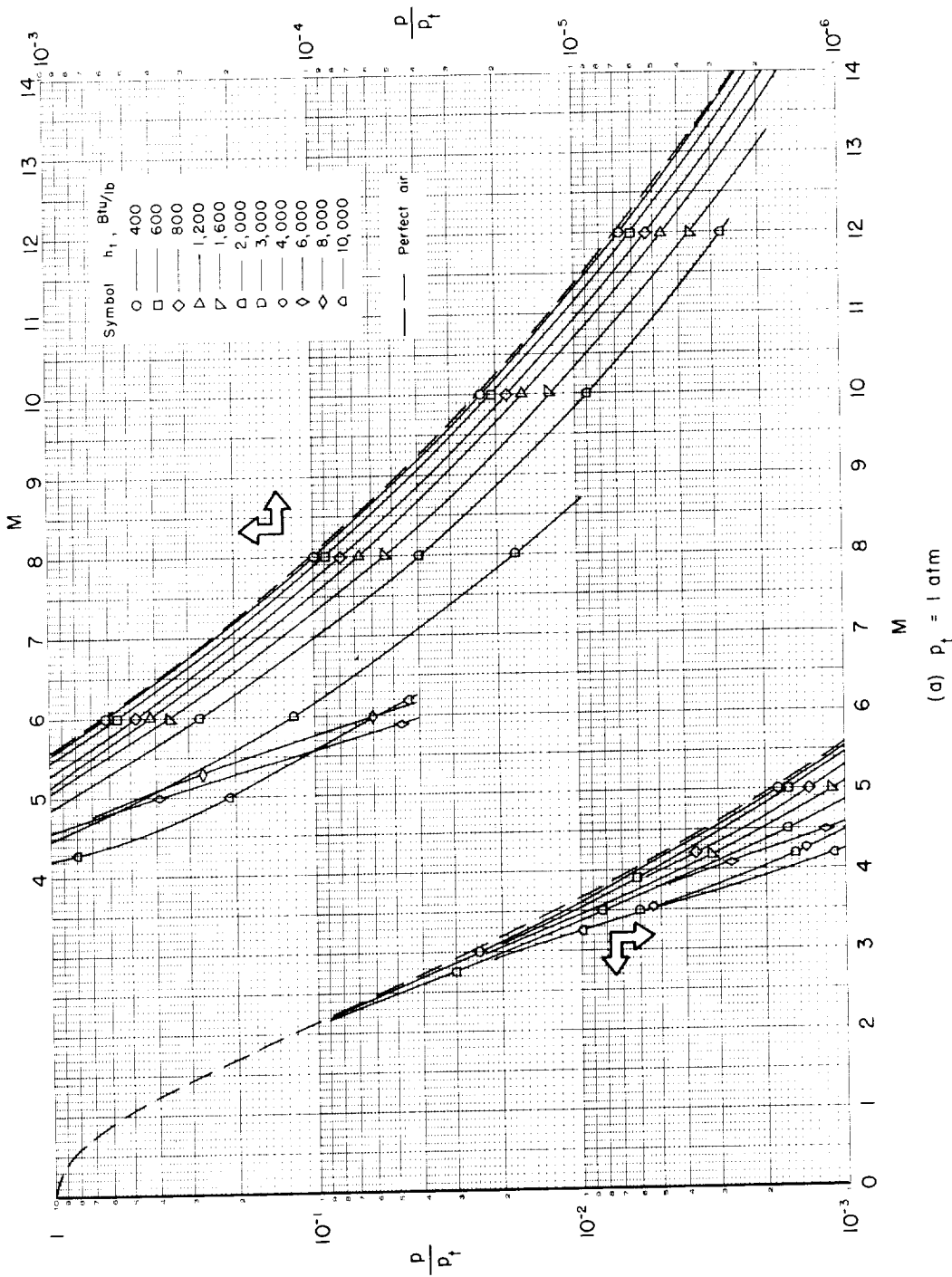
(a)  $P_f = 1 \text{ atm}$ 

Chart 3.- Variation of the ratio of static to total pressure with Mach number.

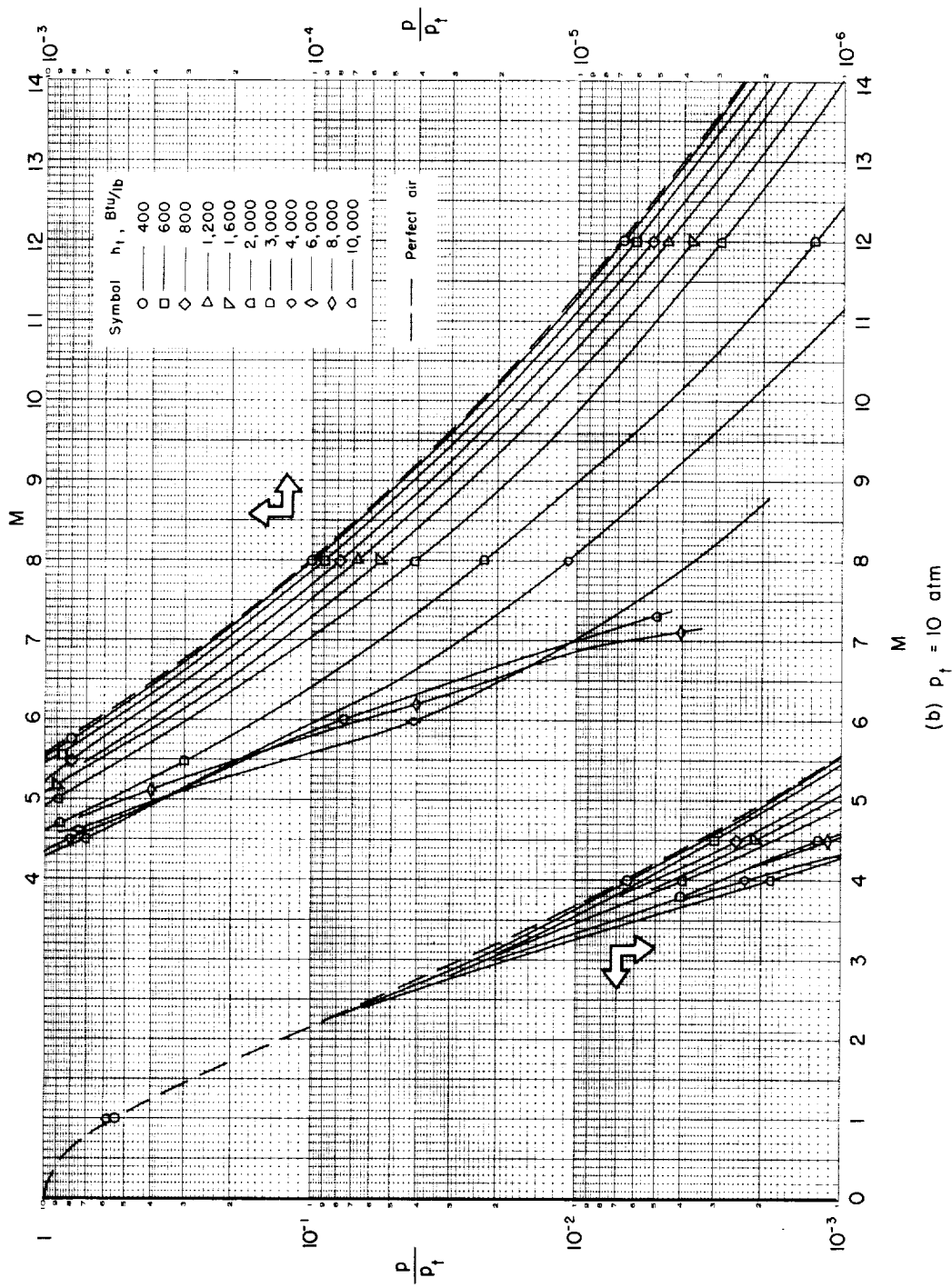
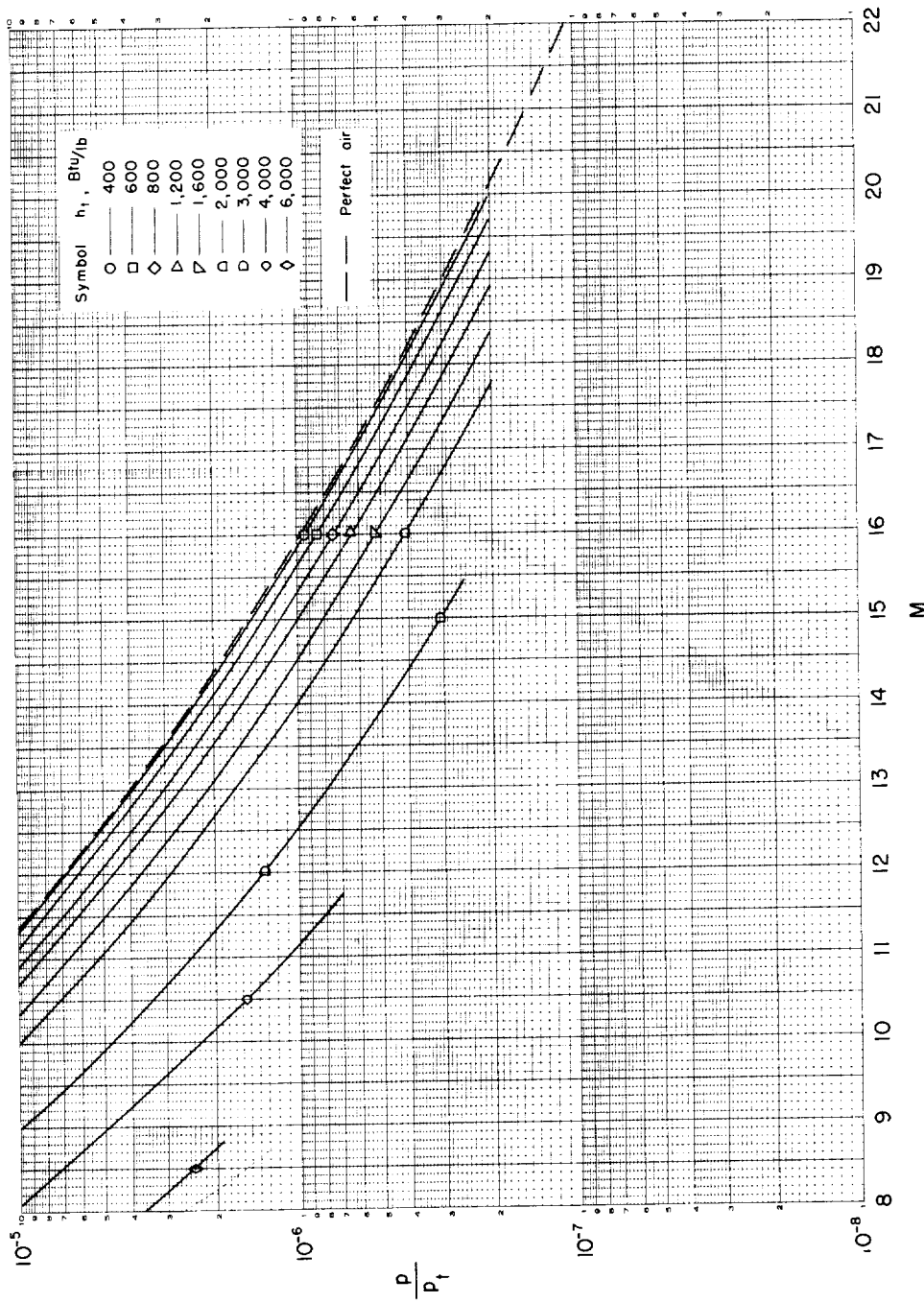
(b)  $P_f = 10 \text{ atm}$ 

Chart 3.- Continued.



(b)  $P_t = 10 \text{ atm} - \text{Concluded.}$

Chart 3.- Continued.

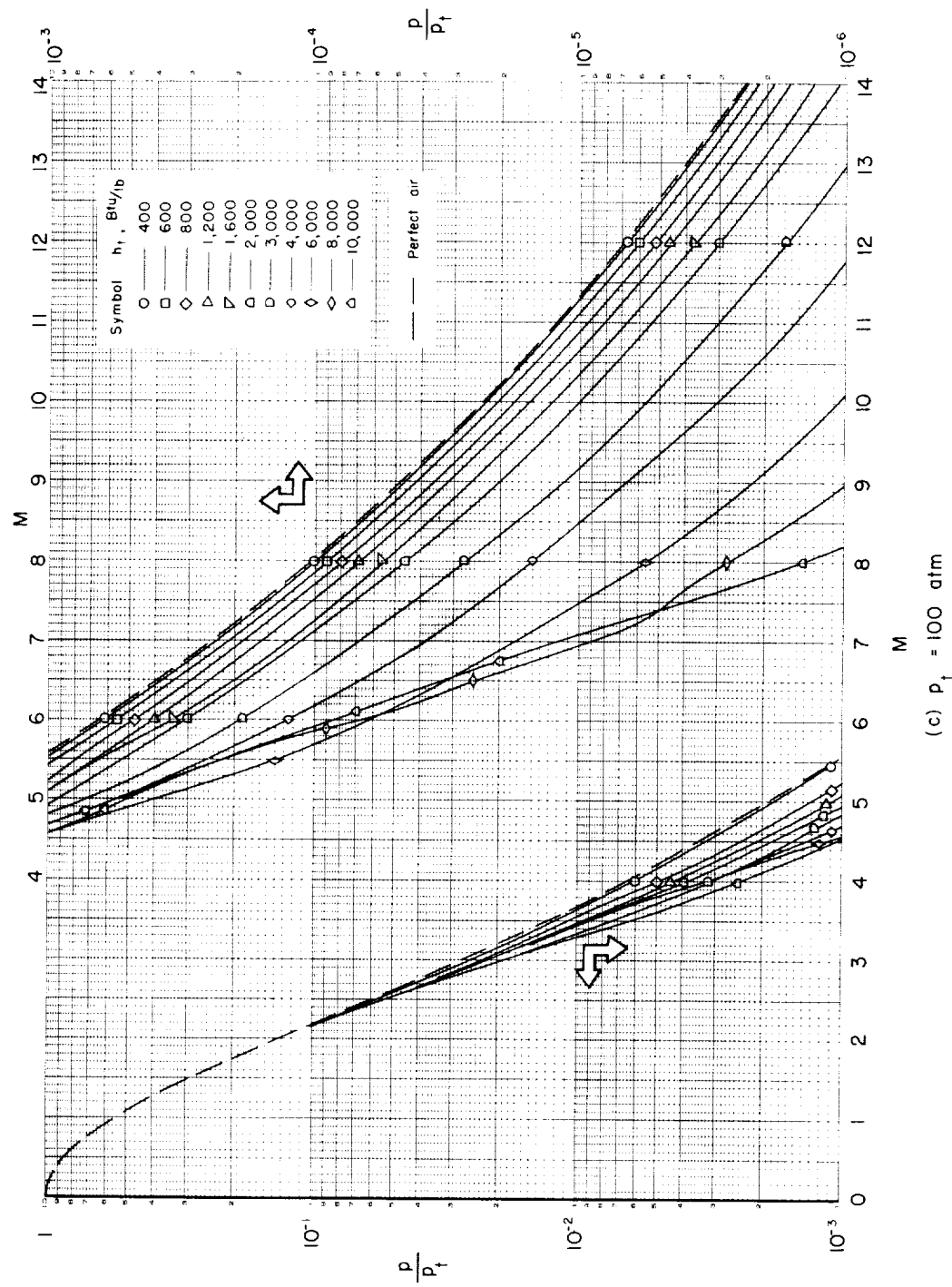
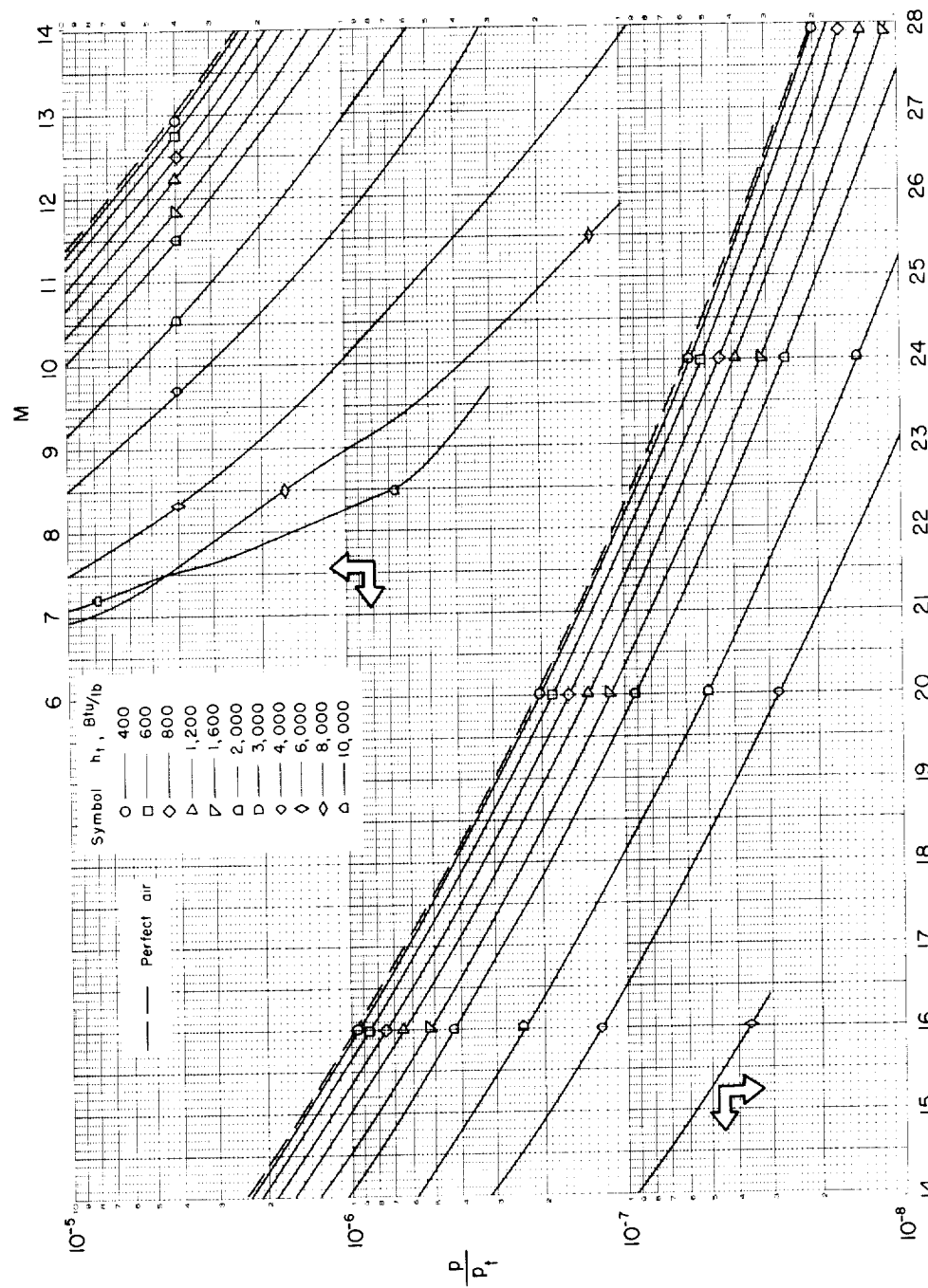
(c)  $P_t = 100$  atm

Chart 3.- Continued.



(c)  $p_1 = 100 \text{ atm} - \text{Concluded.}$

Chart 3.- Continued.

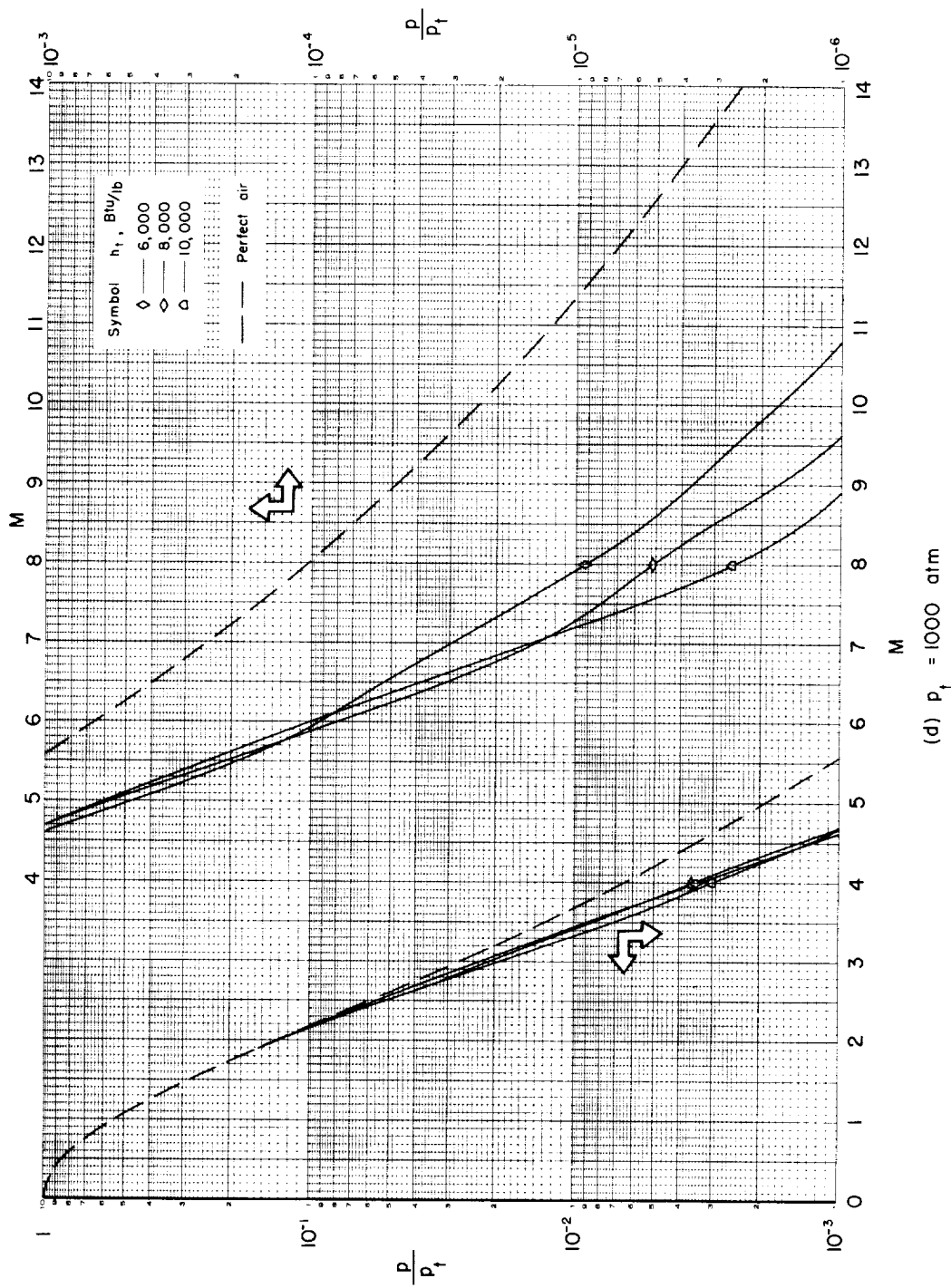
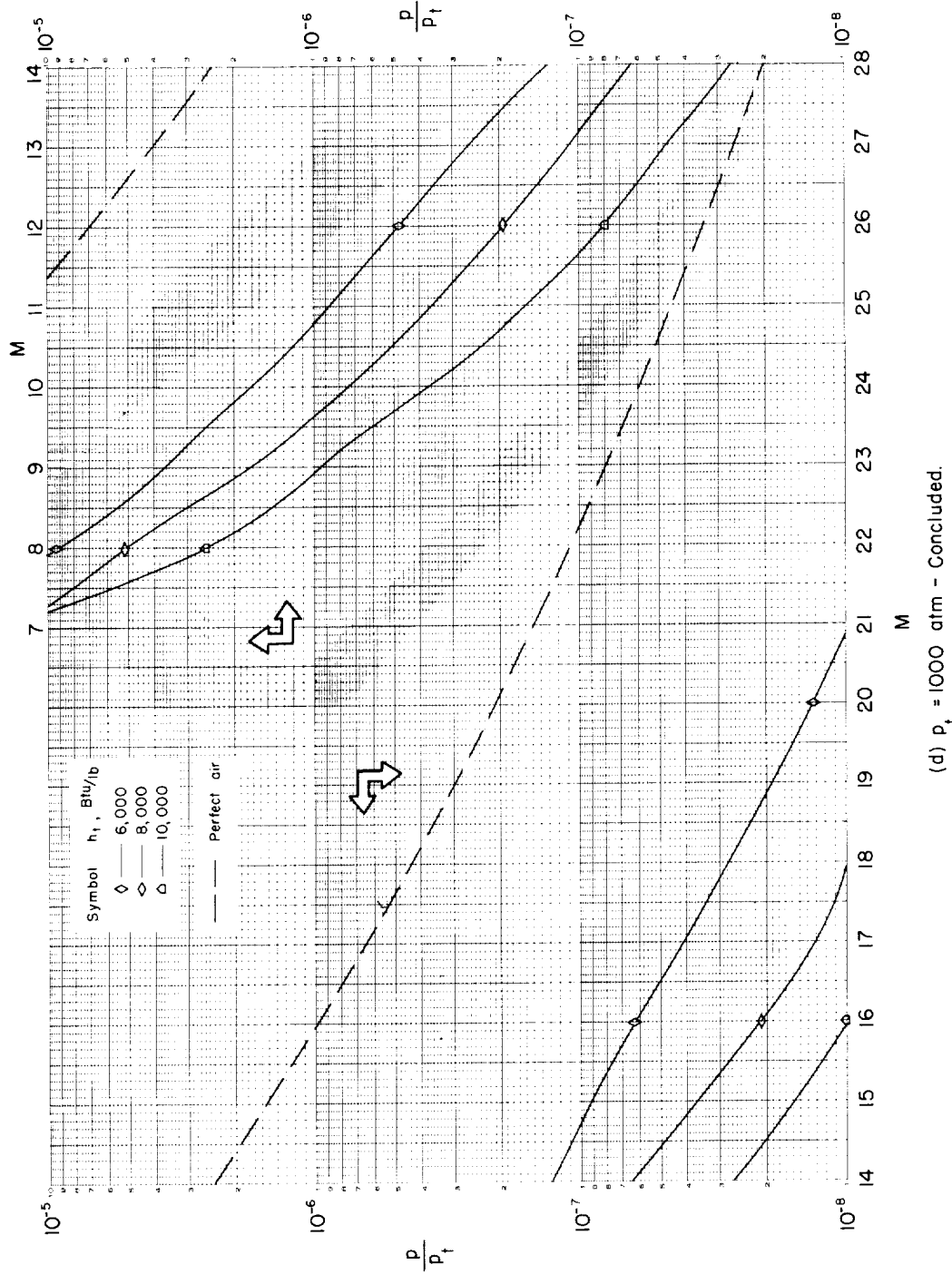


Chart 3-- Continued.



(d)  $P_t = 1000 \text{ atm} - \text{Concluded.}$

Chart 30 - Concluded.

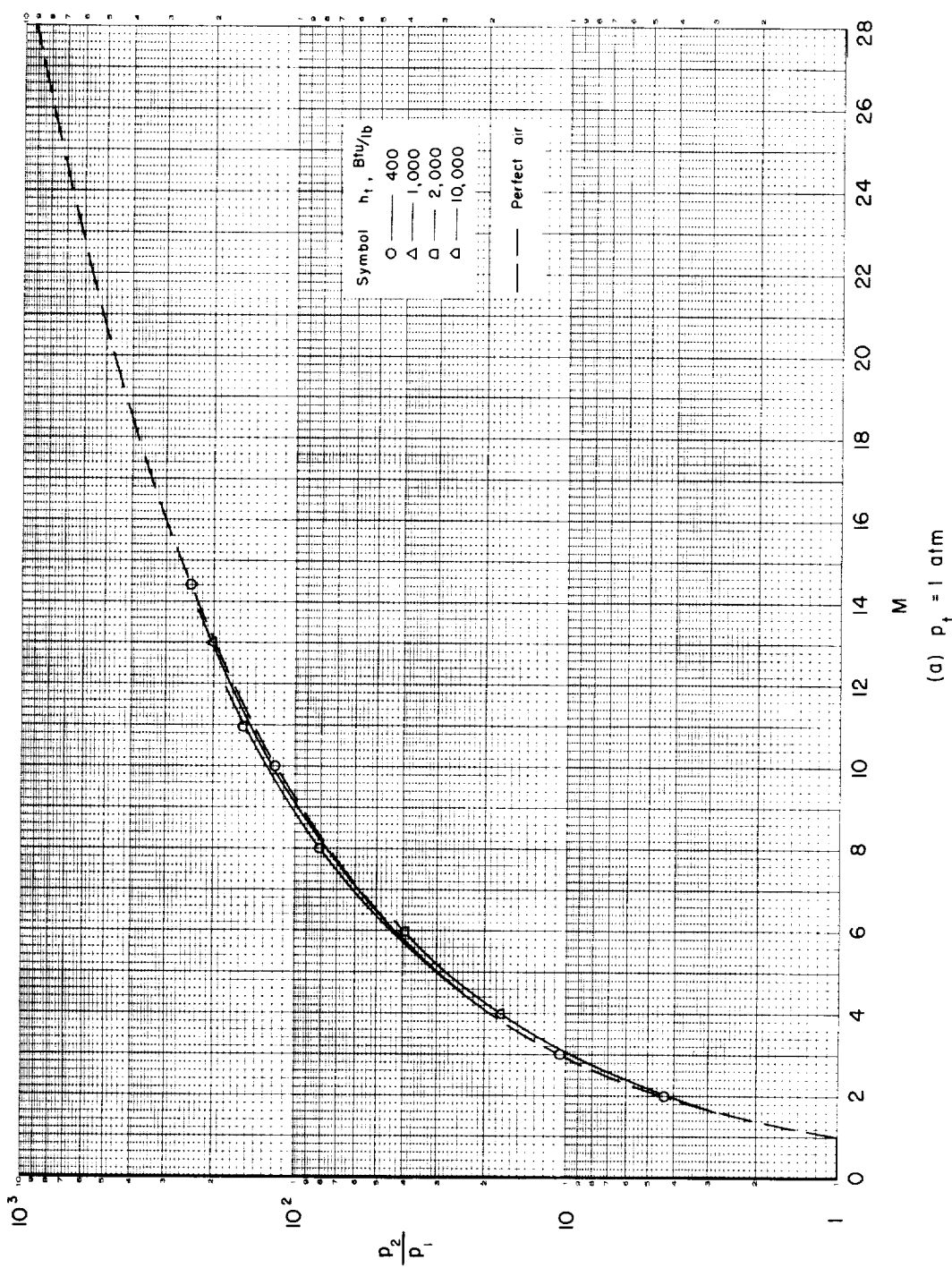


Chart 4.- Variation of pressure ratio across a normal shock wave with Mach number.

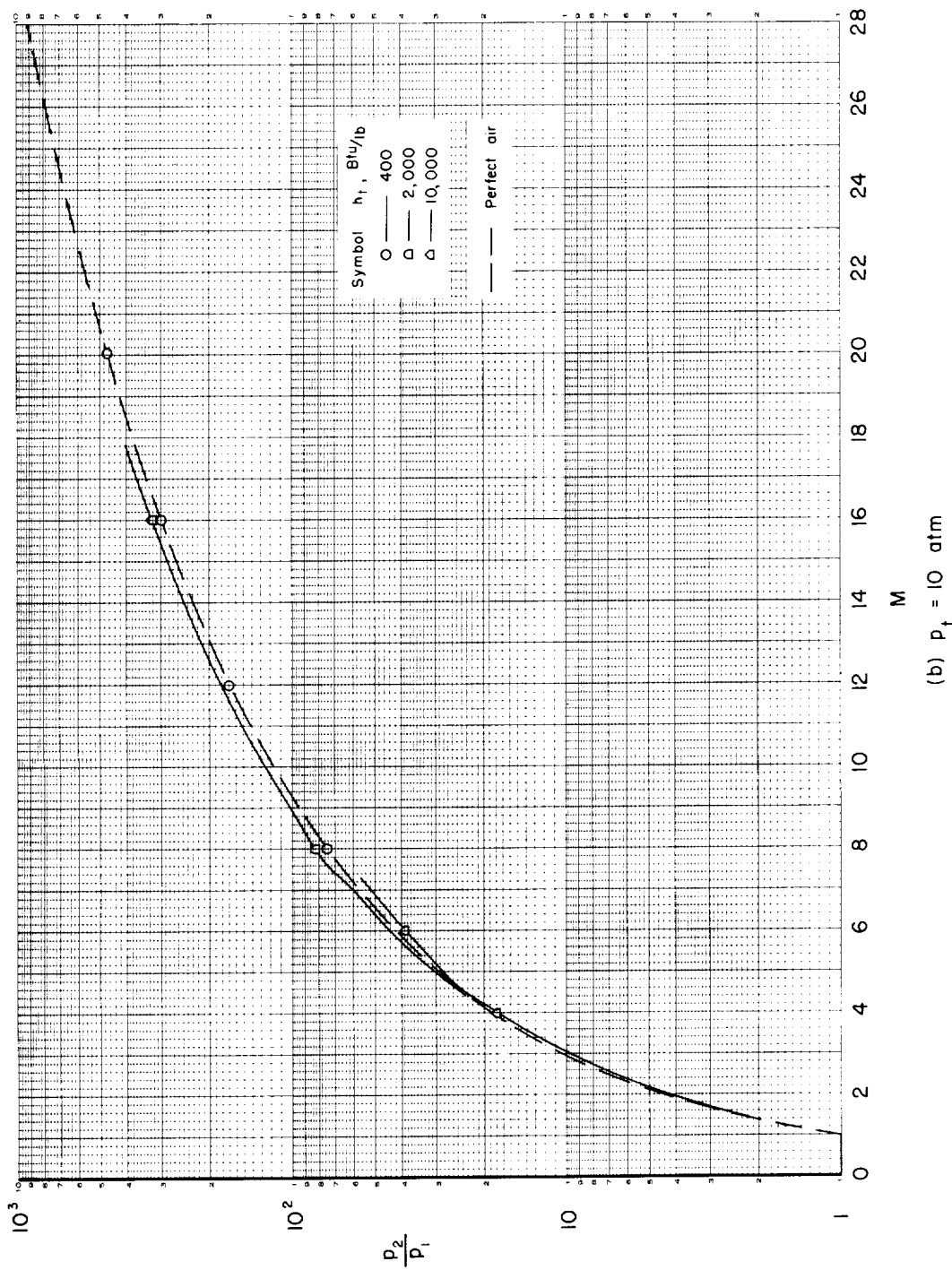
(b)  $P_t = 10 \text{ atm}$ 

Chart 4.- Continued.

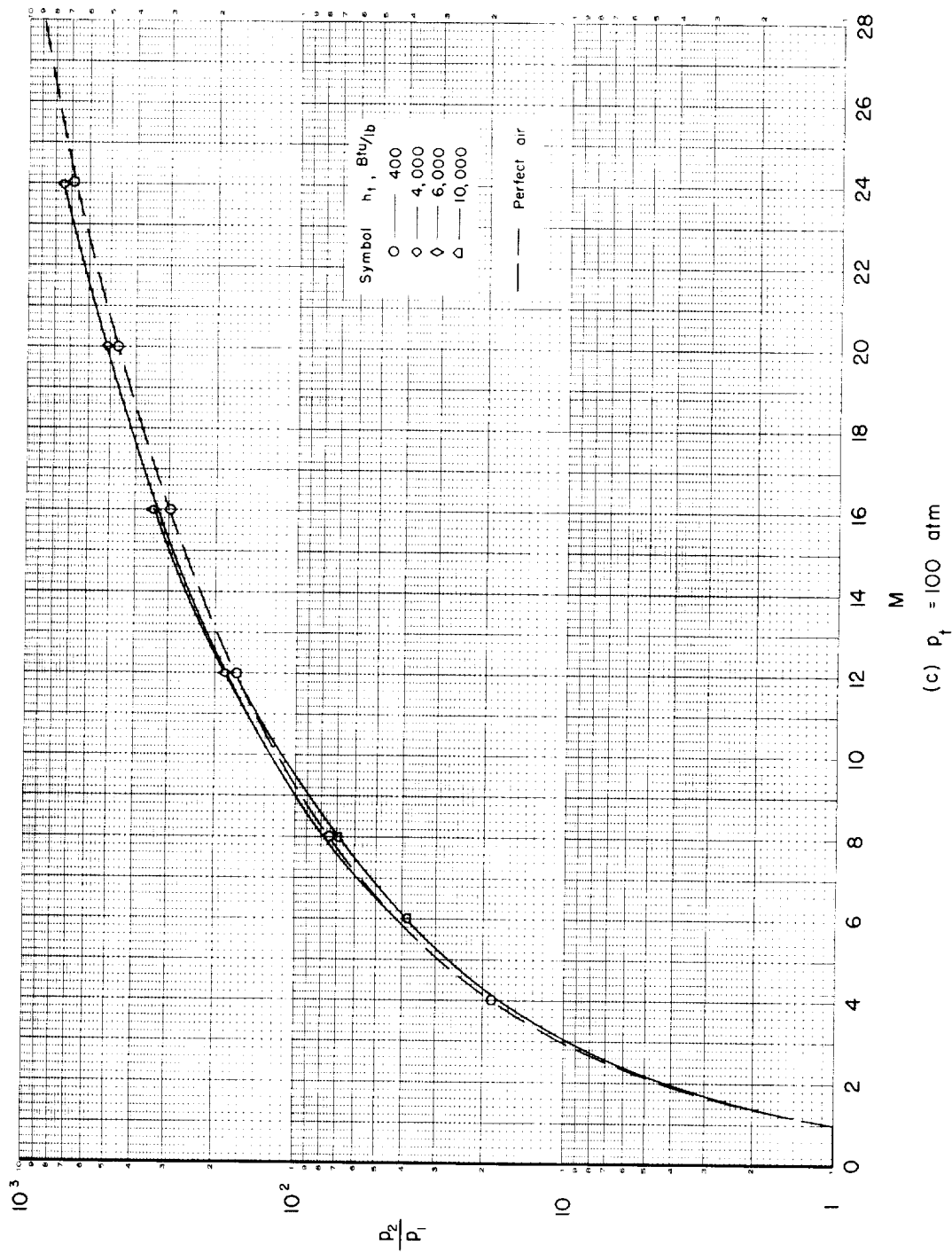
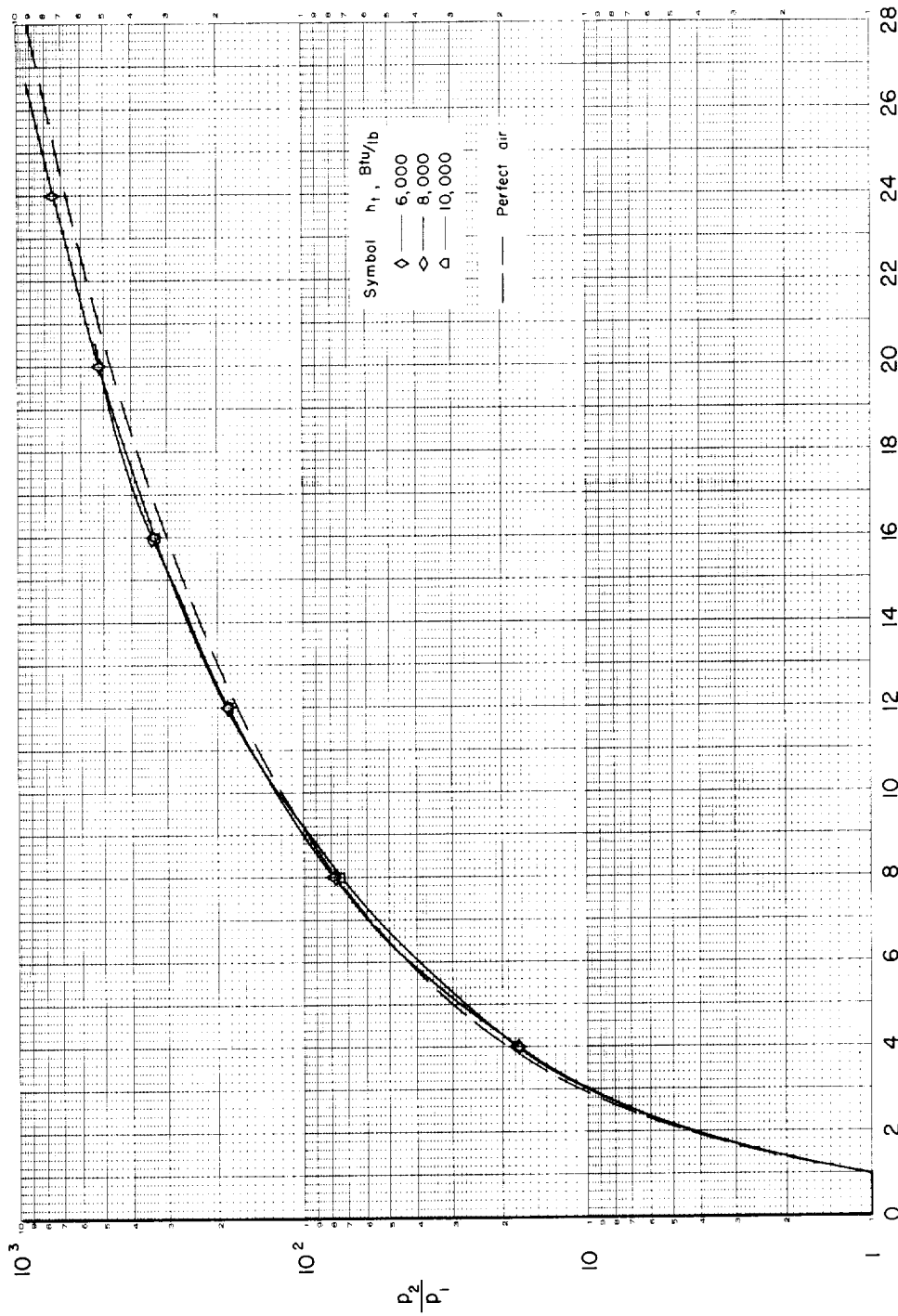


Chart 4.- Continued.  
(c)  $P_1 = 100 \text{ atm}$



(d)  $p_f = 1000$  atm

Chart 4.- Concluded.

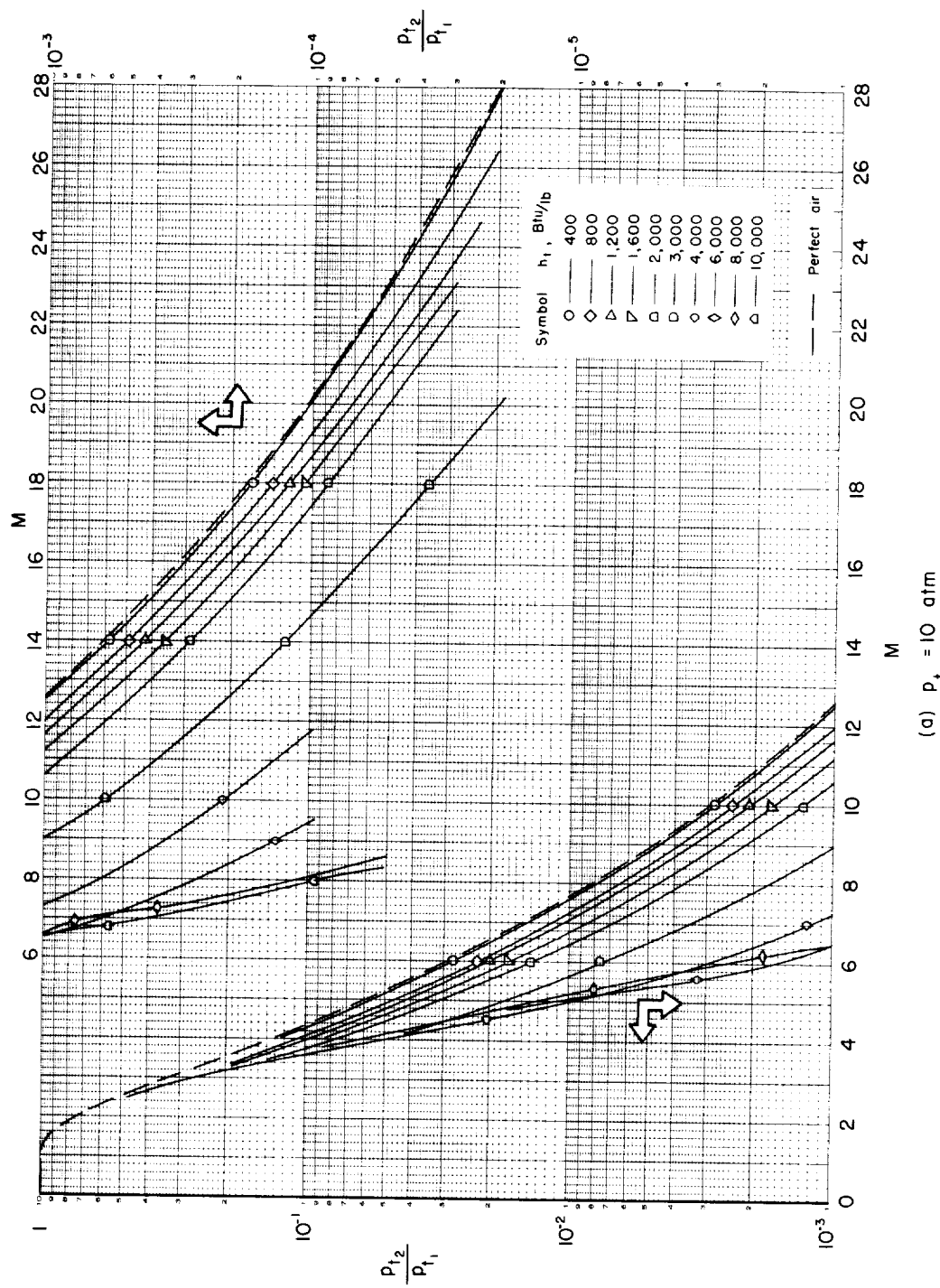


Chart 5.- Variation of total pressure ratio across a normal shock wave with Mach number.

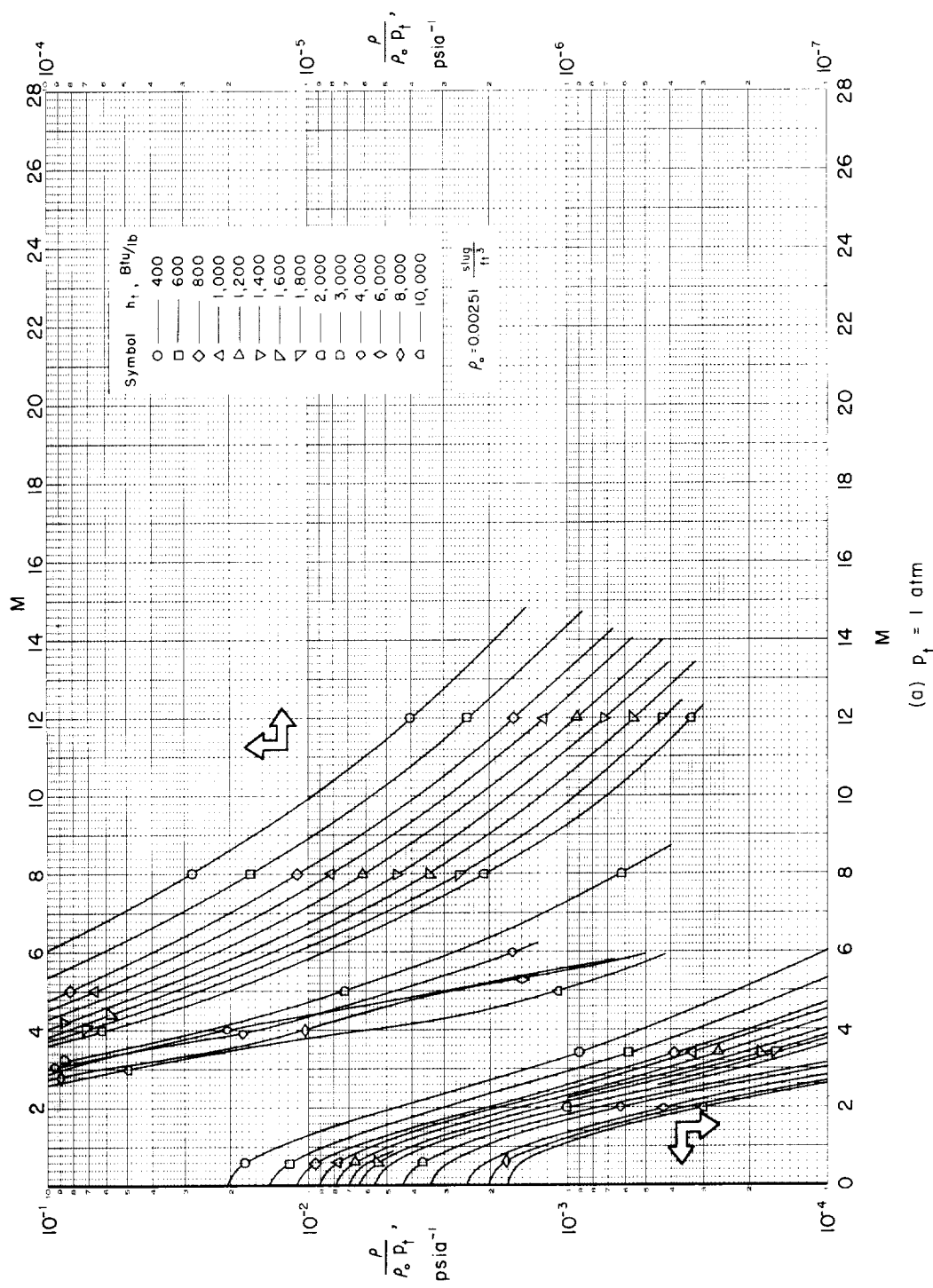
(a)  $P_t = 1 \text{ atm}$ 

Chart 6.- Variation of density parameter with Mach number;  
 $\rho_0 = 0.00251 \text{ slug}/\text{ft}^3$ .

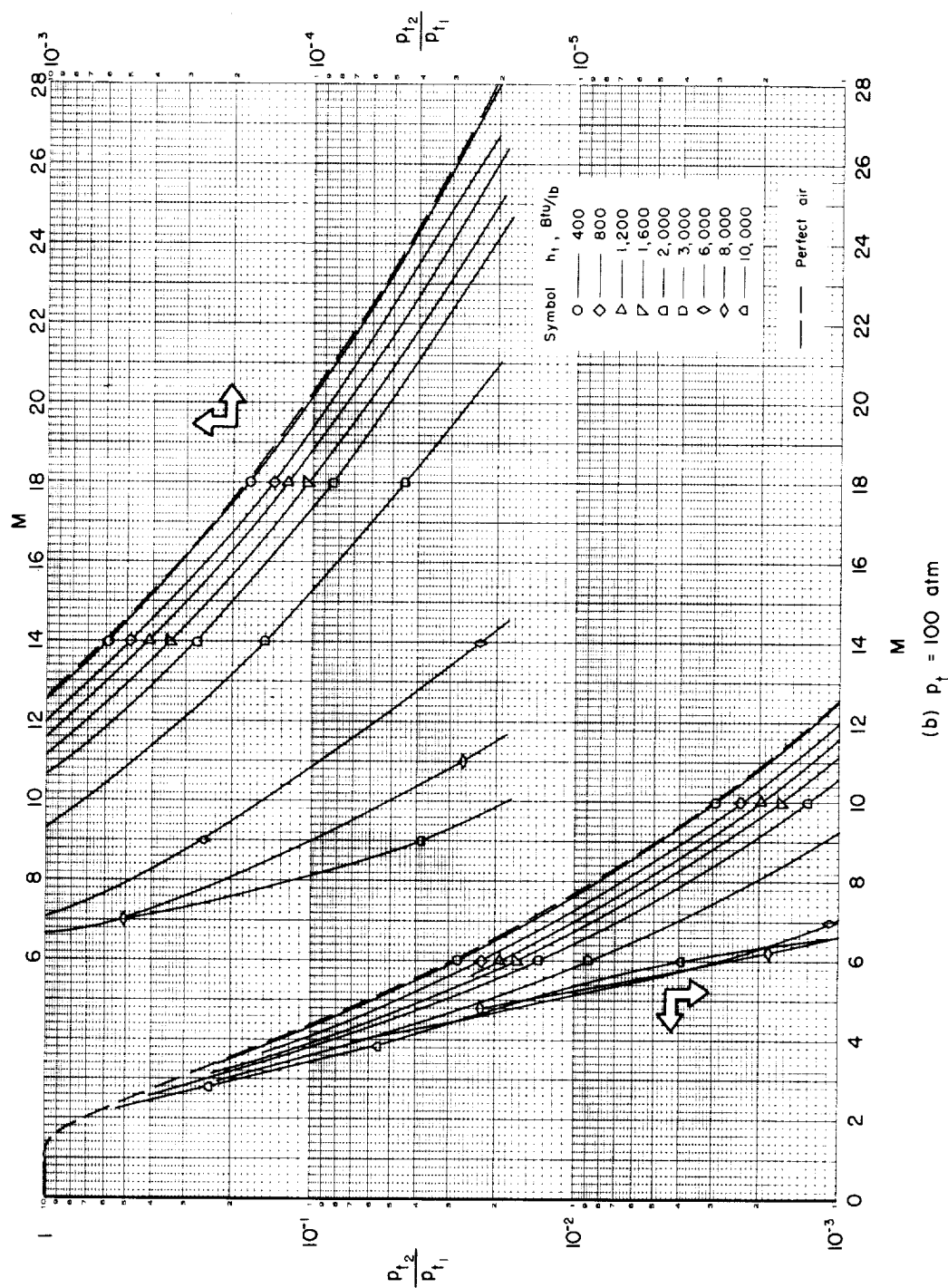
(b)  $p_t = 100$  atm

Chart 5.- Concluded.

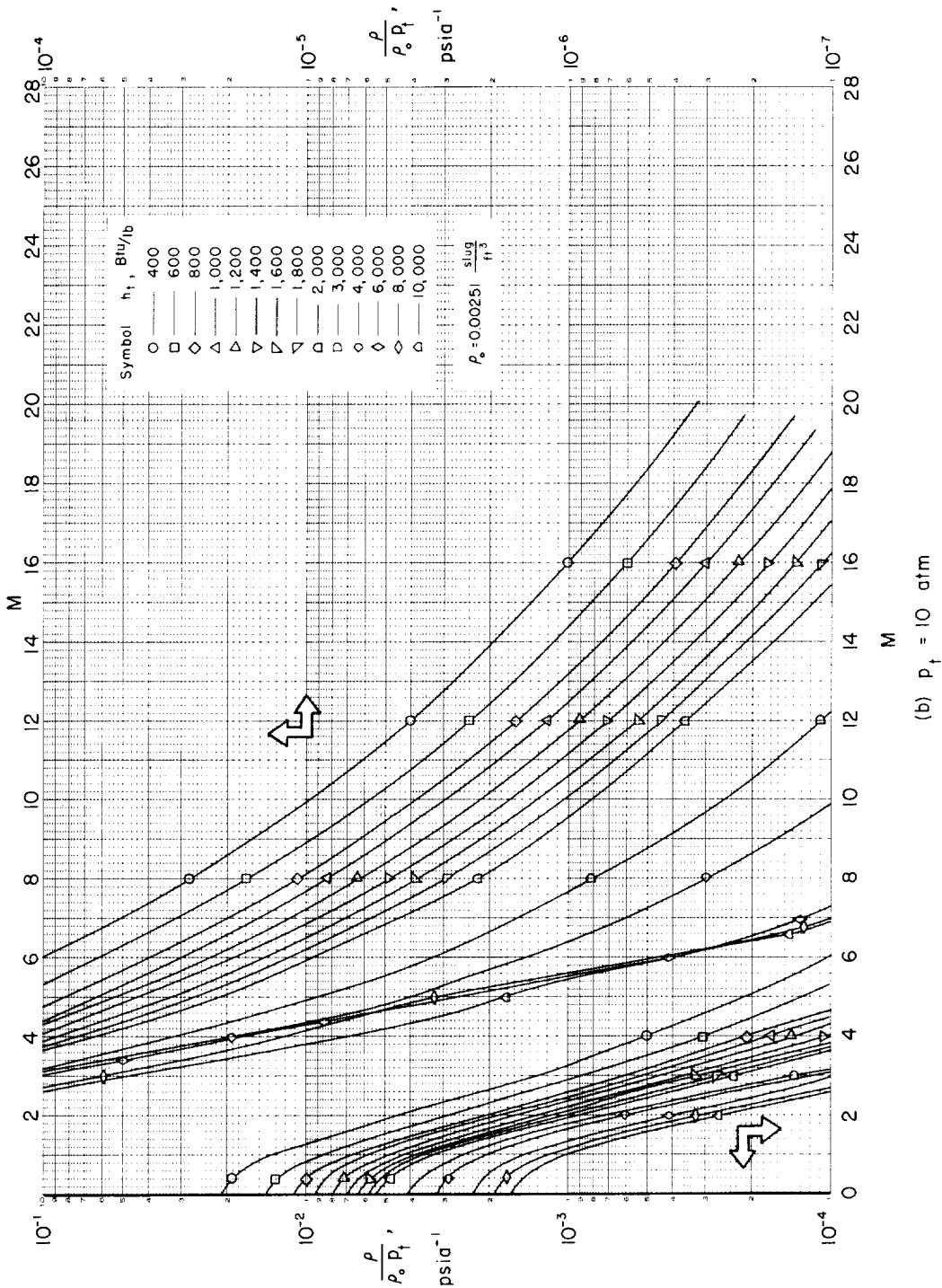
(b)  $P_f = 10 \text{ atm}$ 

Chart 6.- Continued.

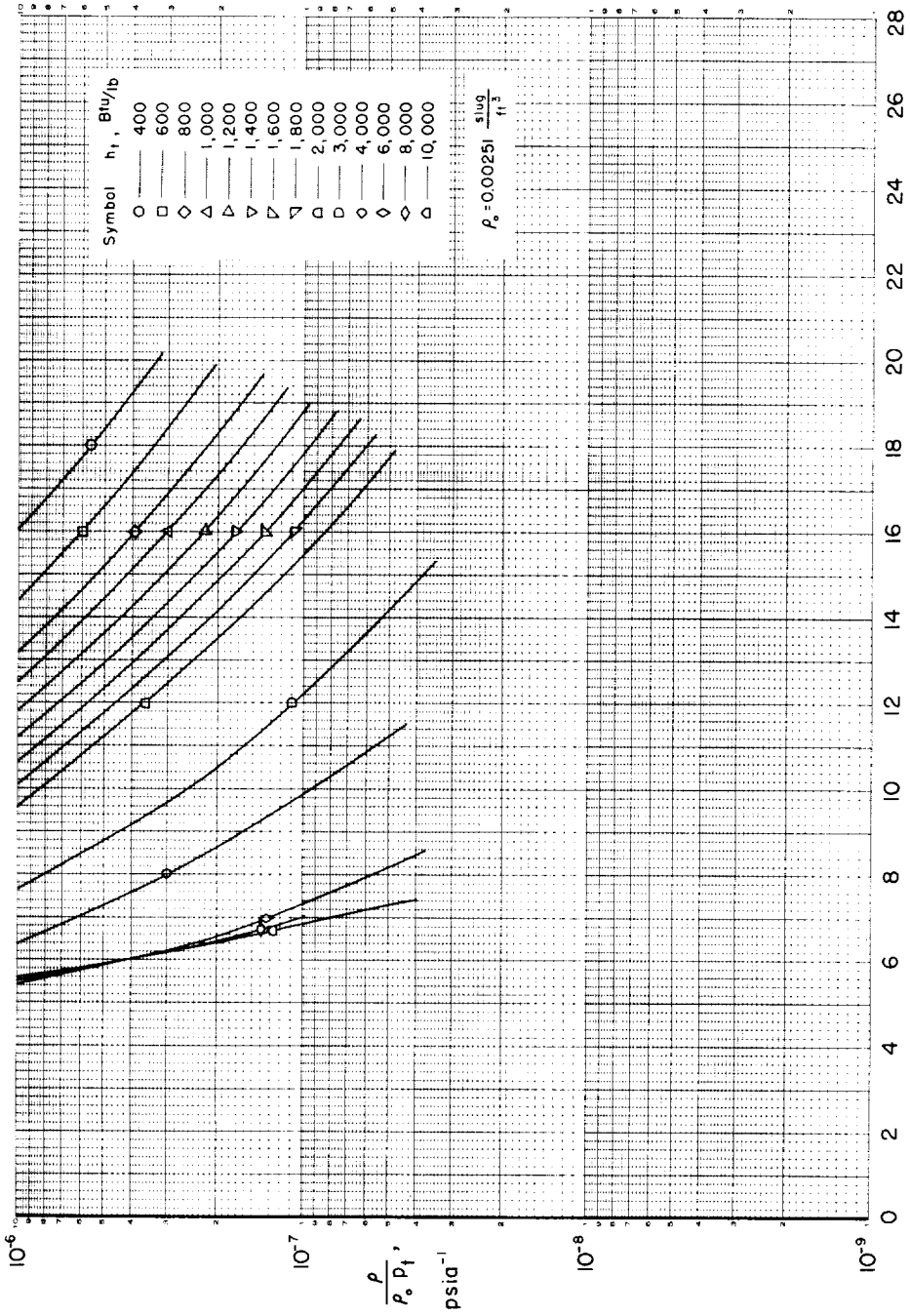
(b)  $p_f = 10$  atm - Concluded.

Chart 6.- Continued.

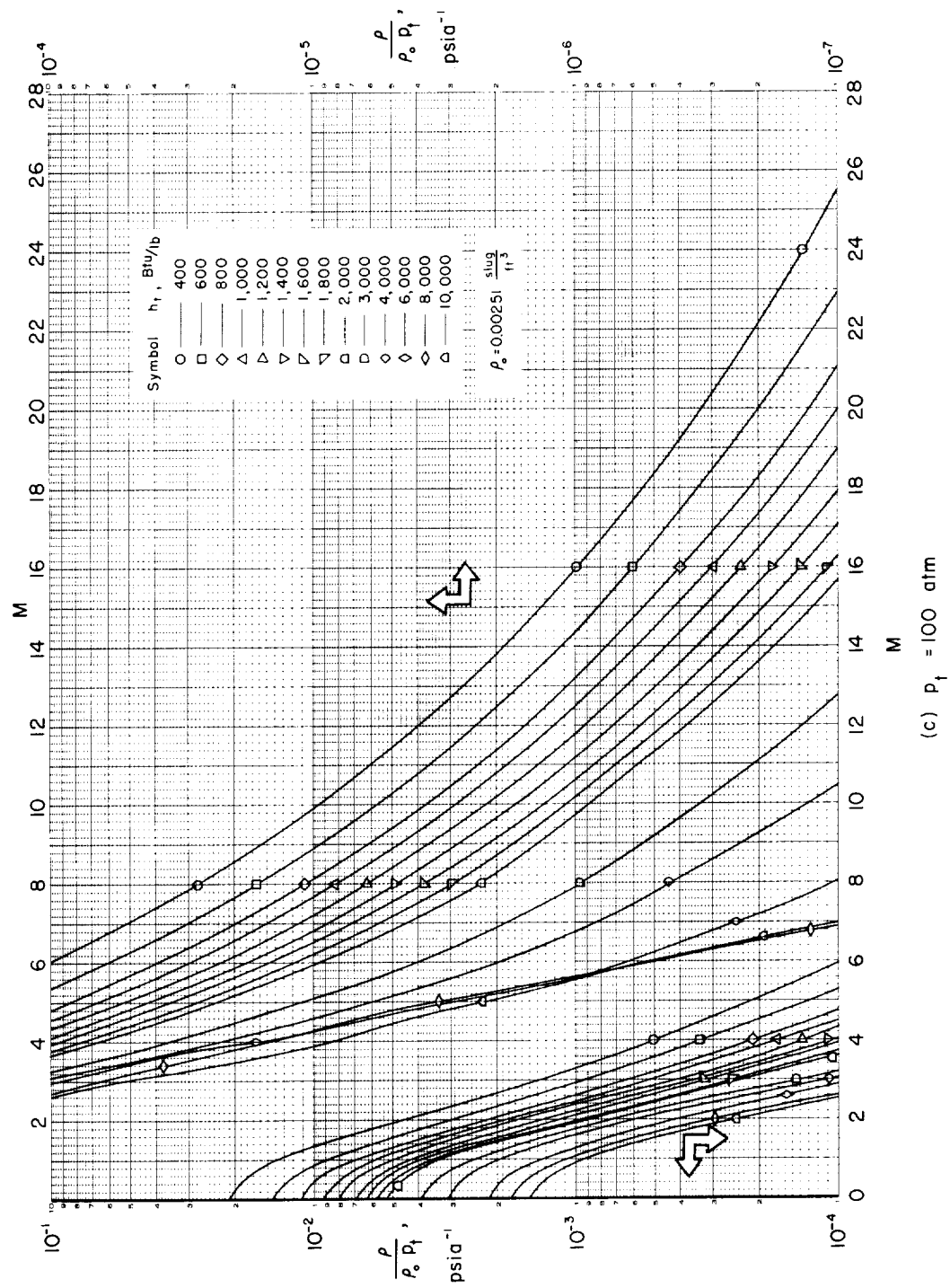


Chart 6.- Continued.

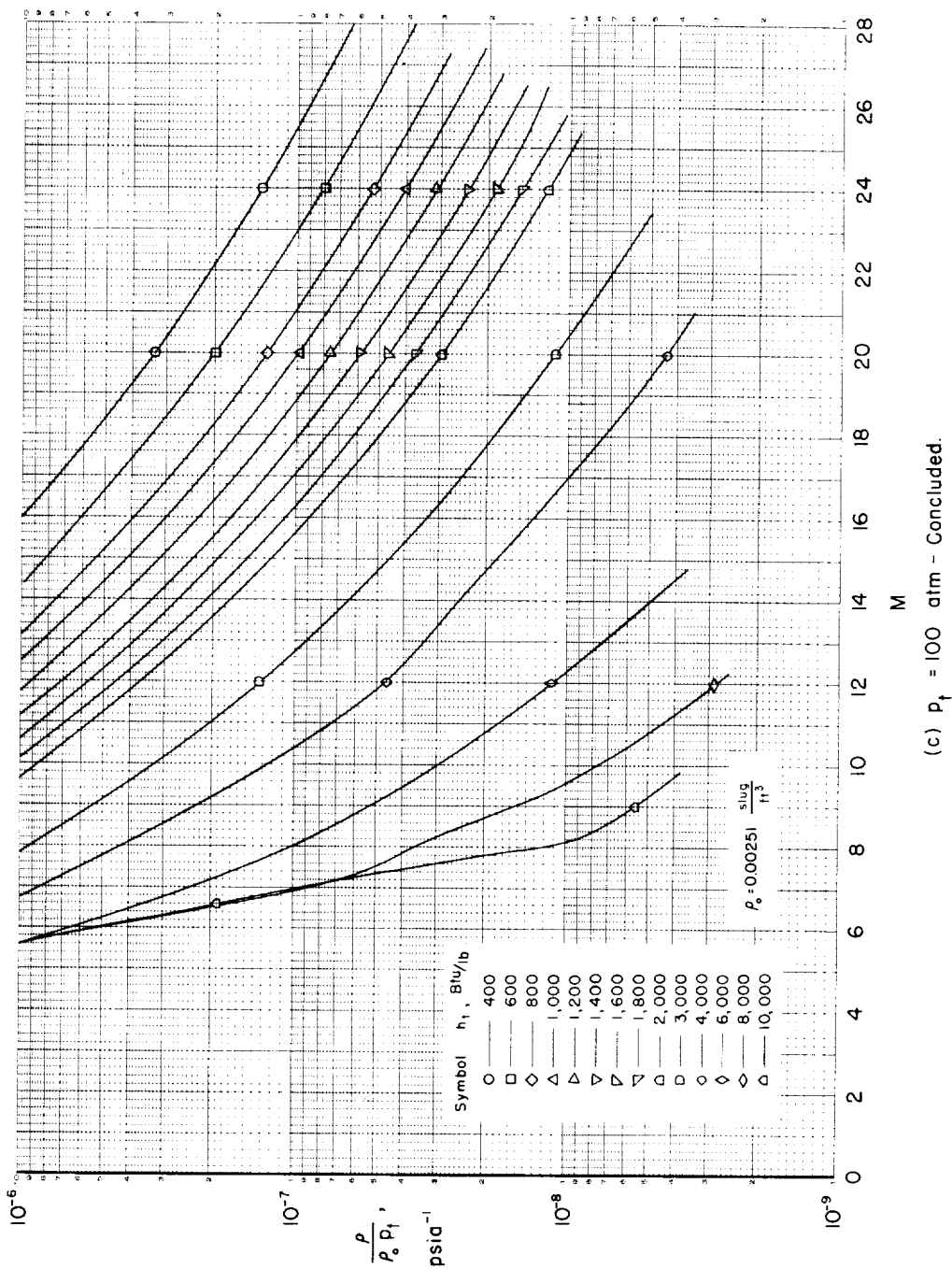


Chart 5.- Continued.

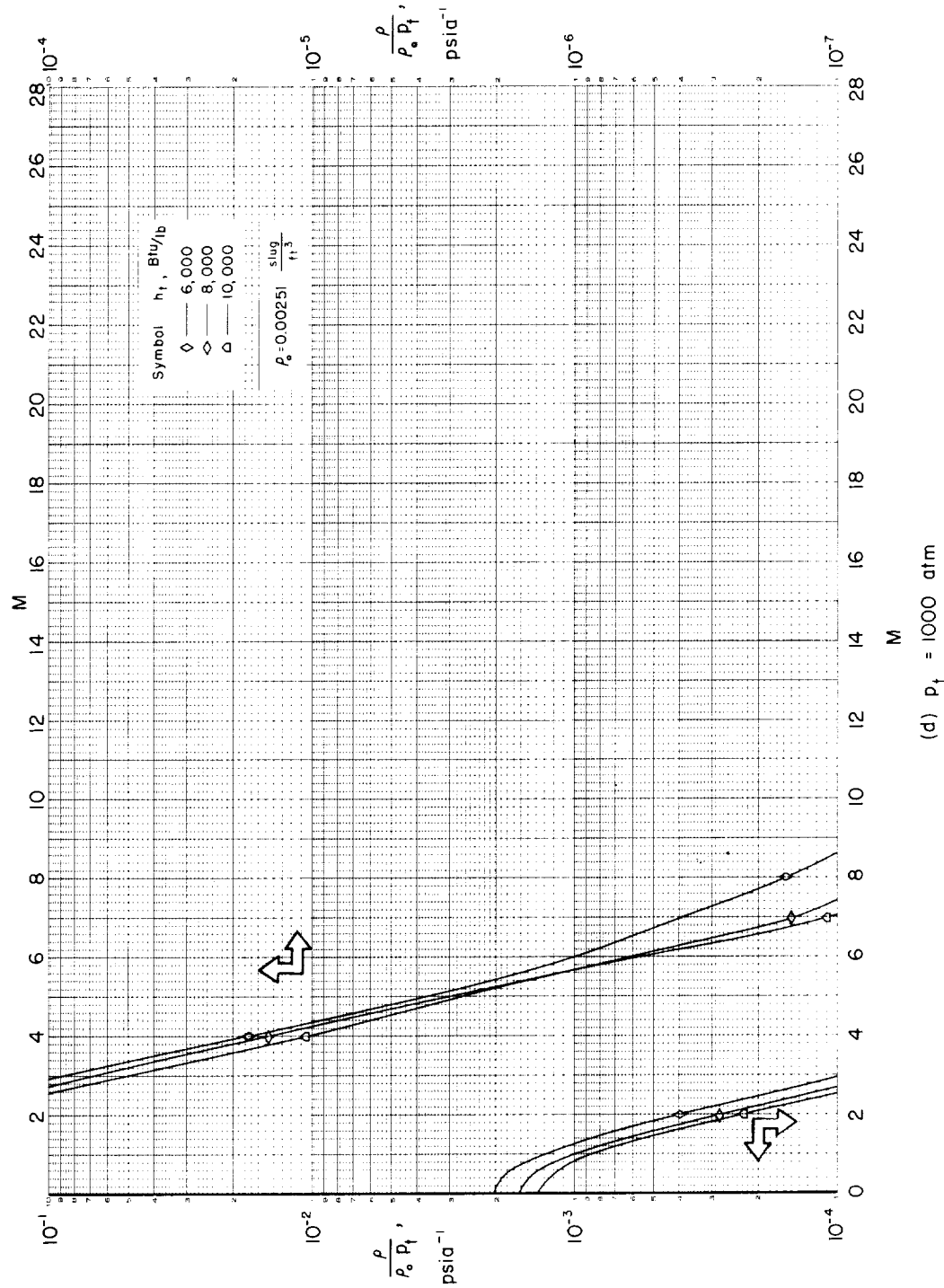
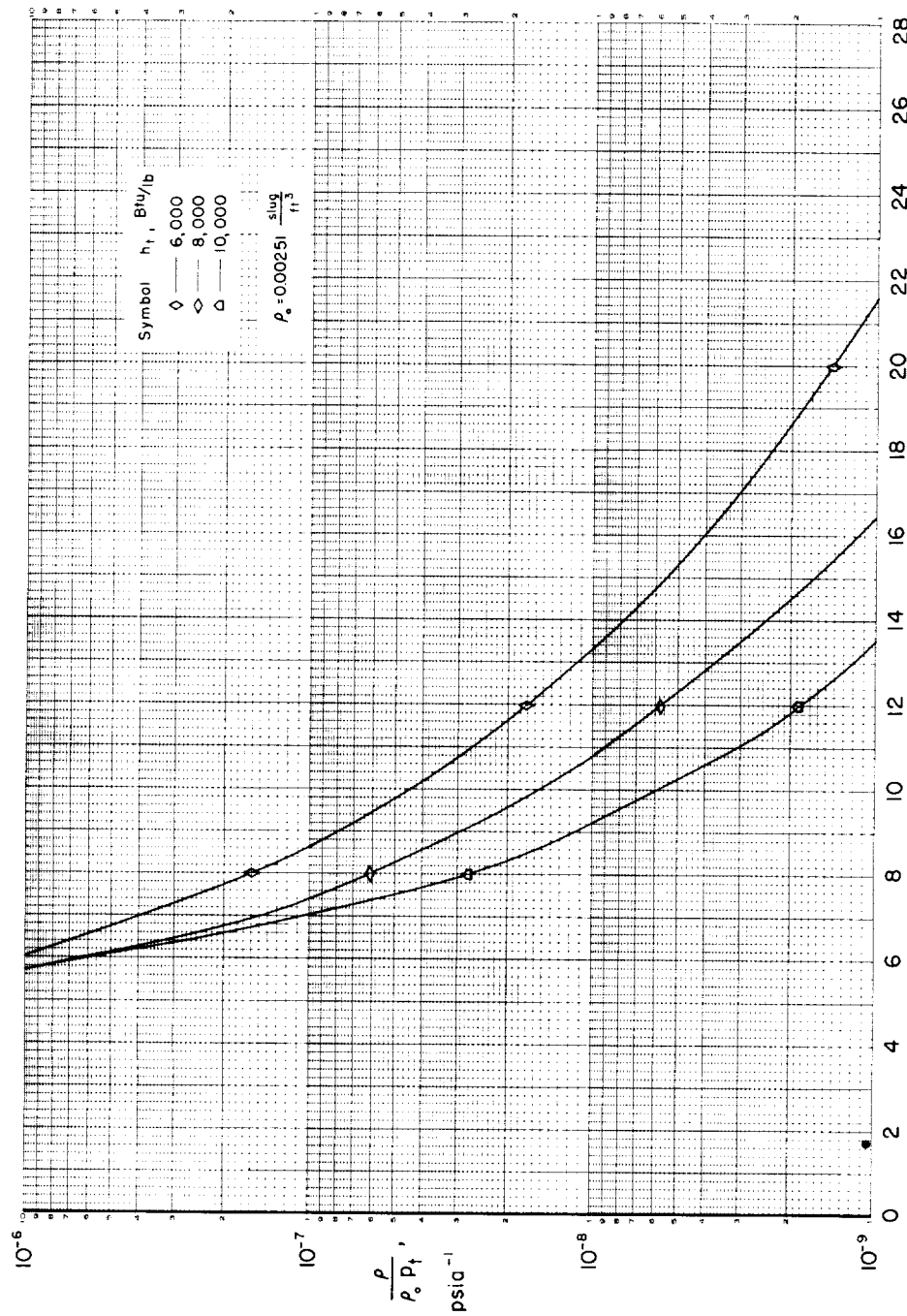


Chart 6.—Continued.



(d)  $P_t = 1000$  atm - Concluded.

Chart 6.- Concluded.

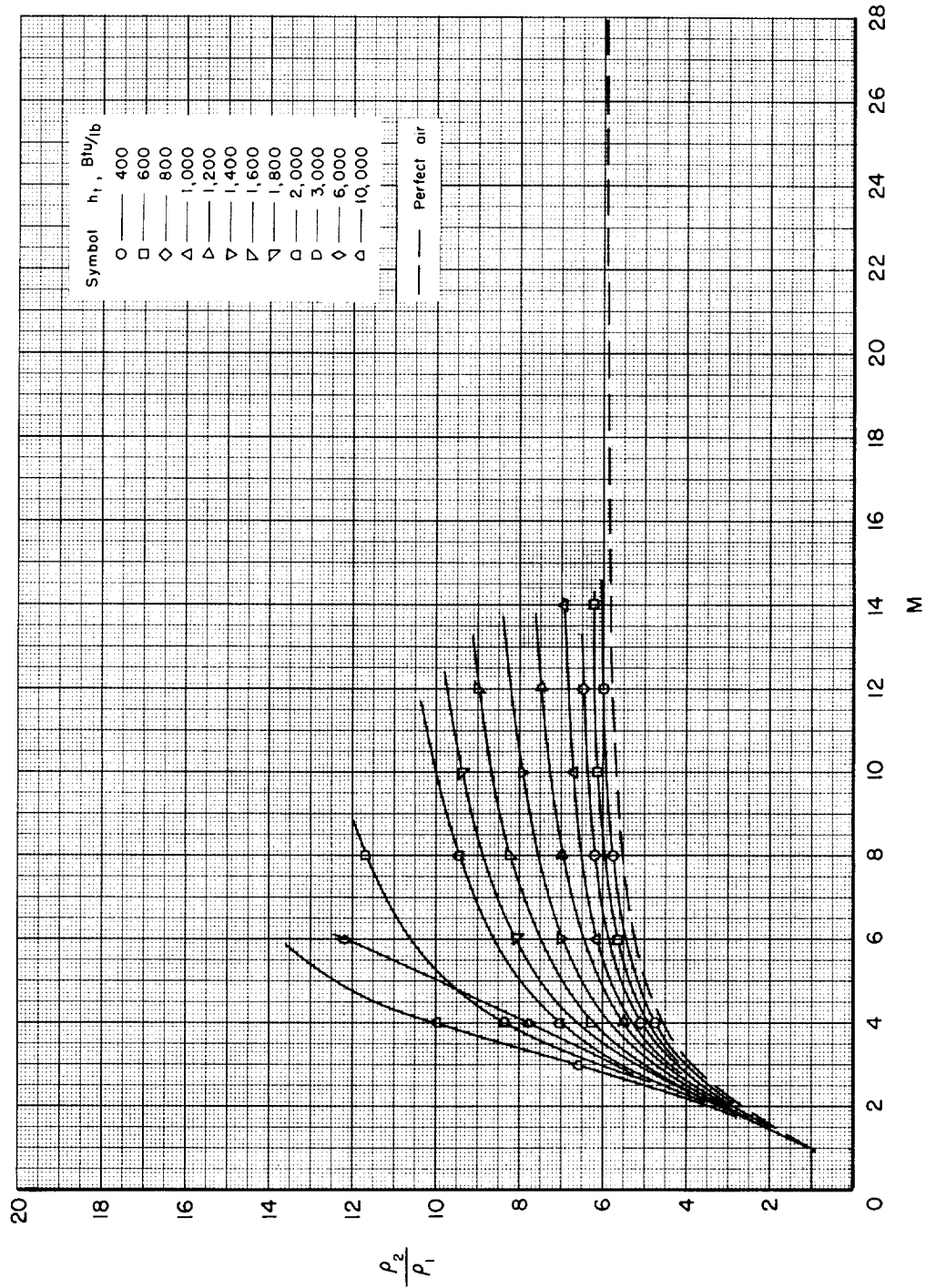


Chart 7•- Variation of density ratio across a normal shock with Mach number.  
(a)  $p_1 = 1 \text{ atm}$

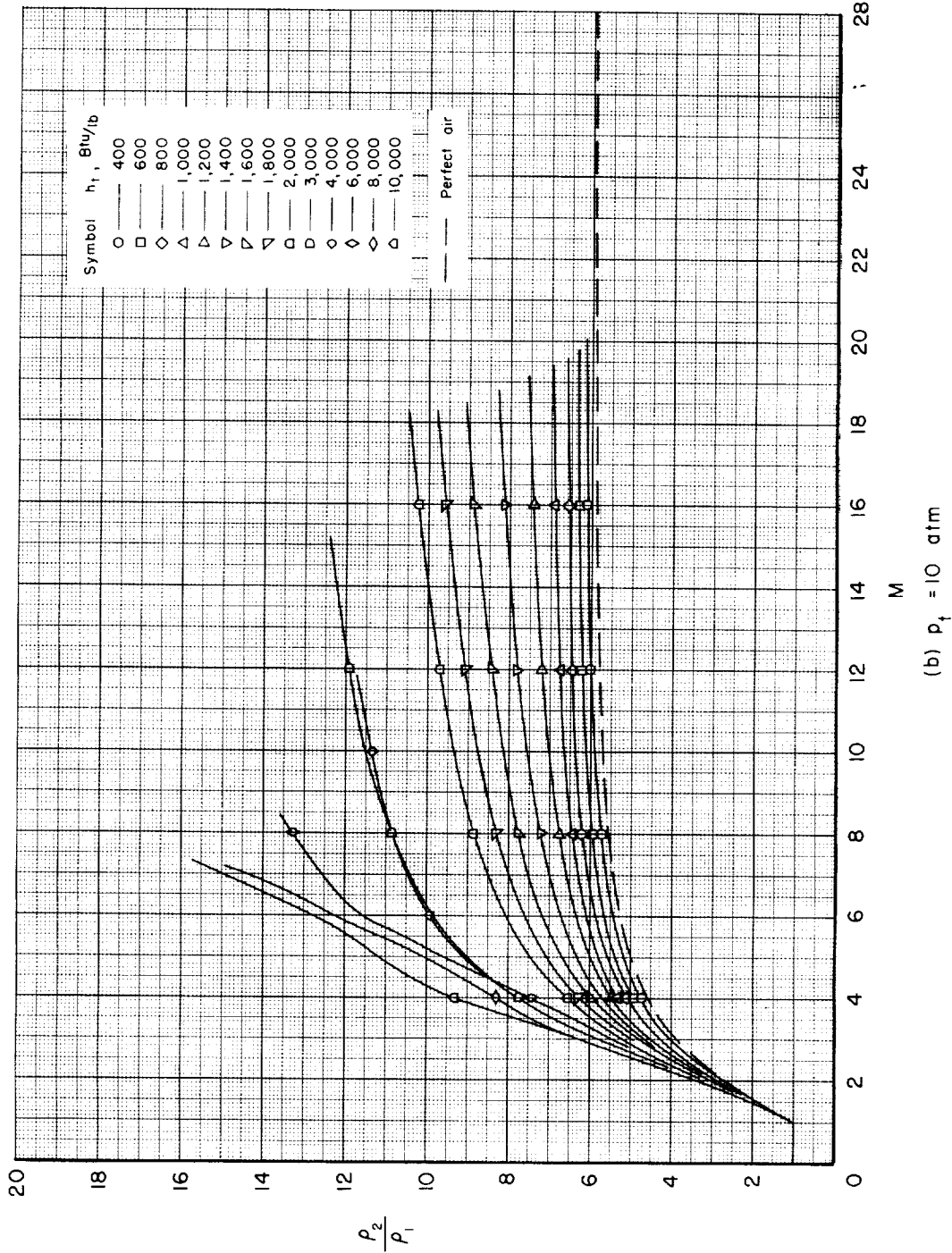
(b)  $p_1 = 10 \text{ atm}$ 

Chart 7.- Continued.

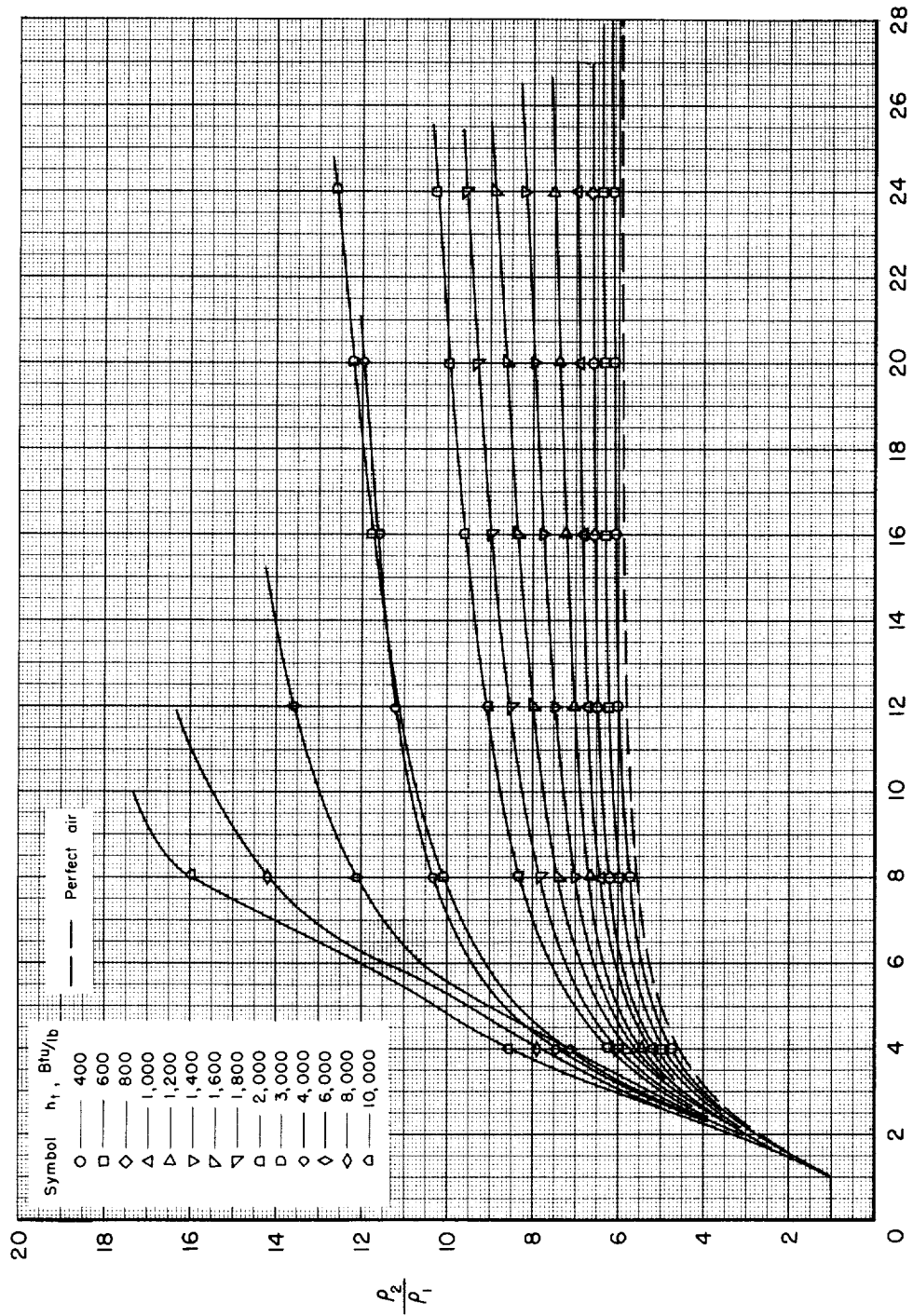
(c)  $P_t = 100$  atm

Chart 7.- Continued.

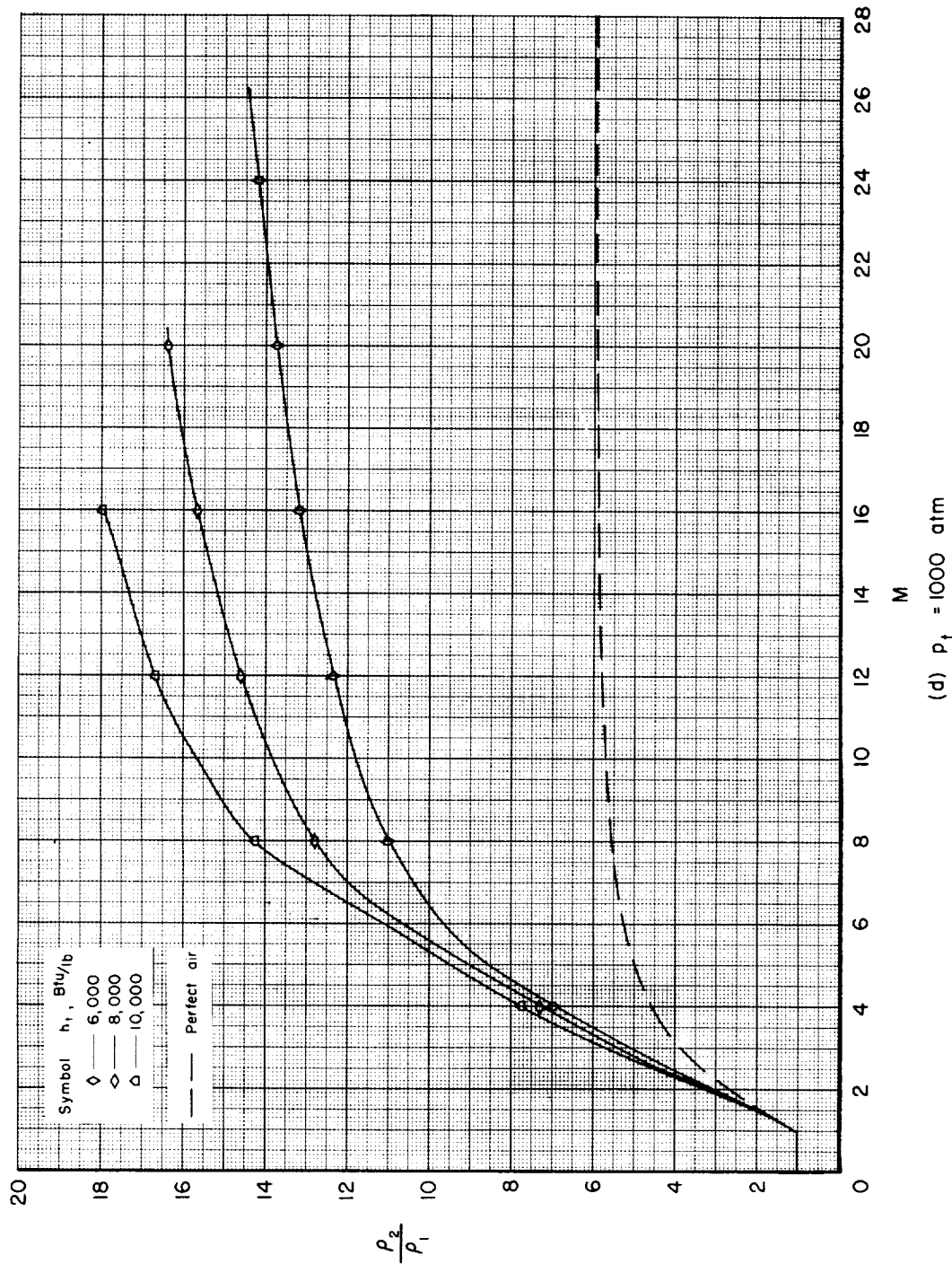


Chart 7.- Concluded.  
(d)  $p_1 = 1000 \text{ atm}$

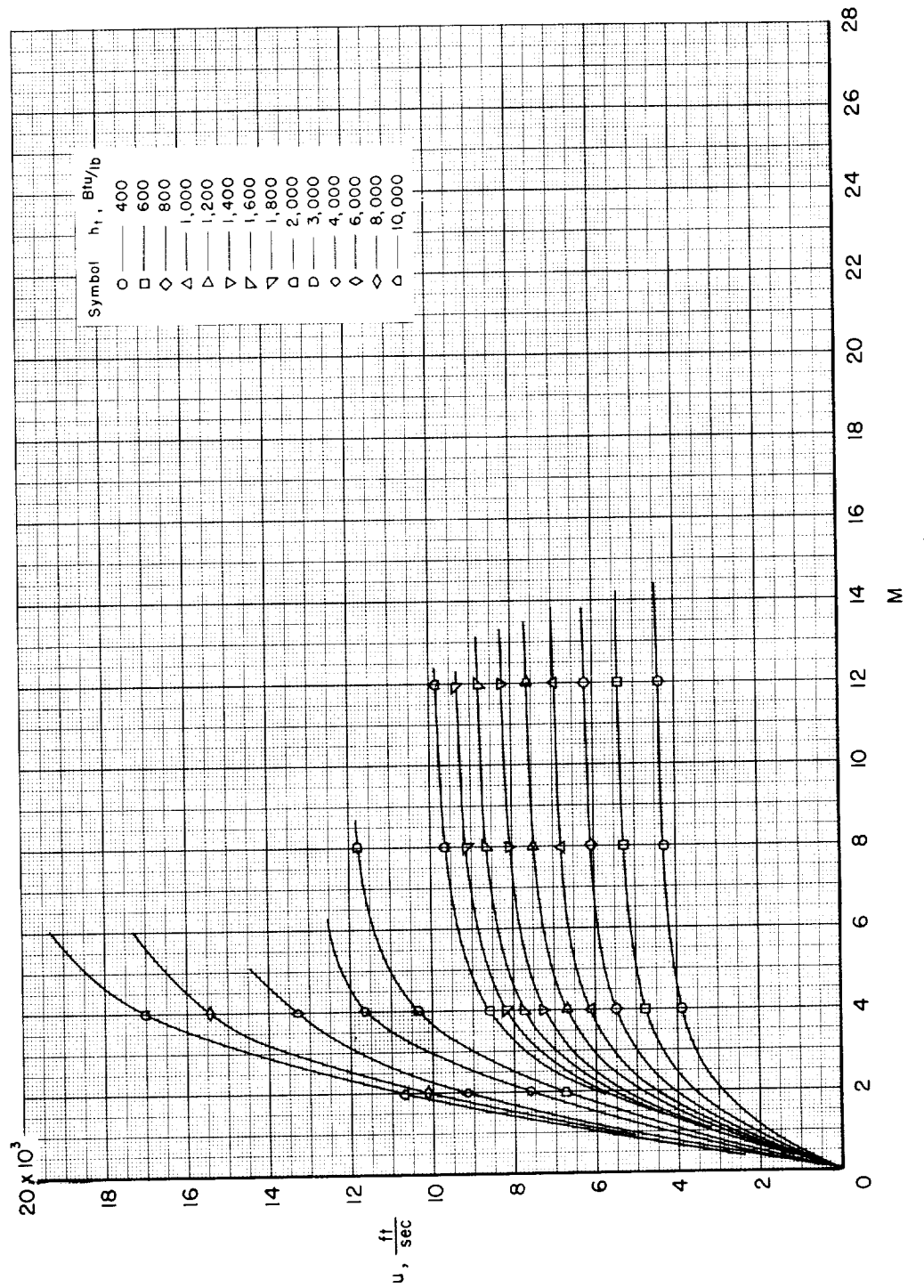


Chart 8.- Variation of velocity with Mach number.

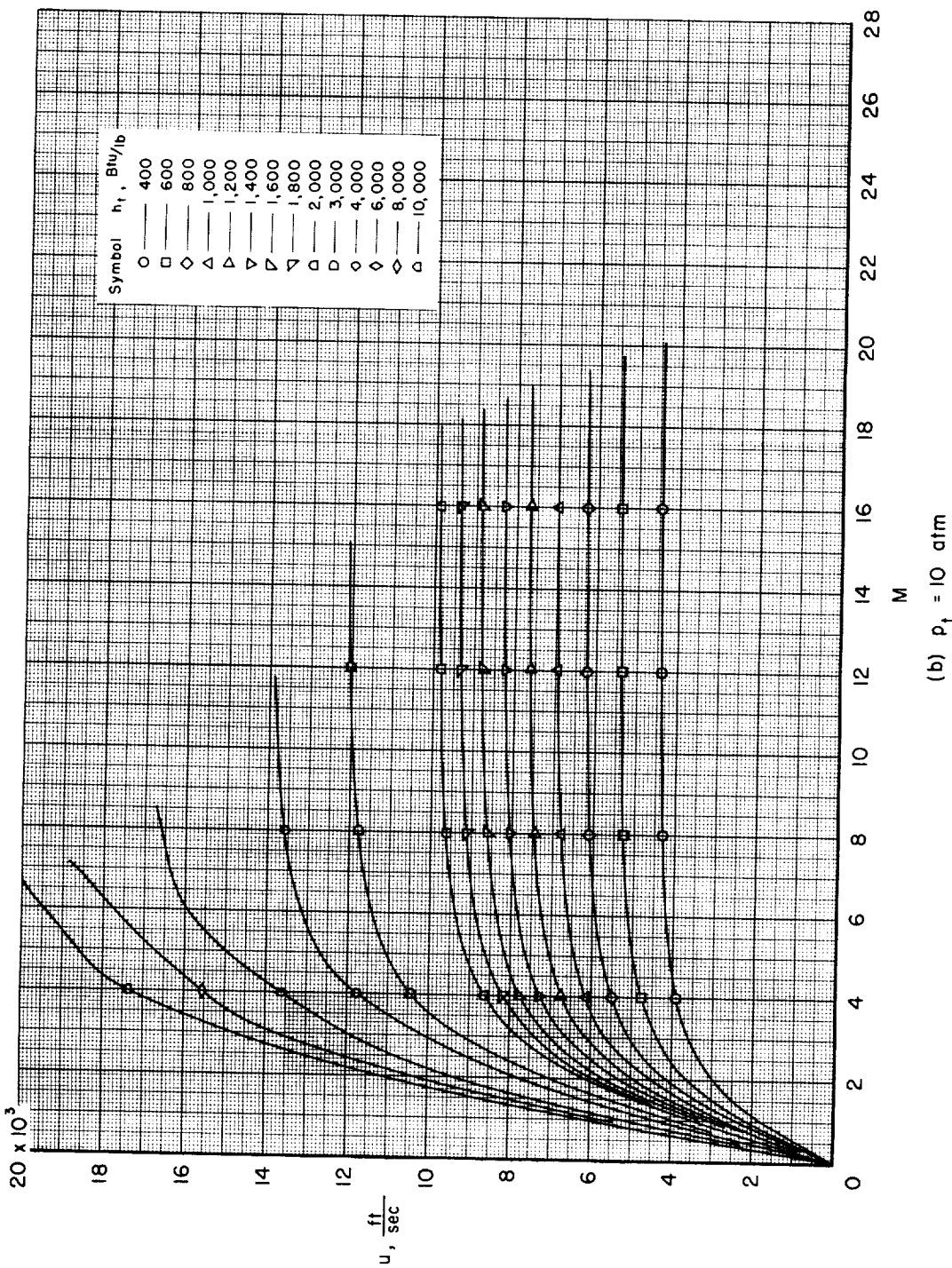
(b)  $p_f = 10$  atm

Chart 8.- Continued.

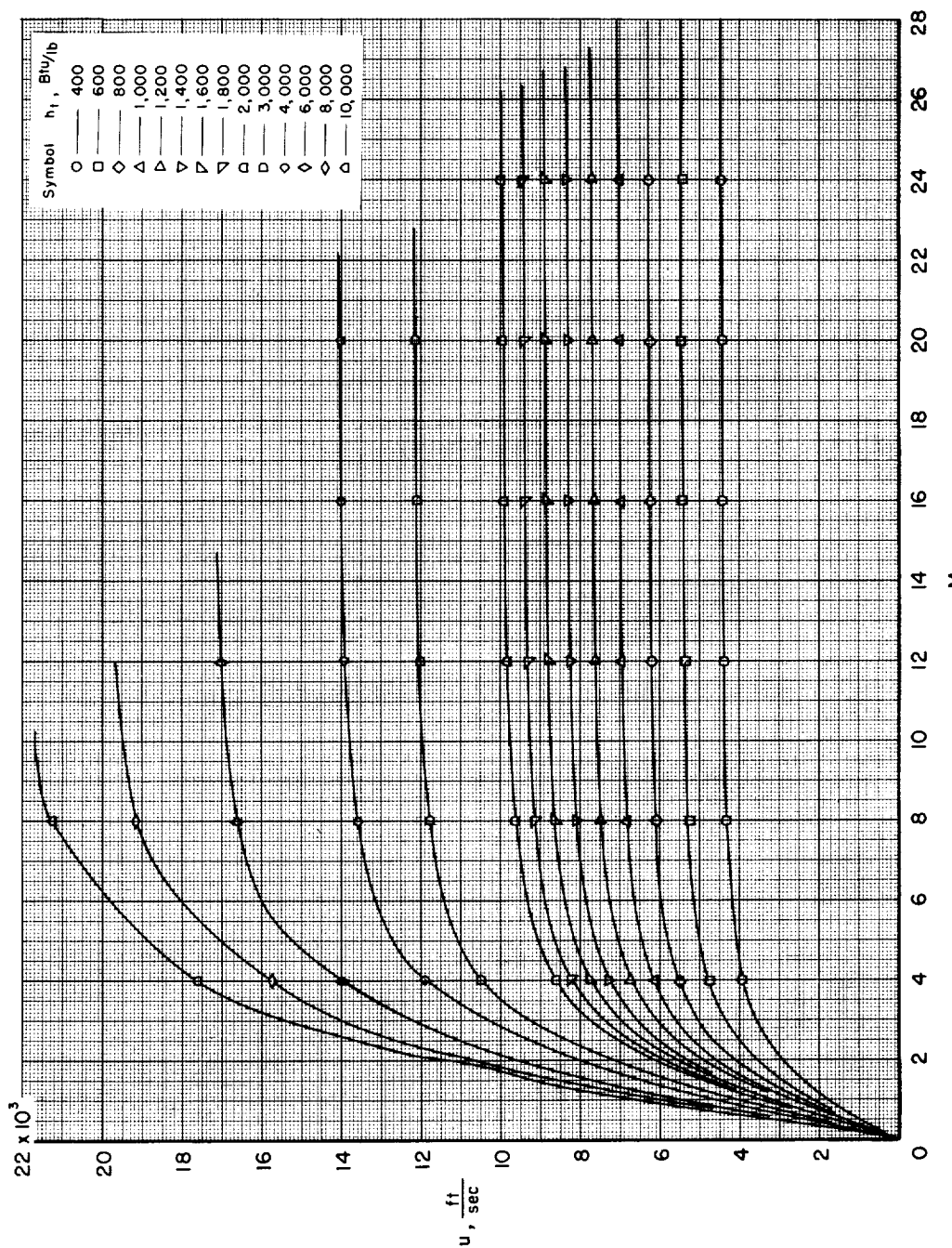
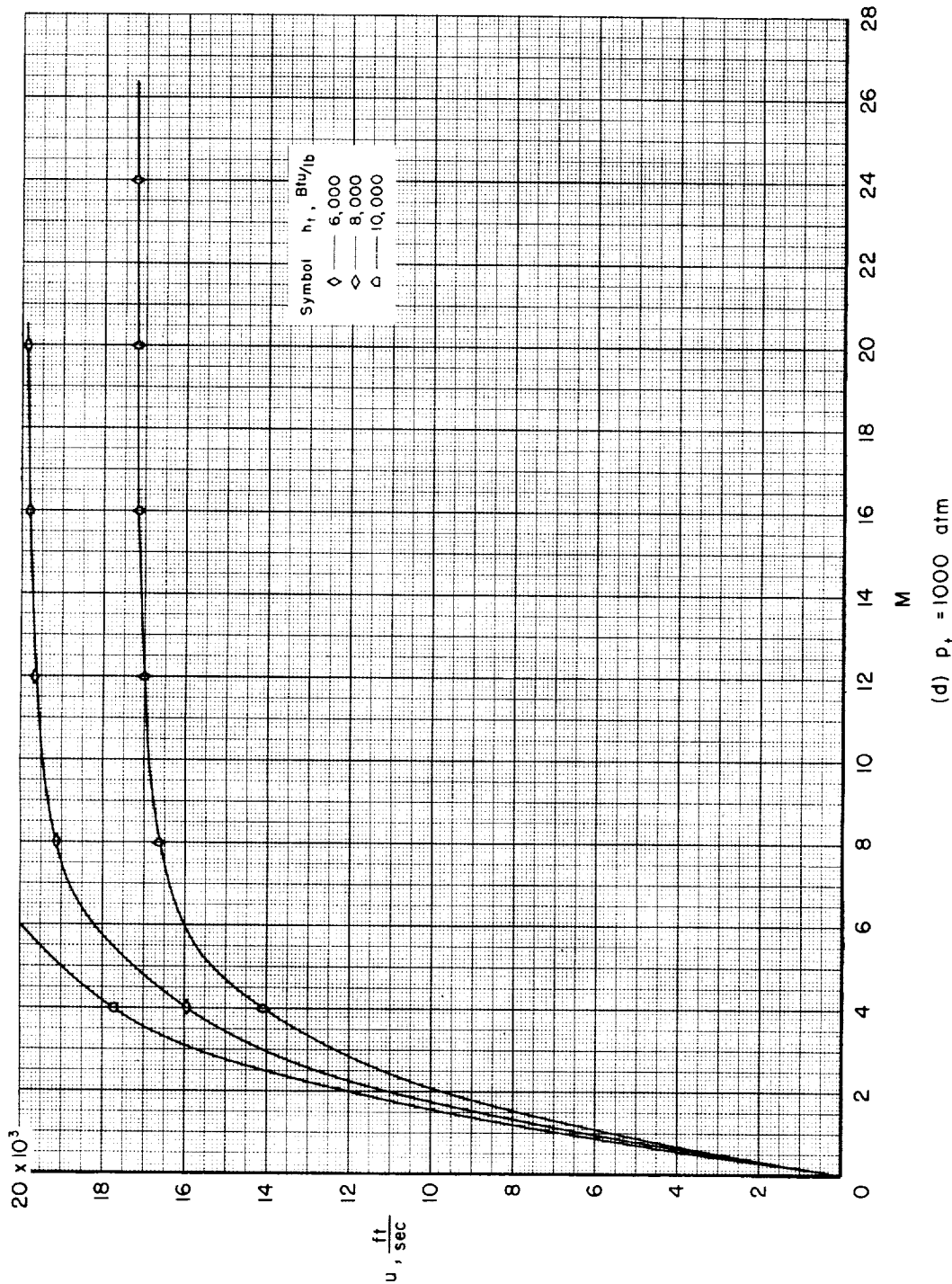


Chart 8.- Continued.

(c)  $p_t = 100 \text{ atm}$



(d)  $p_t = 1000$  atm

Chart 8.- Concluded.

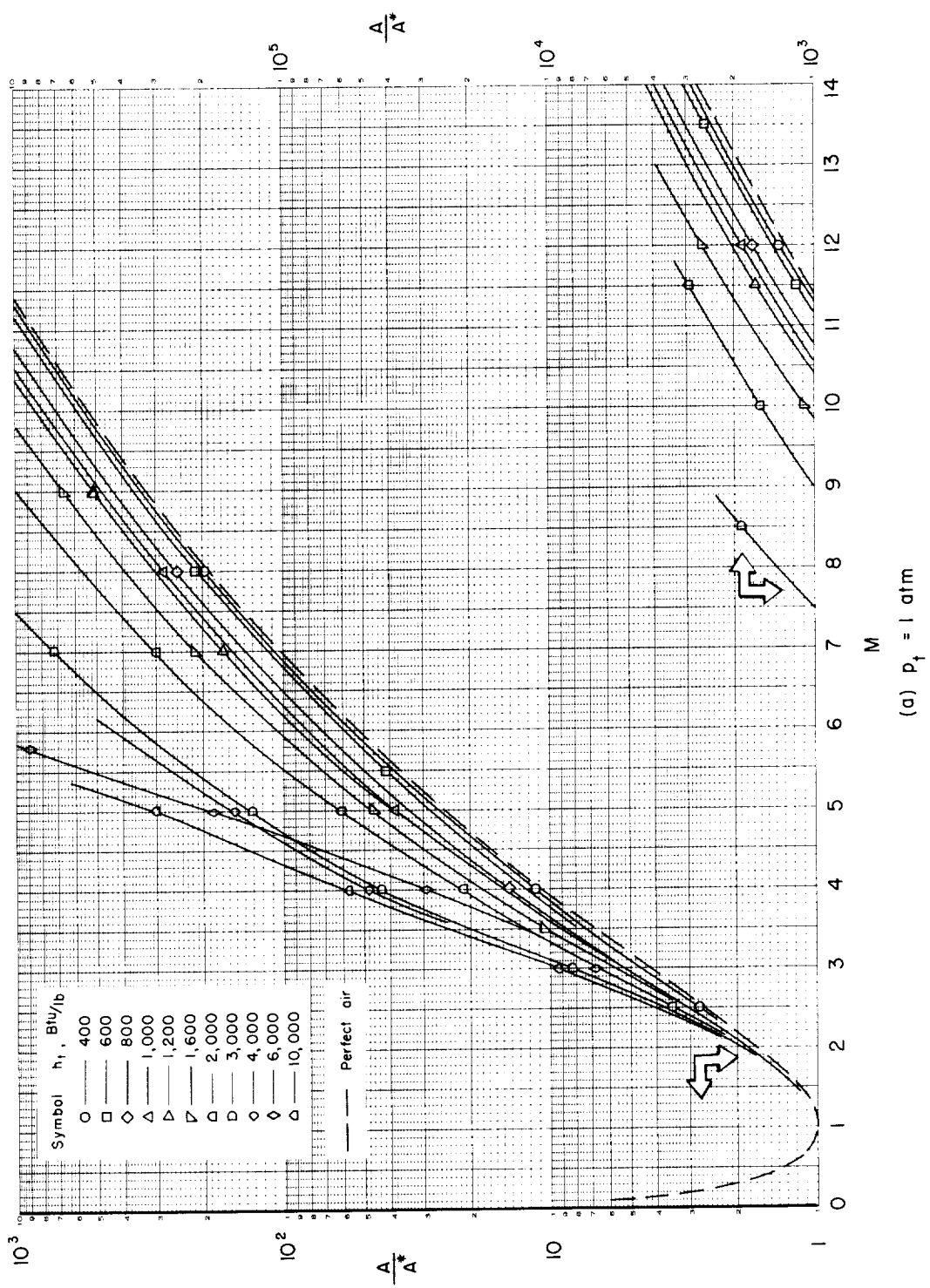


Chart 9.- Variation of area ratio with Mach number.

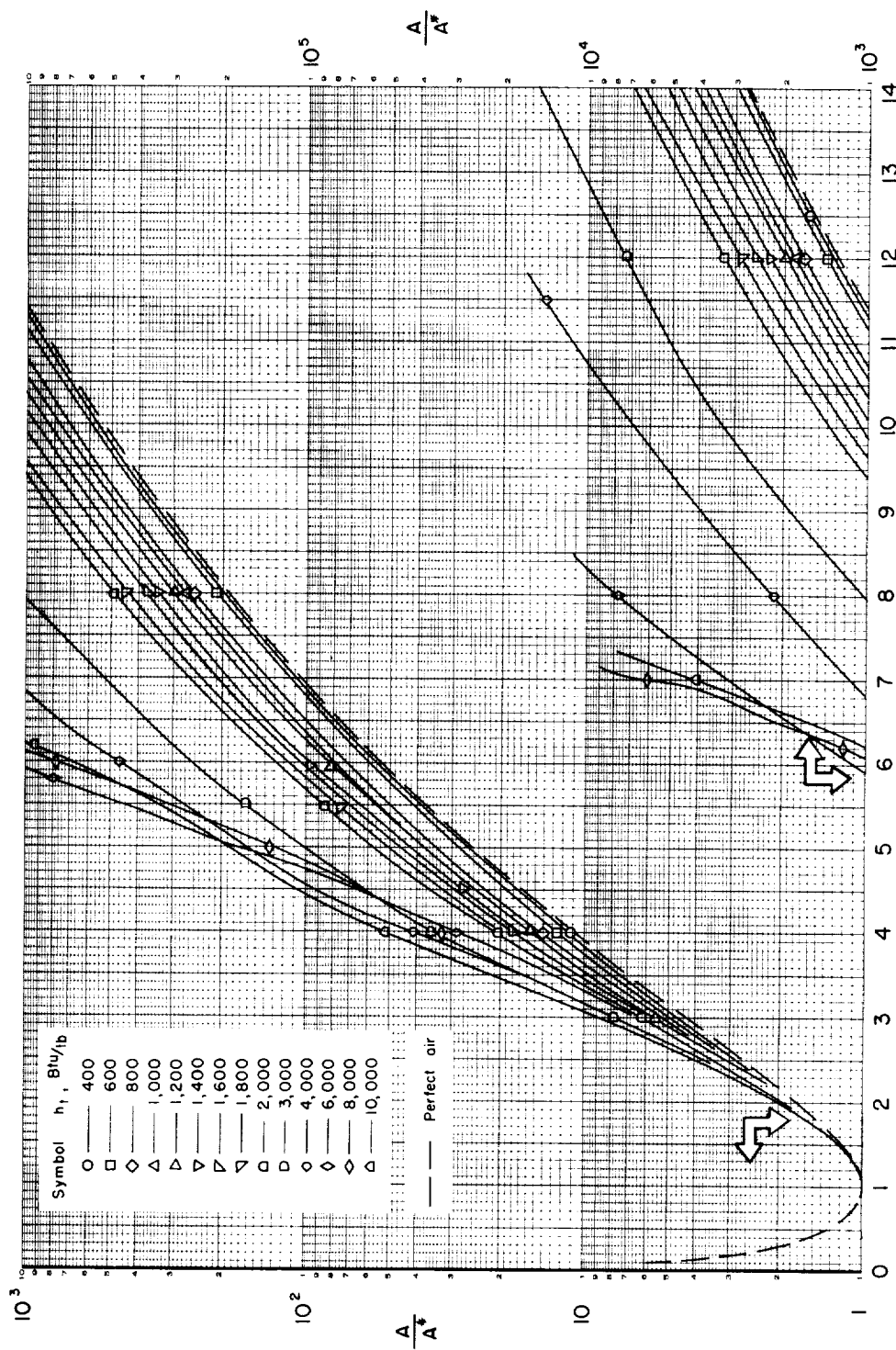
(b)  $p_f = 10 \text{ atm}$ 

Chart 9.- Continued.

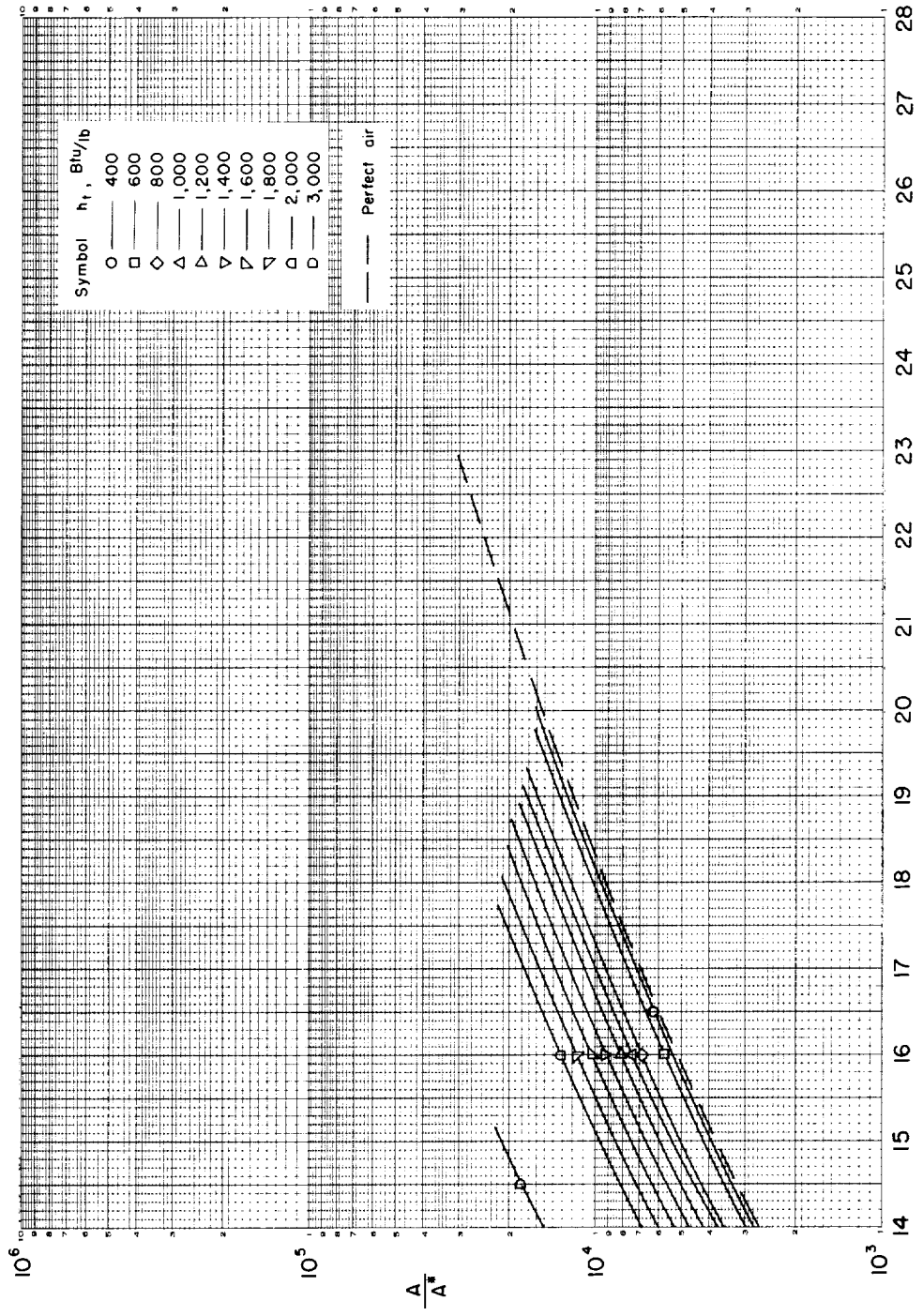
(b)  $p_f = 10 \text{ atm} - \text{Concluded.}$ 

Chart 9.- Continued.

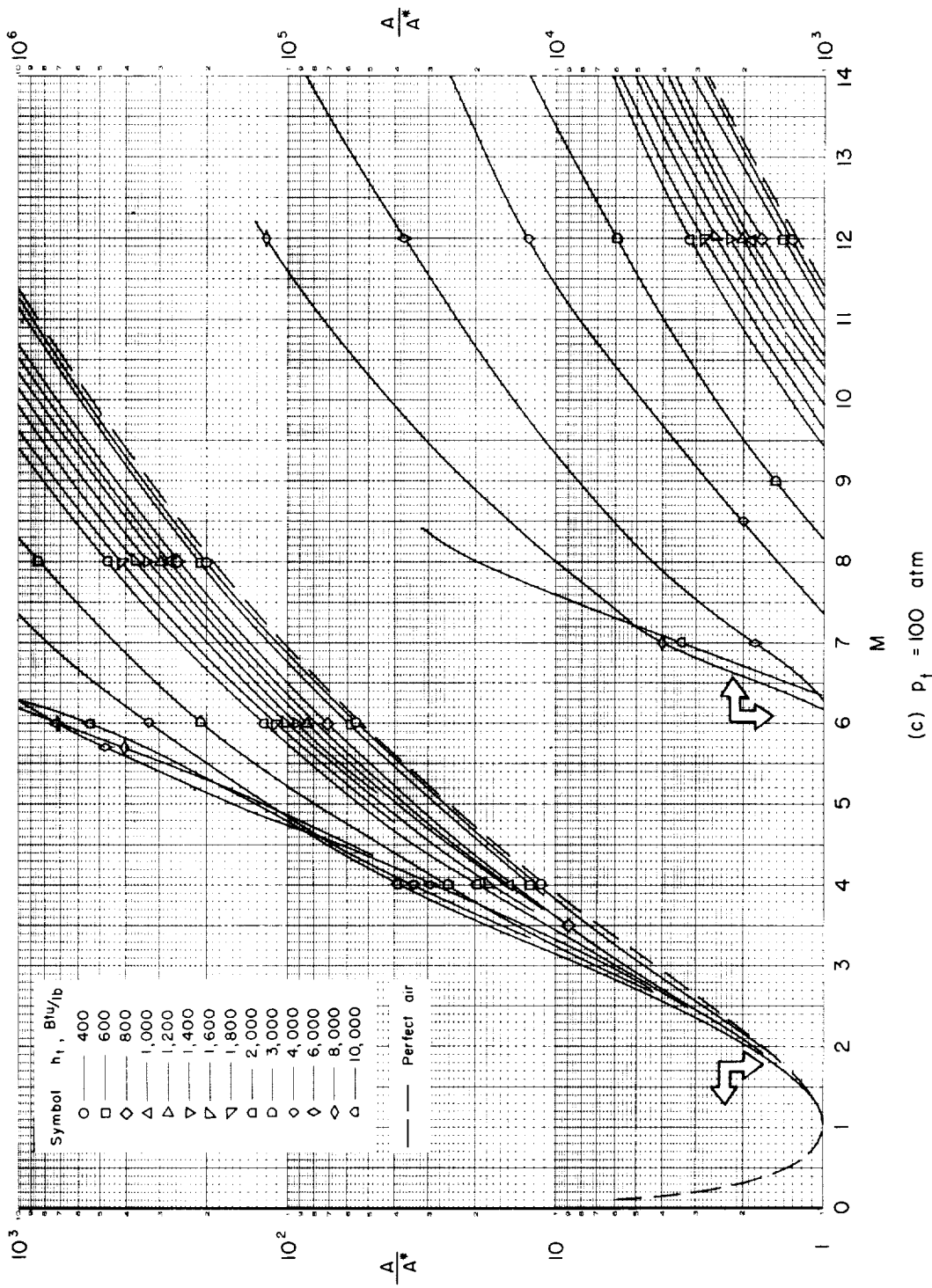
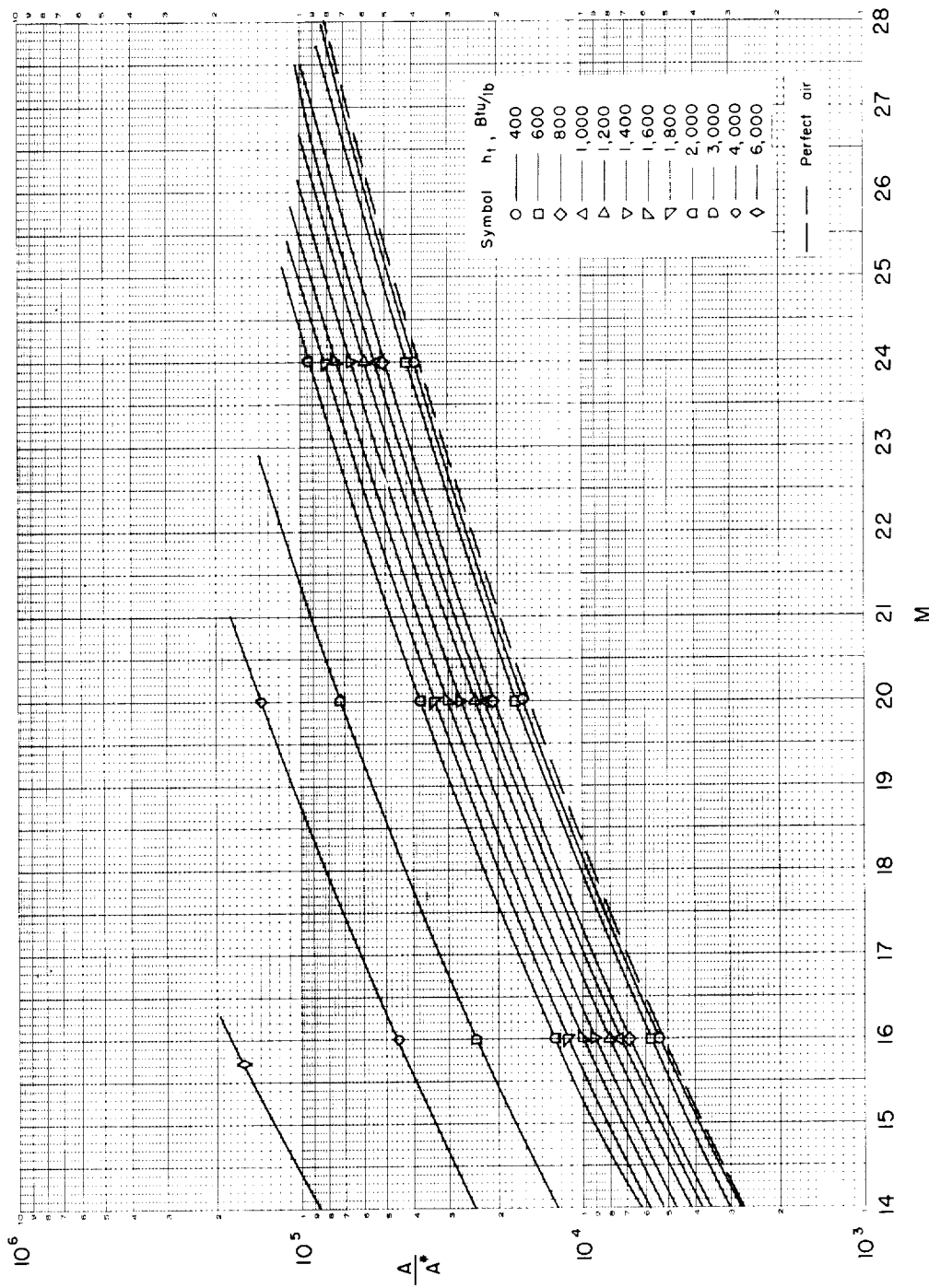
(c)  $P_1 = 100 \text{ atm}$ 

Chart 9.- Continued.



(c)  $p_t = 100$  atm - Concluded.

Chart 9.- Continued.

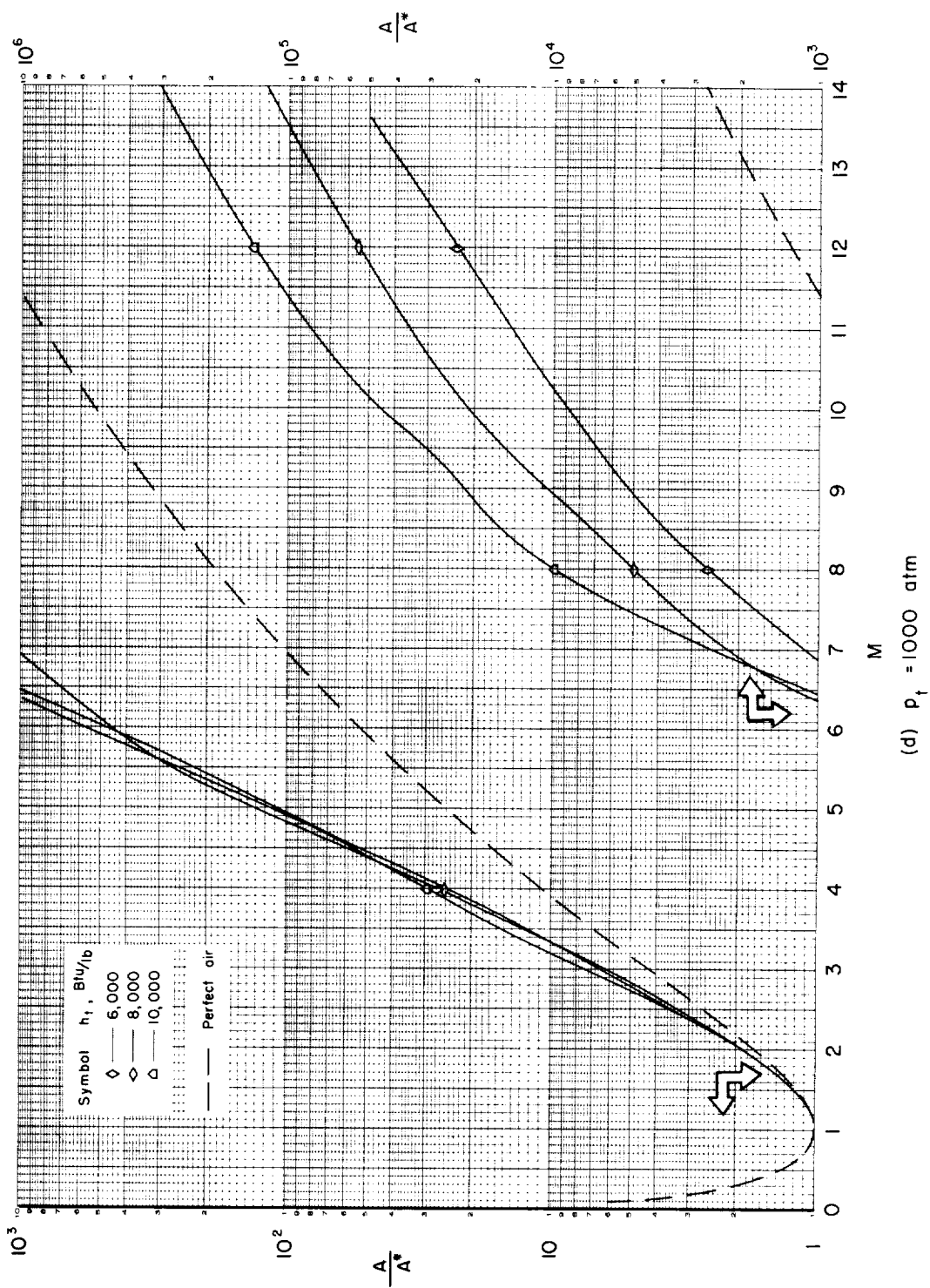
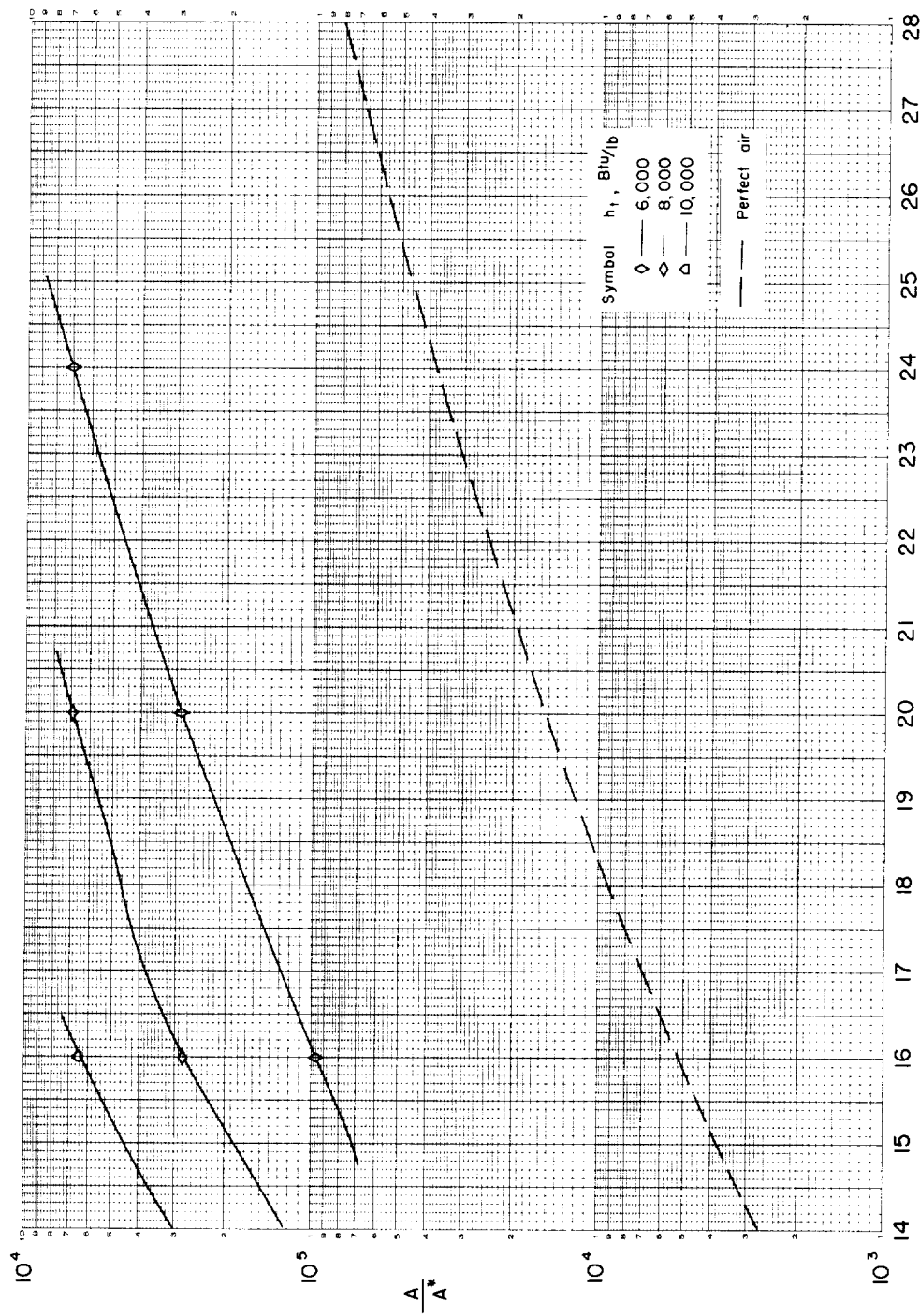
(d)  $p_f = 1000$  atm

Chart 9.— Continued.



(d)  $p_1 = 1000$  atm - Concluded.

Chart 9.- Concluded.

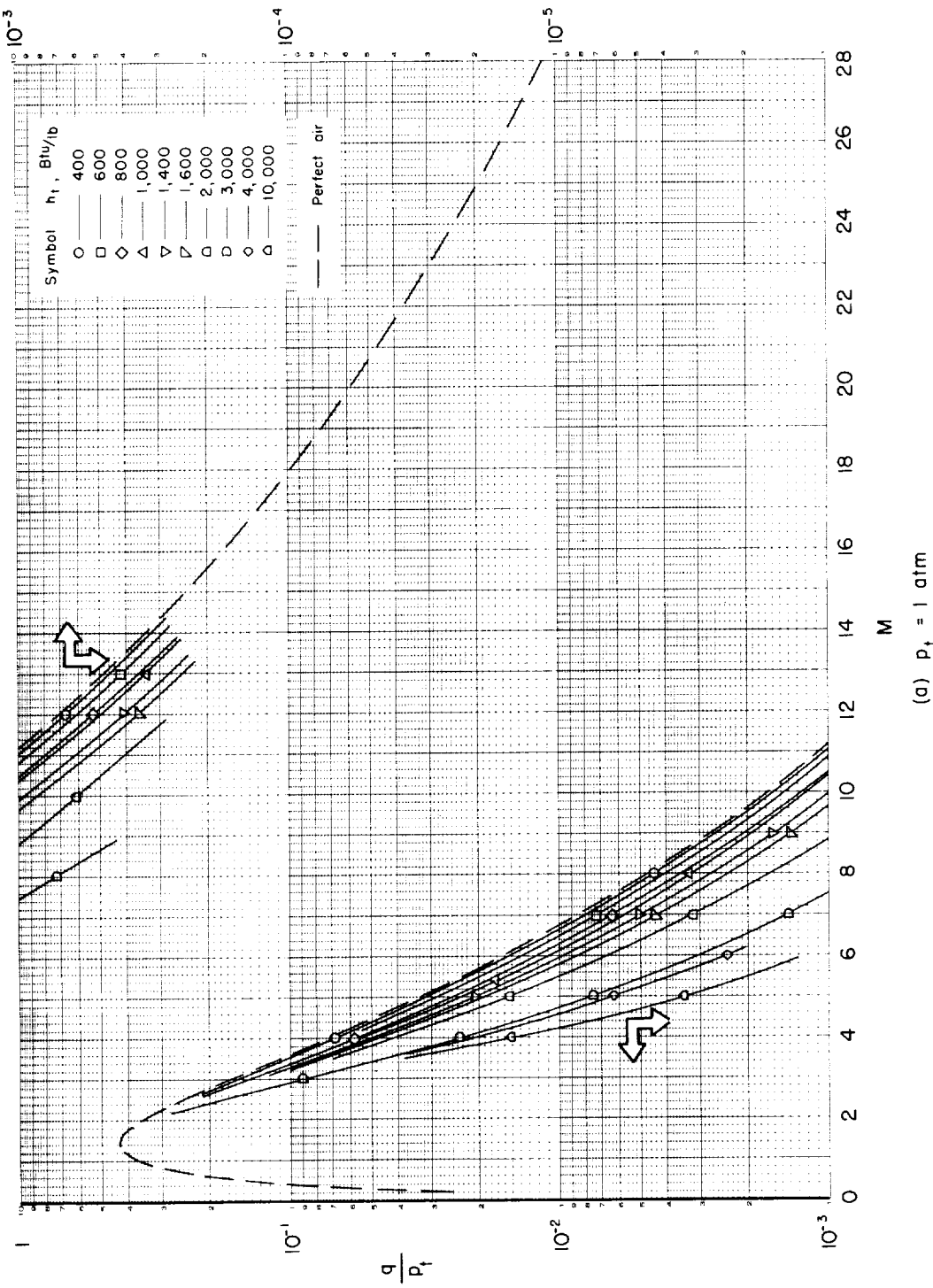
(a)  $P_f = 1 \text{ atm}$ 

Chart 10.- Variation of dynamic pressure with Mach number.

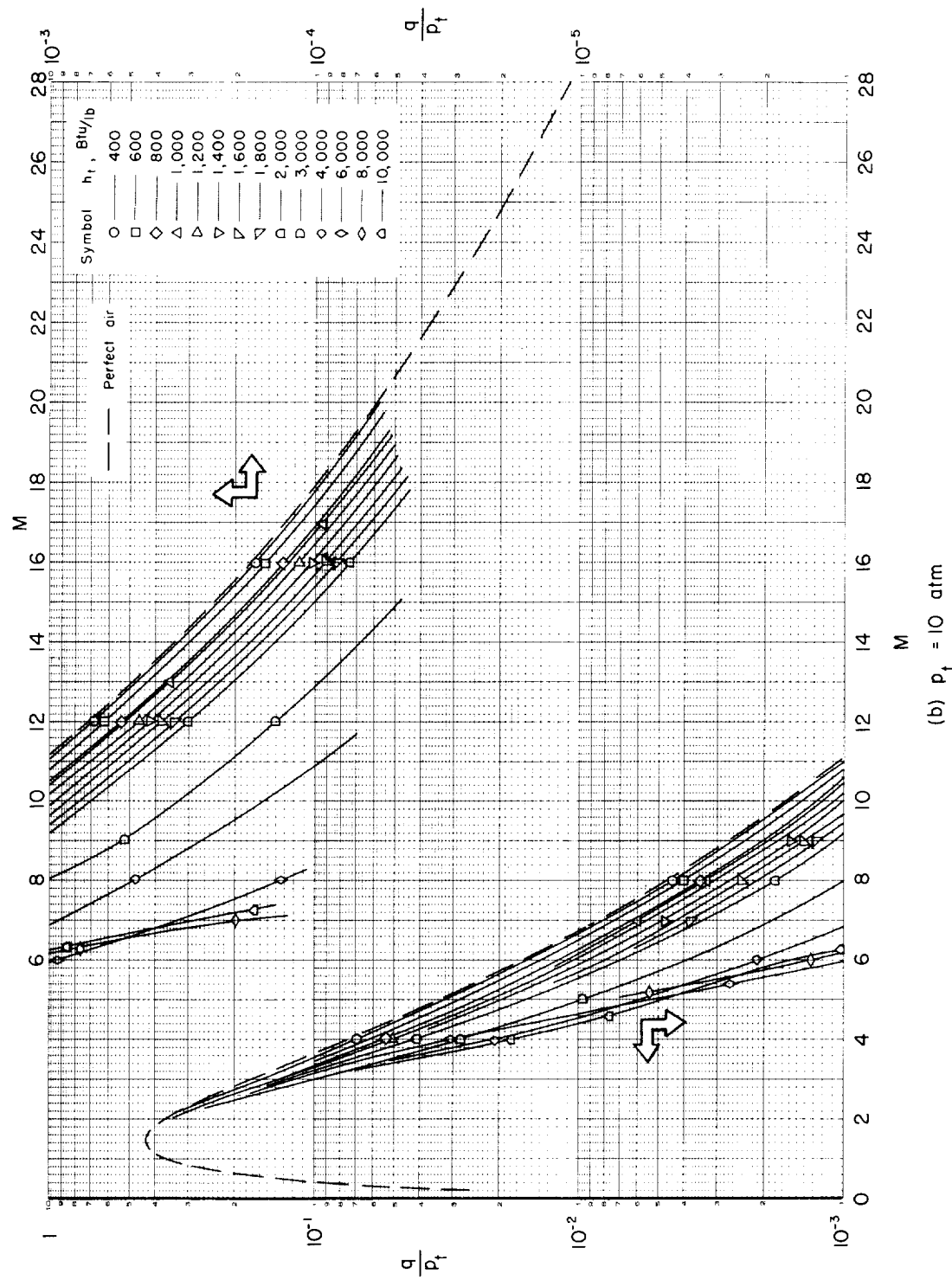


Chart 10.- Continued.

(b)  $p_t = 10 \text{ atm}$

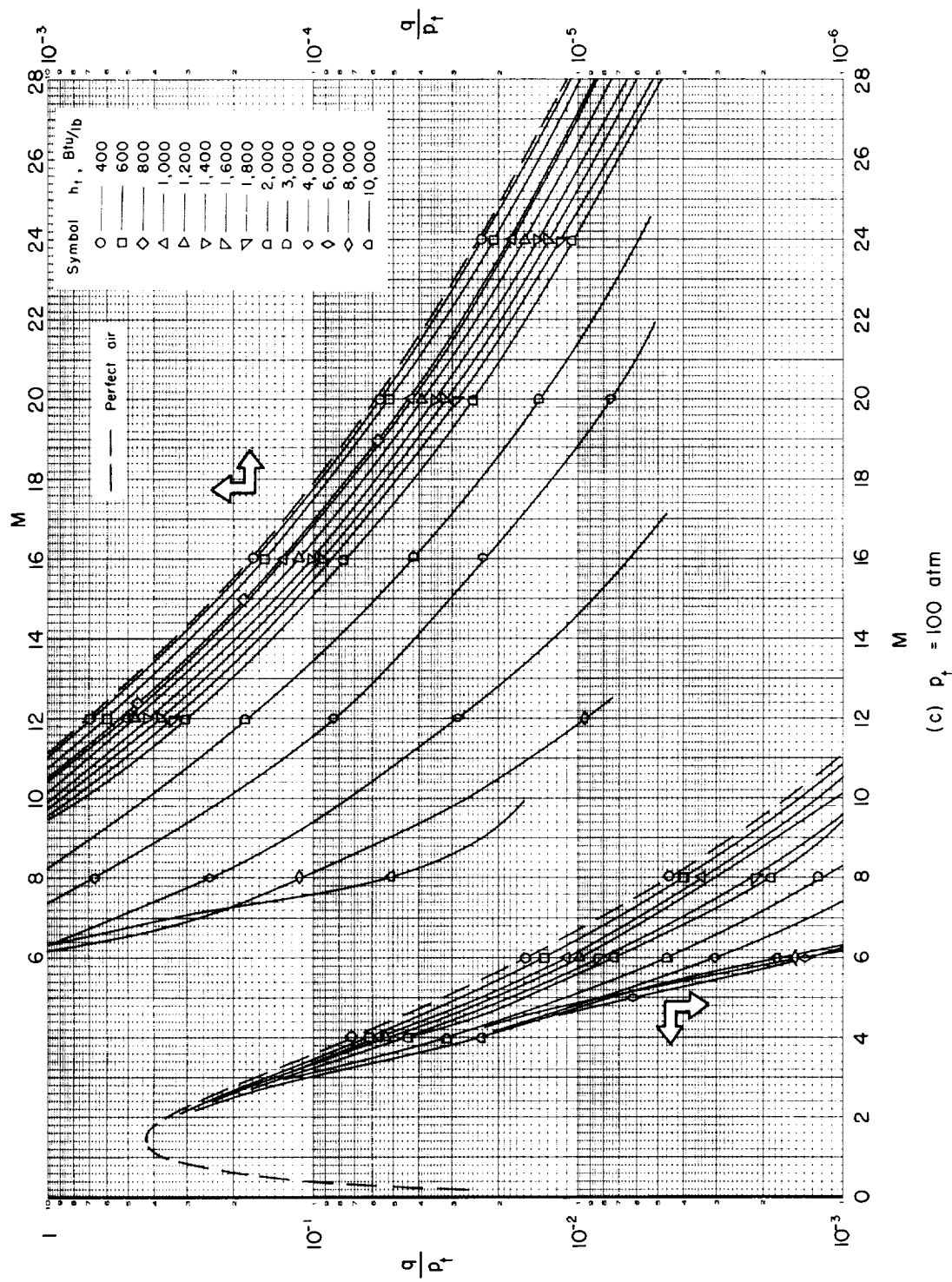


Chart 10.- Continued.

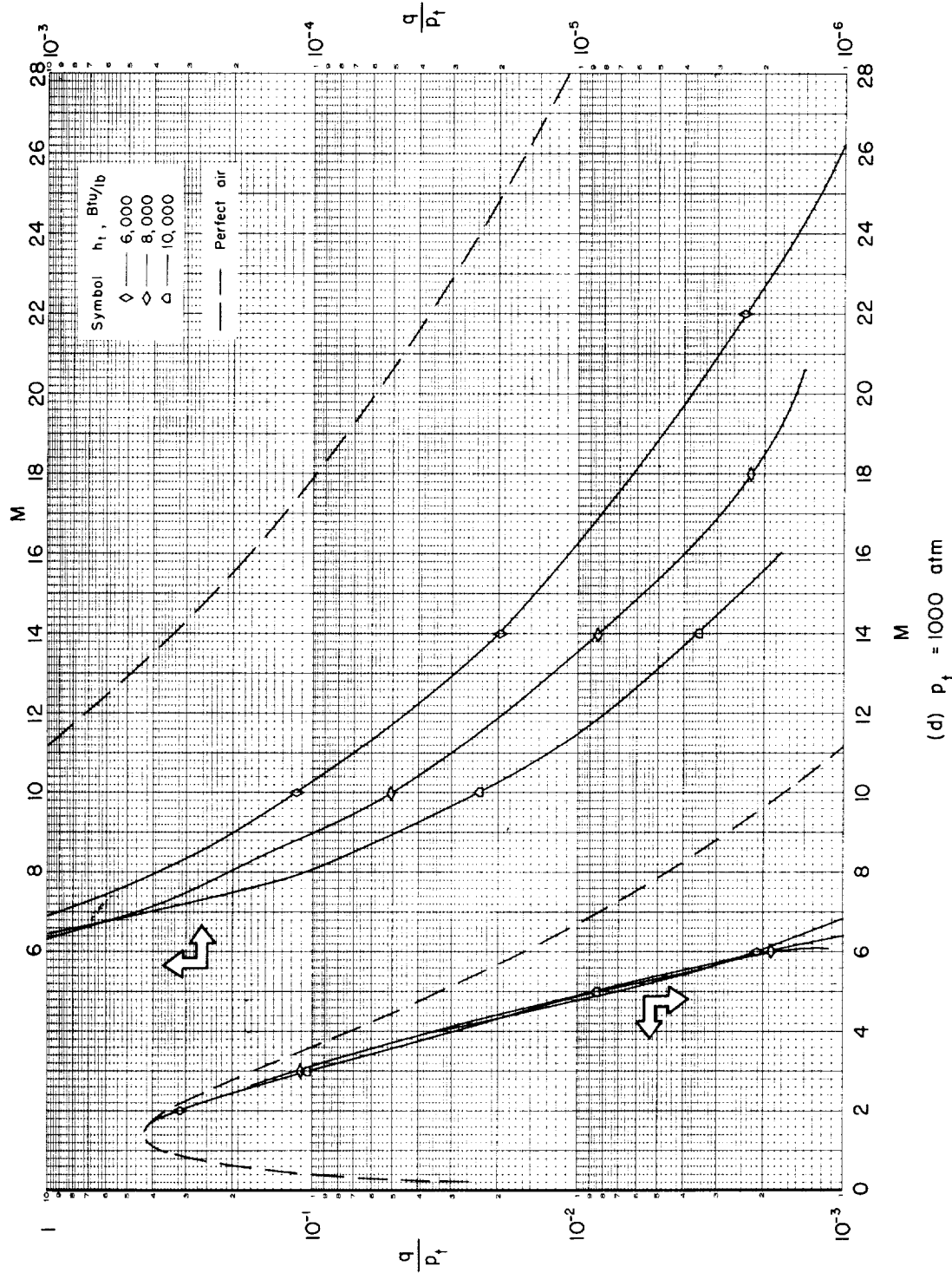
(d)  $p_f = 1000 \text{ atm}$ 

Chart 10.- Concluded.

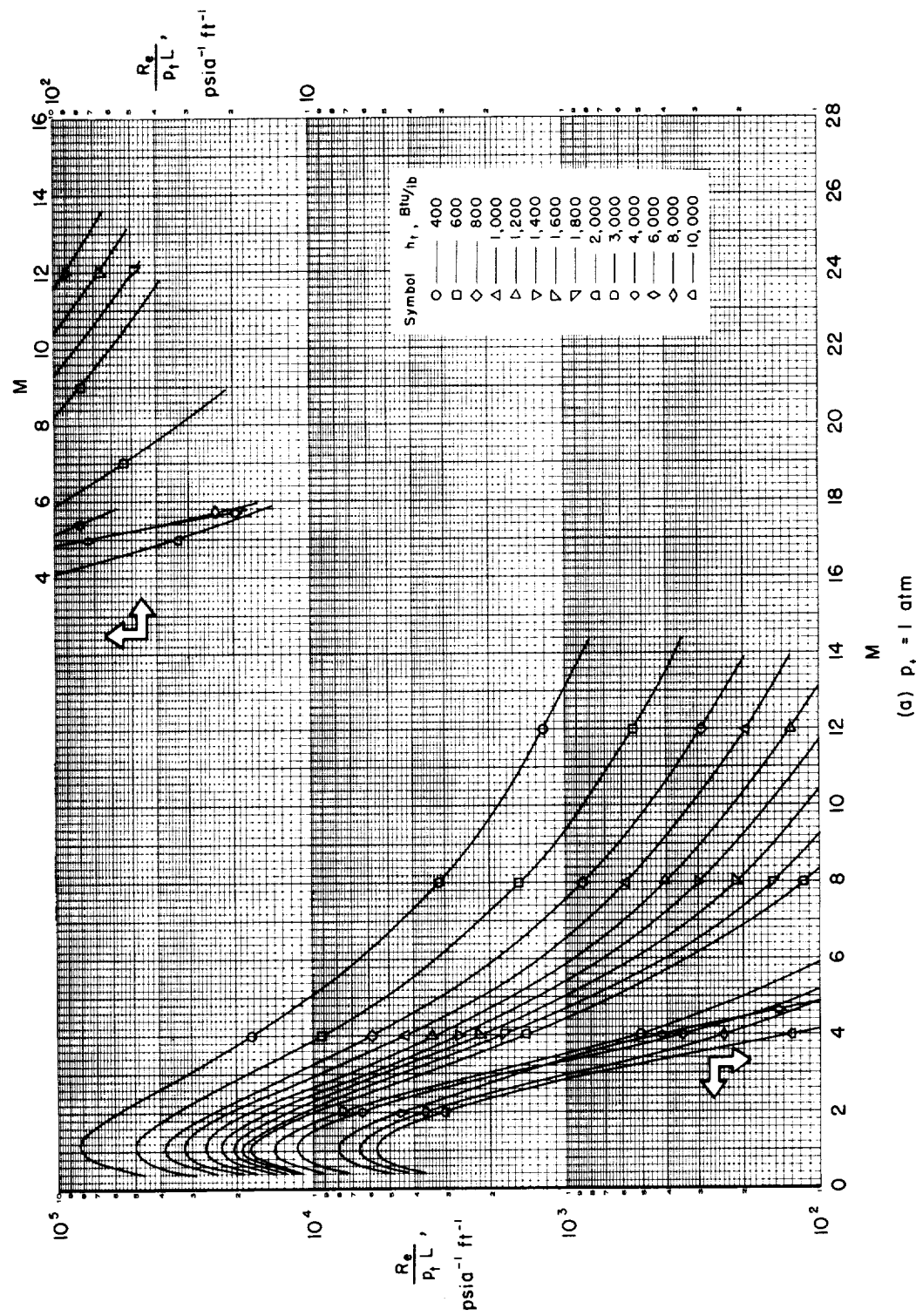
(a)  $p_1 = 1$  atm

Chart 11.- Variation of Reynolds number with Mach number.

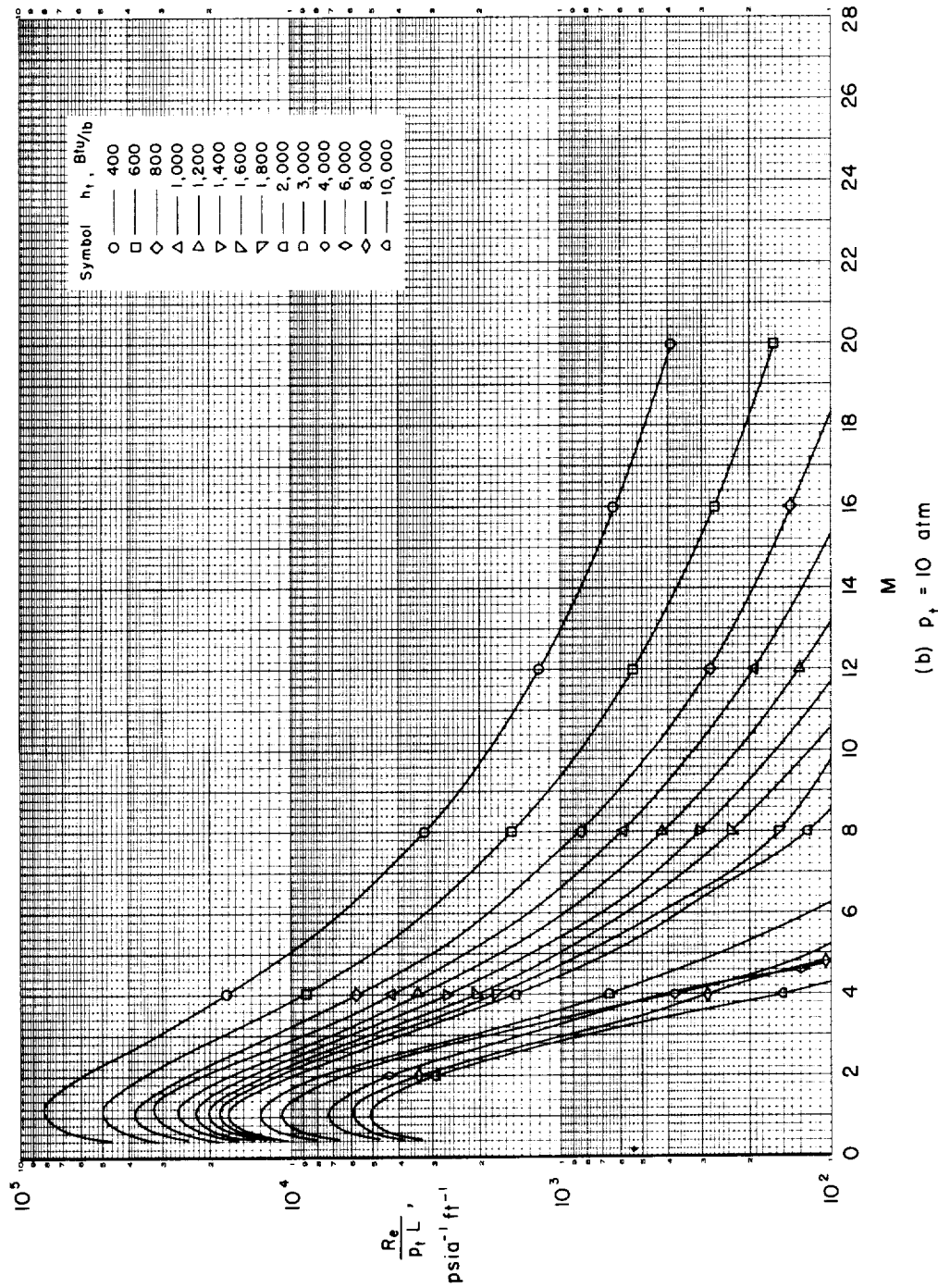
(b)  $p_t = 10 \text{ atm}$ 

Chart 11.- Continued.

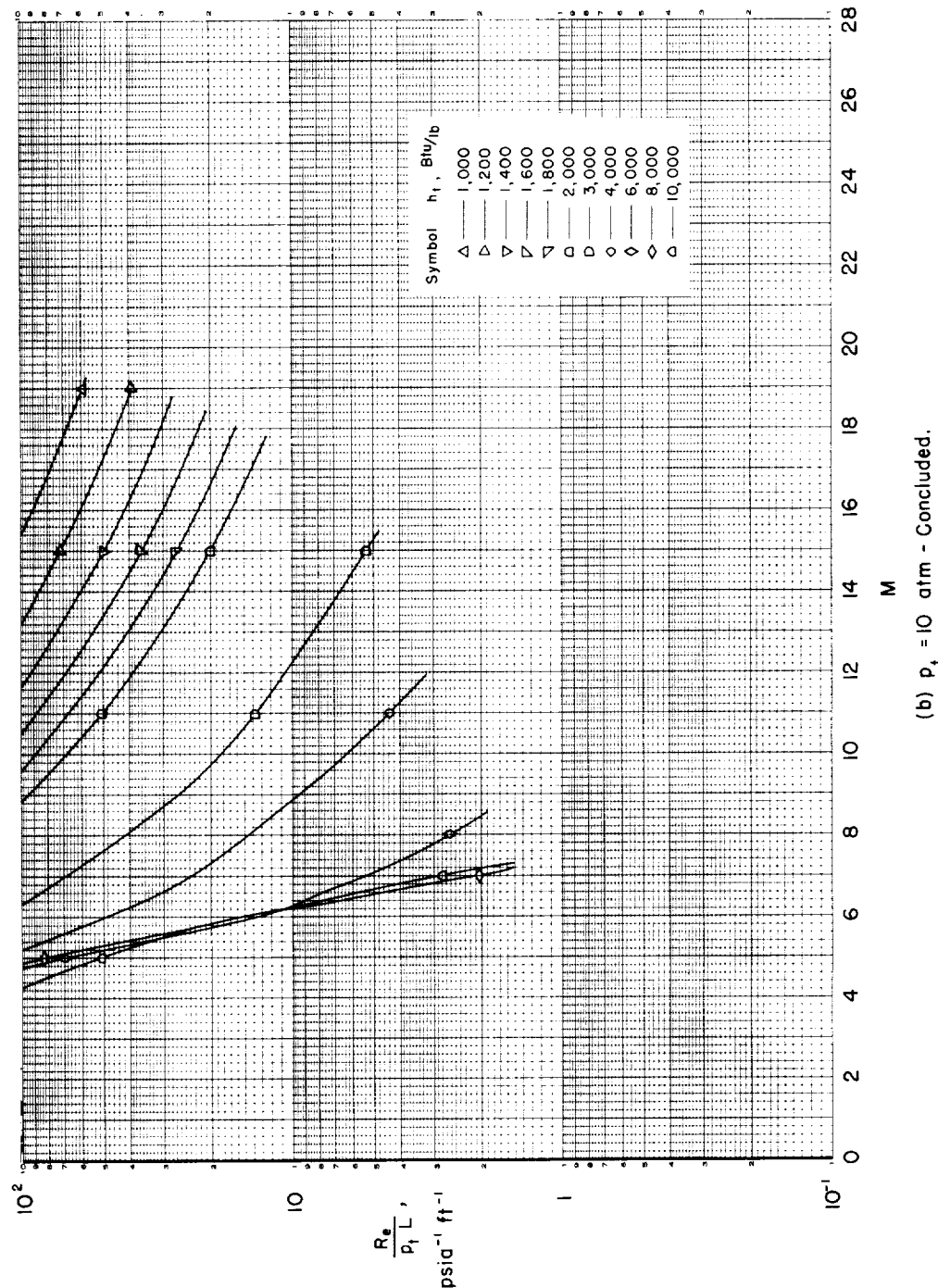
(b)  $p_1 = 10$  atm - Concluded.

Chart 11.- Continued.

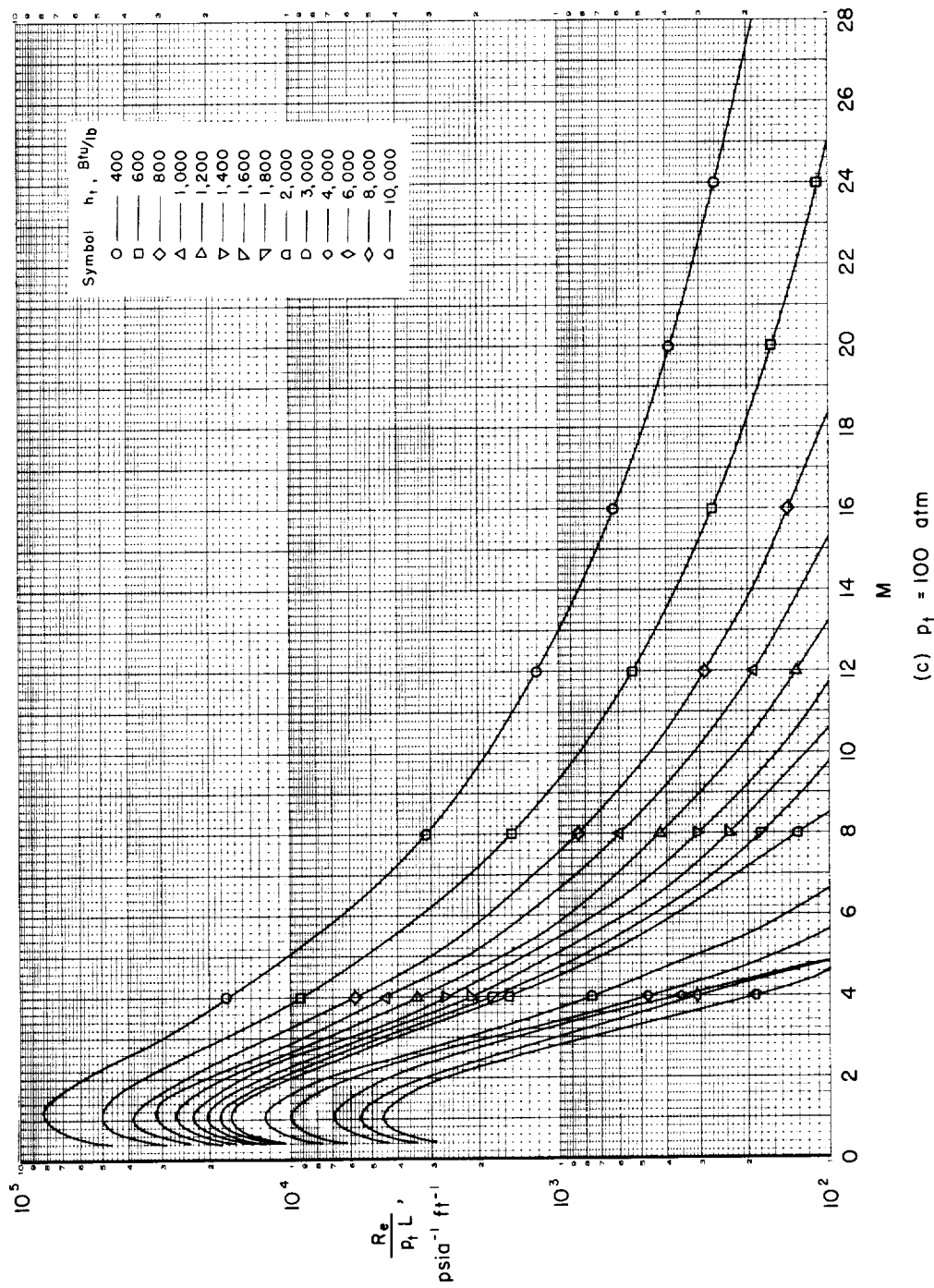


Chart 11.—Continued.

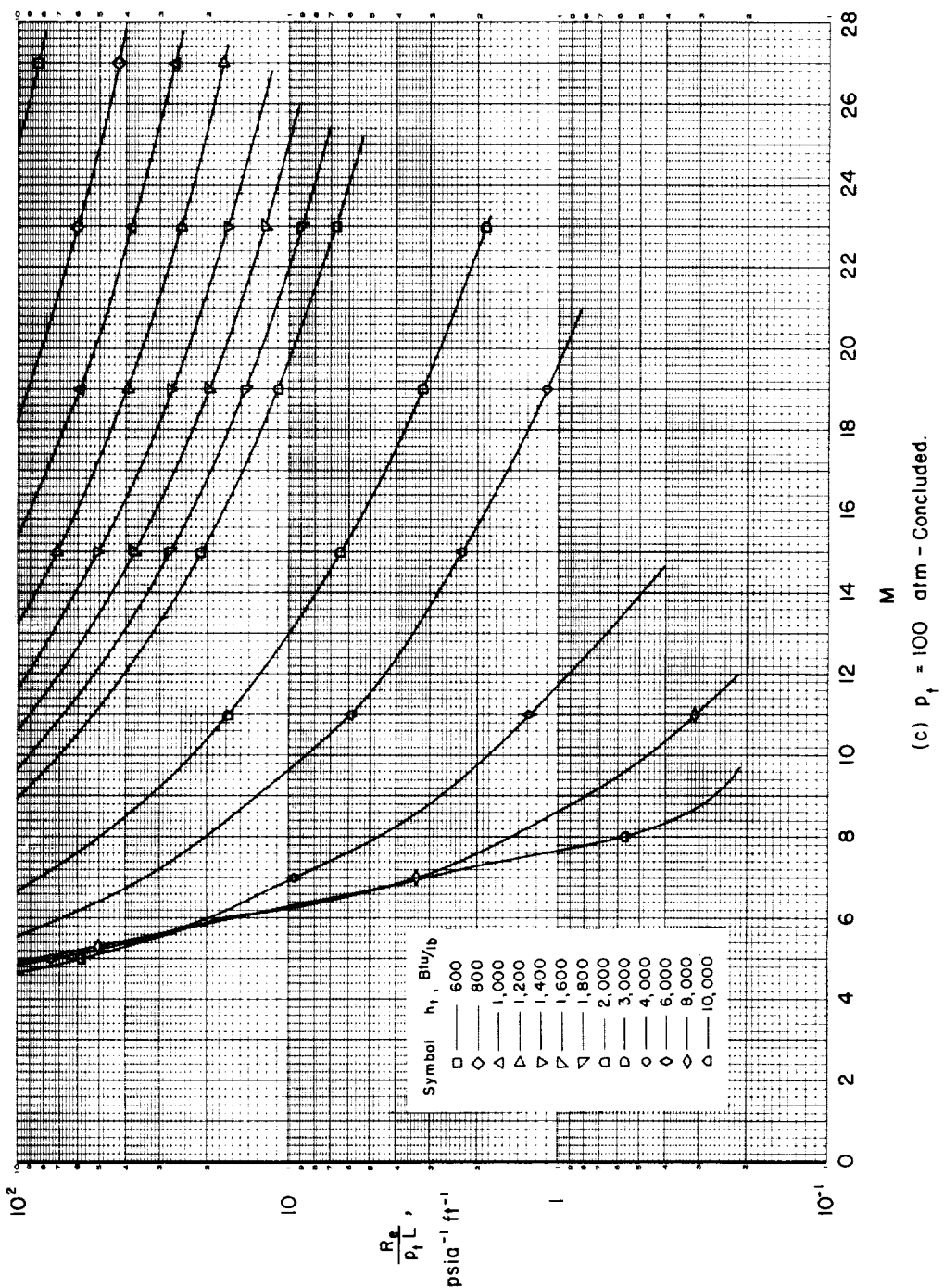
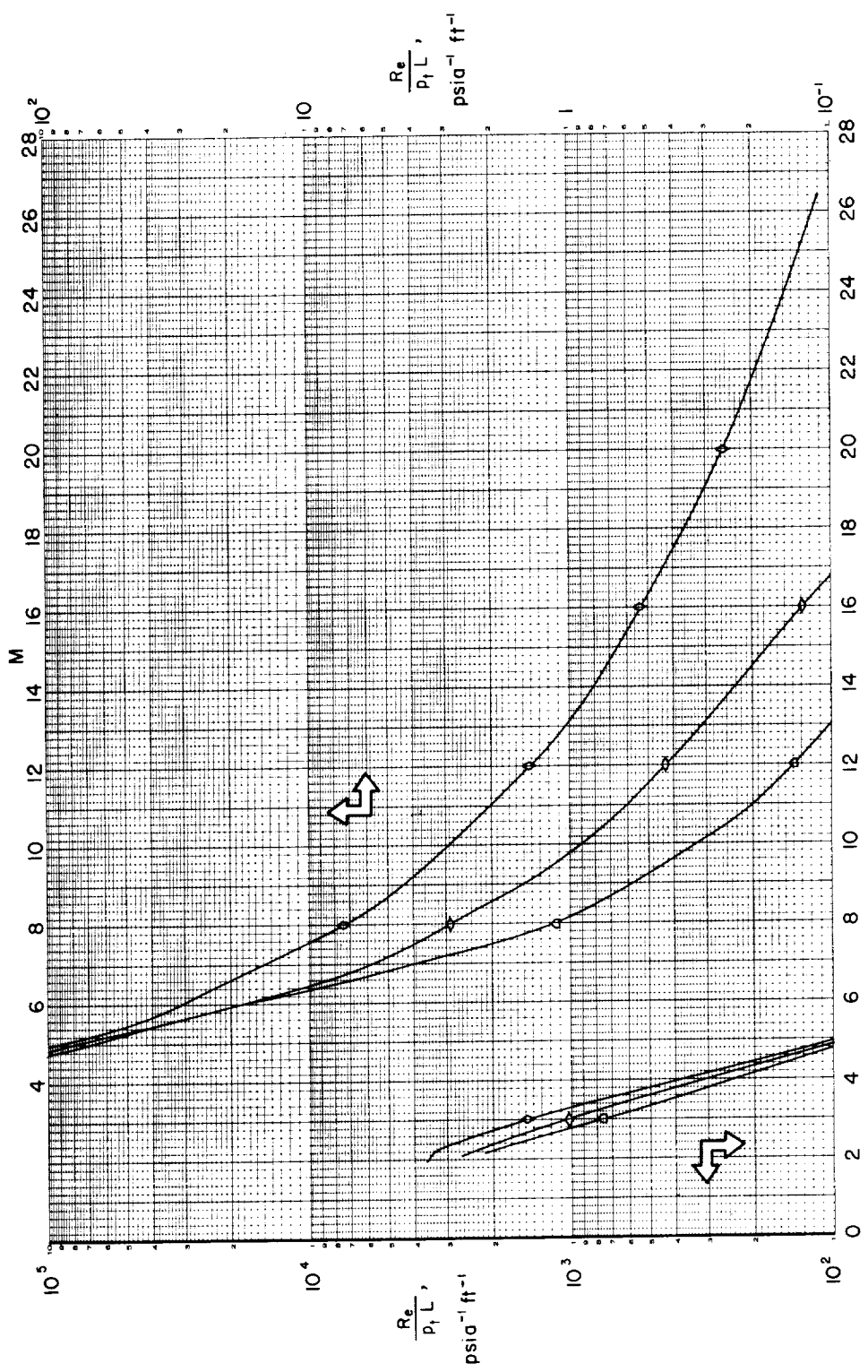


Chart 11.- Continued.



(d)  $p_f = 1000 \text{ atm}$

Chart 11.- Concluded.

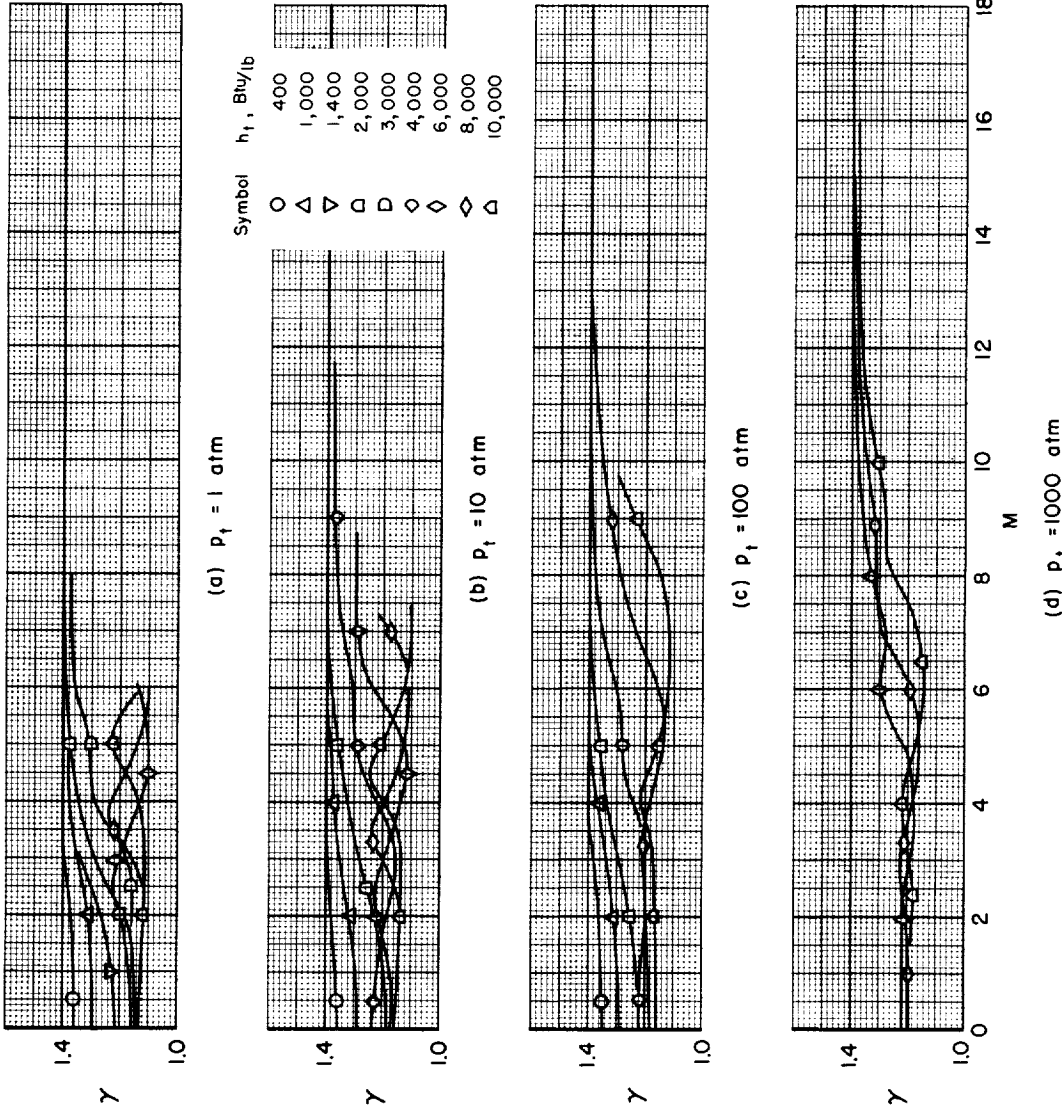


Chart 12.- Variation of isentropic exponent with Mach number.

U H S A

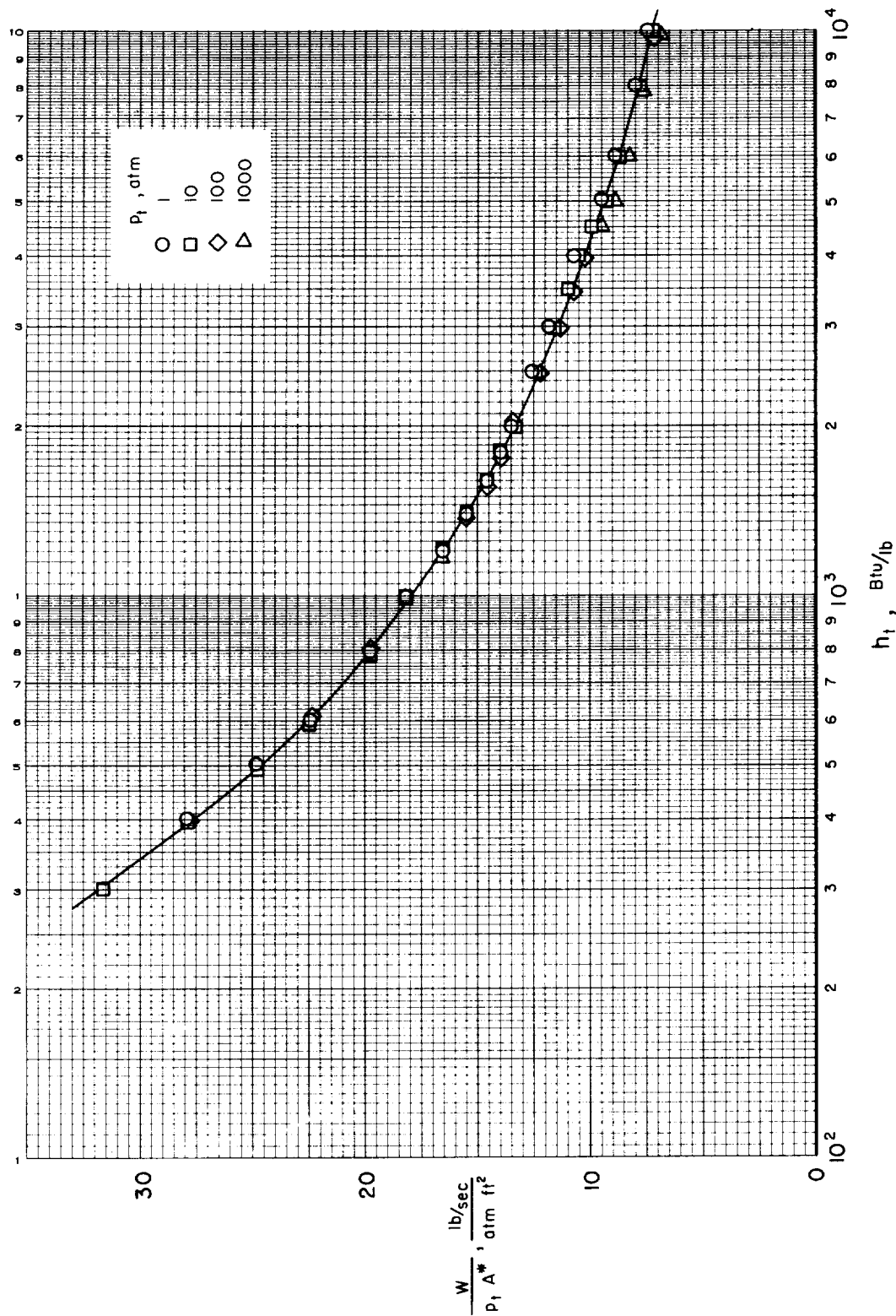


Chart 14.- Variation of weight-flow rate at throat with stagnation enthalpy.

UHSA

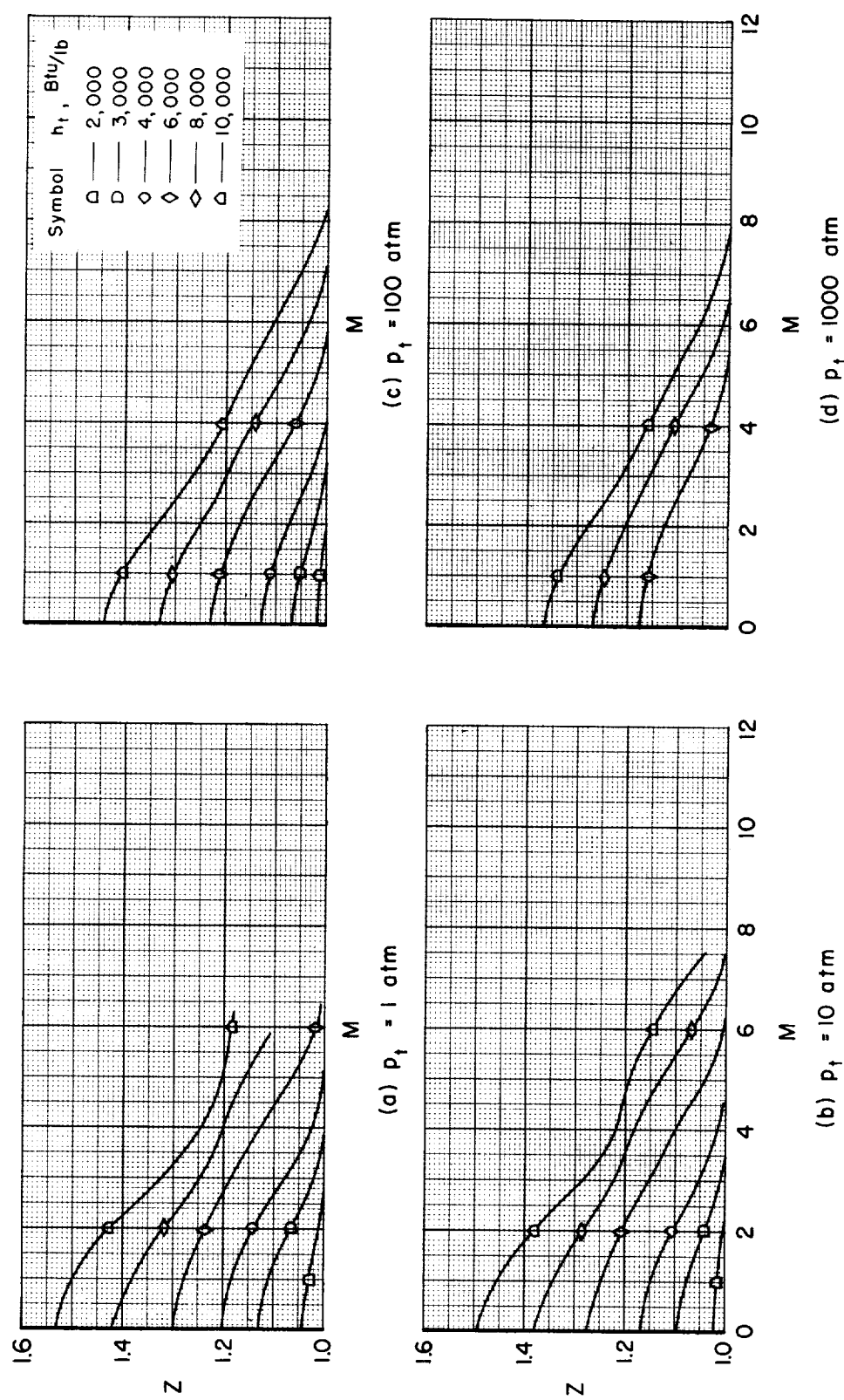


Chart 13.- Variation of molecular weight ratio with Mach number.

